CENTRO DE INVESTIGACIÓN Y DE ESTUDIOS AVANZADOS DEL INSTITUTO POLITÉCNICO NACIONAL

UNIDAD ZACATENCO
DEPARTAMENTO DE BIOMEDICINA MOLECULAR

“El papel de HDAC6 en la migración transendotelial e infiltración de órganos en leucemia linfoblástica aguda de células B”

TESIS

Que presenta

Karina Elizabeth Jiménez Camacho

Para obtener el grado de

DOCTORA EN CIENCIAS

EN LA ESPECIALIDAD DE

BIOMEDICINA MOLECULAR

Directores de Tesis:

Dr. Michael Schnoor

Dra. Rosana Pelayo Camacho

Ciudad de México **Octubre 2023**

RESEARCH CENTER AND ADVANCED STUDIES OF THE NATIONAL POLYTECHNIC INSTITUTE

ZACATENCO UNIT
DEPARTMENT OF MOLECULAR BIOMEDICINE

"The role of HDAC6 in transendothelial migration and organ infiltration in B-cell acute lymphoblastic leukemia"

THESIS

Presented by

Karina Elizabeth Jiménez Camacho

To obtain the degree of

PHILOSOPHY DOCTOR

IN THE SPECIALTY OF

MOLECULAR BIOMEDICINE

Thesis Directors:

Dr. Michael Schnoor

Dr. Rosana Pelayo Camacho

Mexico City **October 2023**

AGRADECIMIENTOS

Al Consejo Nacional de Ciencia y Tecnología (CONACYT), por la beca otorgada durante el periodo 2019-2023 para la realización de este posgrado.

Al CINVESTAV, por haber sido mi lugar de formación y crecimiento.

Al Dr. Michael Schnoor por abrirme las puertas de su laboratorio y por su gran apoyo y observaciones durante el desarrollo de este proyecto.

A mi comité: Dra. Rosana Pelayo, Dr. Vianney Ortiz, Dr. Leopoldo Santos, Dra. Rosaura Hernández y Dra. Elisa Dorantes, por sus valiosas recomendaciones y enriquecedoras discusiones.

Al MVZ Benjamín Emmanuel Chávez Álvarez, por su asistencia y apoyo al trabajar con ratones en el bioterio.

A mis queridos amigos del laboratorio: Dr. Armando Montoya (por ser mi mejor amigo), Dr. Ramón Castellanos (por enseñarme y ser paciente), Dra. Idaira Guerrero, M.C. Iliana León, M.C. Belén Hernández, M.C. Joseph Adomako, M.C. Víctor Correa, Dra. Ana Sánchez y Dra. Hilda Vargas, por su apoyo y por hacer cada día en el laboratorio un lugar tan agradable.

A mis mejores amigos de La Paz que siguen alrededor de CDMX: Dayan Carrión, José Ortega y Marcos Quiroz, por más de 10 años de amistad y hacerme sentir en casa como si el tiempo no pasara.

A mi abuelita Chuyita y a toda mi querida familia, porque siempre me apoyan y echan porras para alentarme a continuar mi camino profesional.

A mis abuelitos en el cielo: Capi, Cuate y Veva, porque su recuerdo me hace sonreír y sentirlos cerca. Por aconsejarme a seguir creciendo y disfrutando del camino de vida que elegí.

DEDICATORIA

A mi mami, Rossy Camacho, por ser mi principal apoyo y motor, por impulsarme a seguir adelante y a disfrutar la vida.

A mi papi, José Jiménez, porque apoyarme sin pensarlo y alentarme a seguir creciendo en mi camino en la investigación y en mi vida.

Soy lo que soy gracias a ustedes.

He llegado hasta aquí por ustedes.

Por siempre agradecida por todo su amor.

Los amo infinitamente.

INDEX

LIST OF FIGURES

LIST OF TABLES

ABBREVIATIONS

ABP	Actin binding protein
ABCC	ATP binding cassette subfamily C
AL	Acute leukemia
ALL	Acute lymphoblastic leukemia
AML	Acute myeloid leukemia
ARP	Actin related protein
ASXL	Additional sex combs like
ATP	Adenosine triphosphate
AURKA	Oncogenic serine/threonine kinase Aurora A
B-ALL	B-precursor cell acute lymphoblastic leukemia
BCR	B-cell receptor
BM	Bone marrow
BSA	Bovine serum albumin
BUZ	Ubiquitin-binding zinc finger
CAR	CXCL12-abundant reticular
CD	Catalytic domain
CFDA	Carboxyfluorescein diacetate
CLL	Chronic lymphoid leukemia
CML	Chronic myeloid leukemia
CNS	Central nervous system
CSF	Cerebral spinal fluid
Cttn	Cortactin
CTV	Cell trace violet
CXCL	C-X-C motif chemokine ligand
CXCR	C-X-C chemokine receptor

DD	Deacetylase domain
DMSO	Dimethyl sulfoxide
DNA	Deoxyribonucleic acid
ECM	Extracellular matrix
EDTA	Ethylenediaminetetraacetic acid
ERK	Extracellular signal-regulated
F-actin	Filamentous actin
FBS	Fetal bovine serum
FISH	Fluorescence in situ Hybridization
GM-CSF	Granulocyte colony stimulating factor
GTP	Guanosine triphosphate
Hb	Hemoglobin
HDAC6	Histone deacetylase 6
HDAC	Histone deacetylases
HDACi	Histone deacetylases inhibitor
HEK	Human embryonic kidney
HSPC	Hematopoietic stem progenitor cells
HSC	Hematopoietic stem cells
HS	Human stroma
HSP	Heat shock protein
HUVEC	Human umbilical vein endothelial cells
ICAM-1	Intercellular Adhesion Molecule 1
IF	Immunofluorescence
IGHV	Immunoglobulin heavy-chain variable
IL	Interleukin
ILE	Inflammatory-leukemia expansion
JAK	Janus kinase

KD	Knock down
kDa	Kilodalton
LFA-1	Lymphocyte function-associated antigen 1
LICs	Leukemia-initiating cells
MFI	Mean fluorescence intensity
MNC	Mononuclear cells
MMP-9	Matrix metalloprotease-9
MPB	Mobilized peripheral blood
MRD	Minimal residual disease
MSC	Mesenchymal stromal cells
MT	Microtubules
MTT	3-(4,5-dimethylthiazol-2-yl)-2,5 diphenyltetrazolium bromide
NAD	Nicotinamide adenine dinucleotide
NEDD9	Neural precursor cell expressed, developmentally downregulated 9
NES	Nuclear exclusion signal
NFκB	Nuclear factor-kappa B
NGS	Next generation sequencing
NLS	Nuclear localization signal
NSG	NOD scid gamma
NTA	N-terminal acidic
N-WASP	Neuronal-Wiskott–Aldrich Syndrome protein
p38MAPK	p38 mitogen-activated protein kinase
PAGE	Polyacrylamide gel electrophoresis
PAK1	p21 activated kinase 1
PB	Peripheral blood

PBS	Phosphate buffered saline
PCAF	P300/CBP-associated factor
PCR	Polymerase chain reaction
PECAM-1	Platelet endothelial cell adhesion molecule-1
PFA	Paraformaldehyde
PI	Propidium iodide
PI3K	Phosphatidylinositol 3-kinase
PKC	Protein kinase C
PKD	Protein kinase D
PLC	Phospholipase C
PS	Phosphatidylserine
PSGL-1	P-selectin glycoprotein ligand-1
PST	Proline-serine-threonine
PTM	Post-translational modification
RPKM	Reads per kilobase million
RT	Room temperature
SDF-1	Stromal derived-factor 1
SD	Standard deviation
SDS	Sodium dodecyl sulfate
SE	Standard error
SH3	Src-homology-3
siRNA	small interfering RNA
SIRT	Sirtuin
LIC	Leukemia initiating cell
STAT	Signal transducer and activator of transcription
SV	Splice variant
TEM	Transendothelial migration

TNF	Tumor necrosis factor
TubA	Tubastatin-A
TGF	Tumor growth factor
TSA	Thricostatin-A
VCAM-1	Vascular adhesion molecule-1
VE	Vascular endothelial
VLA-4	Very Late Antigen-4 or integrin $\alpha_4\beta_1$
WBC	White blood cell
WT	Wild type
ZAP-70	Zeta-chain-associated protein kinase 70
ZnF-UBP	Zinc finger domain- ubiquitin binding
ZO-1	Zonula occludens-1

1. RESUMEN

La leucemia linfoblástica aguda de células B (LLA-B) es el cáncer infantil más común. A pesar de que la mayoría de los pacientes con LLA-B alcanzan la remisión, aproximadamente el 20% sufre una recaída. La mayoría de las recaídas se producen en la médula ósea (MO), de forma aislada o combinada con afectación del sistema nervioso central (SNC), testículos u otros órganos extramedulares. La extravasación de células leucémicas requiere una migración transendotelial controlada por el citoesqueleto de actina. La cortactina es una proteína de unión a actina que se acumula al frente de las células migratorias. Recientemente, demostramos que la cortactina se sobreexpresa en las células B de los pacientes con LLA-B y que correlaciona con una mayor capacidad migratoria, colonización a médula ósea, infiltración de órganos y recaída. La cortactina necesita ser desacetilada por la histona-desacetilasa-6 (HDAC6) para inducir de manera eficiente la motilidad. HDAC6 es una histona desacetilasa de clase II dependiente de zinc con una localización citoplasmática. Se han detectado niveles altos de HDAC6 en tumores sólidos donde se correlacionó con metástasis en pacientes, pero se desconoce si HDAC6 también modula la agresividad de las células B en LLA. En este estudio, investigamos la relevancia de HDAC6 en la migración de células leucémicas *in vitro* e *in vivo*. Encontramos que HDAC6 está sobreexpresado en la línea celular REH de LLA-B en comparación con células B sanas, y que colocaliza con cortactina en el citoplasma. Células derivadas de pacientes con LLA-B también expresan altos niveles de HDAC6 y encontramos una correlación positiva con la recaída. Además, encontramos que se requiere HDAC6 para la polimerización de actina eficiente, la migración transendotelial, la colonización de MO y la invasión de órganos *in vivo*. Nuestros hallazgos destacan el potencial de la inhibición farmacológica de HDAC6 como nueva estrategia terapéutica en pacientes con LLA-B que podría ayudar a prevenir la infiltración a órganos y recaída de la enfermedad.

1.1 ABSTRACT

B- cell acute lymphoblastic leukemia (B-ALL) is the most common childhood cancer. While most of the patients with B-ALL accomplish complete remission, approximately 20% suffer relapse. Most of relapses occur in the bone marrow (BM), alone or in combination with central nervous system (CNS), testis or other extramedullary organs involvement. Leukemic cell extravasation is a migratory process that requires actin cytoskeleton remodeling. Cortactin is an actin-binding protein that accumulates at the leading edge of migrating cells. Recently, we demonstrated that cortactin is overexpressed in B cells from B-ALL patients and that it correlates with higher migratory capacity, BM colonization, organ infiltration and relapse. Cortactin needs to be deacetylated by the histone deacetylase-6 (HDAC6) to induce efficient cell motility. HDAC6 is a class II zinc-dependent histone deacetylase with a cytoplasmic localization. High HDAC6 levels have been detected in solid tumors where it correlates with metastasis in patients, but whether HDAC6 modulates B-ALL cell aggressiveness has not yet been explored. In this study, we investigated the relevance of HDAC6 in leukemic B cell migration *in vitro* and *in vivo*. We found that HDAC6 is overexpressed in the B-ALL cell line REH in comparison to healthy B cells, and that HDAC6 colocalizes with cortactin in the cytoplasm. B-ALL patient-derived cells also possess high HDAC6 levels and we found a positive correlation with relapse. Furthermore, we found that HDAC6 is required for efficient actin polymerization, transendothelial migration, BM colonization and organ invasion *in vivo*. Our findings highlight the potential of HDAC6 pharmacological inhibition as a new therapeutic strategy in B-ALL patients, which could help to prevent organ infiltration and disease relapse.

2. INTRODUCTION

2.1 Statistics of childhood leukemia

Childhood cancer comprises only a small proportion of the global cancer burden. In high-income countries, more than 80% of children with cancer survive after diagnosis (Lam et al., 2019; World Health Organization, 2021). However, approximately 90% of children who develop cancer worldwide live in low- and middle-income countries (Force et al., 2019). Unfortunately, these children have low survival rates due to inadequate sanitary resources, inaccurate diagnosis, limited access to drugs, and therapy abandonment (Zapata-Tarrés et al., 2021).

Acute leukemias (AL), especially acute lymphoblastic leukemias (ALL), are the most common childhood cancers throughout the world, accounting for about 30% of all cases (Siegel et al., 2023). The reported incidence worldwide is 153,000 new cases and 47,600 deaths (Lancet, 2019).

For Mexico City, the frequency of ALL is among the highest in the world (Pérez-Saldivar et al., 2011). In public hospitals, the B cell subtype in pediatric patients is found with frequencies of 76.1-81.4%, followed by the T-cell subtype (12.4-23.6%) (Mejía-Aranguré et al., 2022). For the B-ALL subtype, the immunophenotypes of children were determined for 113 pediatric AL cases with 26.5% corresponding to pro-B, 19.5% to pre-B and 32% to combined pro-B and pre-B differentiation stages (Balandrán et al., 2016). Thus, B-lineage leukemias dominate within the pediatric lymphoid leukemias.

2.2 B-cell acute lymphoblastic leukemia biology

B-cell acute lymphoblastic leukemia (B-ALL) is a clonal malignant disease characterized by the presence of abnormally large numbers of hematopoietic B-precursor cells (blasts) within the bone marrow (BM) due to an uncontrolled proliferation and inhibition of lymphoid differentiation resulting in the

suppression of normal hematopoiesis (Huang et al., 2020; Terwilliger & Abdul-Hay, 2017; Vilchis-Ordoñez et al., 2015).

The etiology of B-ALL is not well understood. A minority of cases can be associated with genetic syndromes such as Down syndrome and Fanconi anemia (Paul et al., 2016; Terwilliger & Abdul-Hay, 2017). Viral infections can alter DNA methylation patterns in genes associated with cell proliferation leading to progression of ALL (Rahmani et al., 2018). Additional predisposing factors comprise exposure to ionizing radiation, pesticides, and certain solvents (Paul et al., 2016; Terwilliger & Abdul-Hay, 2017, causing cytotoxicity and DNA damage in the BM (Mansell et al., 2019).

The fetal environment is also thought to play a vital role in the development of pediatric ALL, with the hypothesis that as cells proliferate during fetal development, random alterations can occur creating a preleukemic clone (M. Greaves, 2018; Paul et al., 2016). In some cases, the postnatal acquisition of secondary genetic changes drives conversion to leukemia. In the majority of cases, B-ALL appears as a *de novo* malignancy in previously healthy individuals, involving a variety of genetic alterations: chromosome abnormalities, such as hyperdiploidy or translocations, point mutations and deletions (Cobaleda & Sánchez-García, 2009; Greaves & Wiemels, 2003; Terwilliger & Abdul-Hay, 2017). These oncogenic conversions may interfere with the networks controlling B-cell differentiation. For example, B-cell blasts might lose their capacity to respond to external signals that regulate differentiation; could acquire the capacity for unlimited self-renewal; or may activate molecular pathways that mimic a particular stage of its normal differentiation (Cobaleda & Sánchez-García, 2009; Pui et al., 2008).

2.2.1 B-ALL clinical features and diagnosis

Most of the clinical manifestations of B-ALL reflect the accumulation of malignant, poorly differentiated lymphoid cells within the bone marrow, peripheral blood, and extramedullary sites. Patients can present a range of

ailments such as fever, weight loss, infections, easy bruising, bleeding, and fatigue due to cytopenia. Also, patients may exhibit leukemic cell infiltration in the central nervous system (CNS), testis, lungs, and spleen, among other organs (Loghavi et al., 2015; Paul et al., 2016; Terwilliger & Abdul-Hay, 2017). Diagnosis is performed by determining the presence of 20% or more B lymphoblasts in the peripheral blood or bone marrow. B lymphoblasts are larger than normal lymphocytes and bestow higher nuclear to cytoplasmic ratio with irregular nuclear contour (Rose et al., 2020). Evaluation of cell morphology, cytogenetics, flow cytometry immunophenotyping, age, and white blood cell (WBC) count is effective for confirming the first diagnosis and classify the risk (Paul et al., 2016; Terwilliger & Abdul-Hay, 2017; Vrooman et al., 2018). Cytogenetics represent an important step, where FISH (Fluorescence in situ Hybridization) karyotyping can be helpful in the identification of recurrent translocations (Chiaretti et al., 2014). Immunophenotyping by flow cytometry analysis is the diagnostic gold standard, with the most important surface markers for diagnosis of B-ALL being CD19, CD20, CD22, CD24, CD34 and CD79a (Kulis et al., 2022). The earliest B-lineage markers are CD19, CD22 (membrane and cytoplasm) and CD79a. A positive reaction for any two of these three markers is indicative of pro-B ALL. Further presence of cytoplasmic heavy μ chain identifies the pre-B group, while the existence of surface immunoglobulin light chains defines mature B-ALL (Chiaretti et al., 2014).

2.2.2 Treatment of B-ALL

After identifying the features mentioned above, intensity of treatment relies on risk stratification. Children of age between 1 and 10 years old is a standard risk feature, with more aggressive disease seen in infants of age less than 1 year and those older than 10 years stratified as high risk, as well as those patients with WBC greater than 50,000/mL (Cooper & Brown, 2015). The treatment of B-ALL typically consists of chemotherapy that lasts approximately 3 years involving a multidrug regimen with different phases: induction, consolidation,

and maintenance (Figure 1), with CNS prophylaxis (intrathecal chemotherapy and/or cranial irradiation) given at intervals throughout therapy (Bhojwani & Pui, 2013; Frishman-Levy et al., 2015; Paul et al., 2016; Terwilliger & Abdul-Hay, 2017). The goal of the induction phase is to achieve complete remission and to restore normal hematopoiesis, where drugs like vincristine, anthracyclines such as daunorubicin or doxorubicin and corticosteroids (e.g. prednisone or dexamethasone) are administered (Huang et al., 2020). Then, consolidation treatment with similar drugs but modified schedule and higher doses is applied to eradicate drug-resistant residual leukemic cells and prevent leukemic regrowth, thus reducing the risk of relapse (Jabbour et al., 2005). Finally, the maintenance therapy is administered for a period of 2 to 3 years to prevent relapse and prolong remission, consisting of daily 6-mercaptopurine, weekly methotrexate, and monthly vincristine and prednisone (Paul et al., 2016; Pui & Howard, 2008; Rudin et al., 2017).

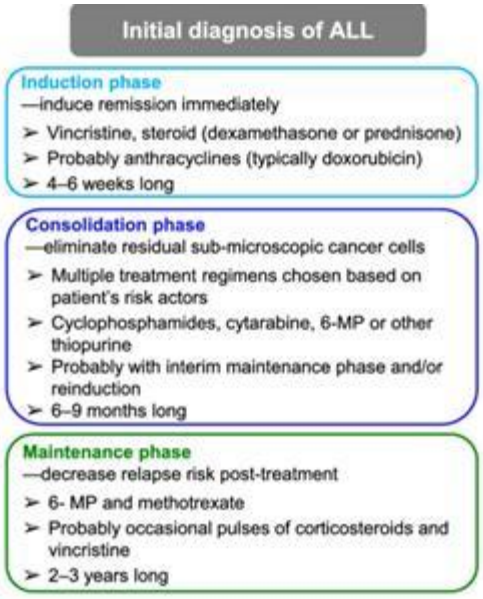

Figure 1. Treatment phases of pediatric B-ALL.

Immediately post-diagnosis, the induction phase of ALL treatment starts with a multi-drug regimen to eliminate leukemic cells and induce remission. Once complete remission is accomplished, the therapies used are intensified to prevent relapse and eliminate any residual cancer cell (consolidation phase). Last is the maintenance phase focused on antimetabolite therapy to reduce the risk of relapse. 6-MP, 6-mercaptopurine. (Modified from Rudin et al., 2017).

2.2.3 Leukemic relapse

Even though the majority of B-ALL patients complete remission, about 15-20% suffer relapse, with an overall survival of less than 10% (Terwilliger & Abdul-Hay, 2017). Most of relapses occur during treatment or within the first 2 years after treatment but can also emerge 10 years after diagnosis (Gaynon, 2005).

Standard regimens for relapsed B-ALL patients are mostly based on different combinations of the same drugs used in frontline therapy in various doses and schedules (Locatelli et al., 2012). However, leukemic blasts at relapse are more drug resistant than blasts at initial diagnosis. Thus, developing new treatment strategies is a priority (Locatelli et al., 2012).

Overall survival is influenced by the site of relapse and duration of first complete remission. Most of the relapses occur in the BM, in an isolated form or combined with involvement of CNS or testes. The best prognosis is seen in isolated extramedullary relapses, whereas in isolated BM relapses the worst outcomes are observed. Patients with combined bone marrow and extramedullary relapse have an intermediate prognosis (Nguyen et al., 2008; Bailey, Lange, Rheingold, & Bunin, 2008). Relapse isolated in the CNS is much less frequent (Locatelli et al., 2012). Leukemic blasts may enter the CNS from the BM of the skull into the subarachnoid space via the bridging veins or the cerebrospinal fluid (CSF) via the choroid plexus, invade cerebral parenchyma via brain capillaries, or infiltrate the leptomeninges via bony lesions of the skull (Pui & Jeha, 2007) .

By studying genome wide DNA-copy-number alterations in 61 B-ALL patients, the cells responsible for relapse were identified as ancestral to the primary leukemia cells; and the relapse clones were usually present as minor subpopulations at first diagnosis that expanded during treatment and became more aggressive (Bhojwani & Pui, 2013; Mullighan et al., 2008). Minimal residual disease (MRD) is the existence of post-therapeutic (chemotherapy, immunotherapy, or radiotherapy) leukemia cells within the BM, therefore, the

detection of MRD through polymerase chain reaction (PCR), flow cytometry, or next-generation sequencing (NGS) is critical to define the risk of leukemia relapse, (Kruse et al., 2020).

Moreover, a subpopulation presenting the characteristics of dormancy, drug resistance and leukemia-initiating properties has been identified (Ebinger et al., 2016). Upon removal of this population from their *in vivo* microenvironment, it lost dormancy and drug resistance, suggesting a reversible nature and a critical role for the interaction between B-ALL cells and the protective niche in the bone marrow for their expansion and survival (Dobson et al., 2020; Ebinger et al., 2016; Pramanik et al., 2013).

2.3 The BM microenvironment can favor leukemia progression

The BM is a vascularized, innervated, and complex organ within the bone where hematopoiesis occurs. It hosts a network of hematopoietic and non-hematopoietic cells, including mesenchymal stromal cells (MSC), osteoblasts, fibroblasts, adipocytes, and endothelial cells. These cells control hematopoietic processes through the secretion of extracellular matrix molecules, cytokines, chemokines, hormones, and growth factors (Congrains et al., 2021; Dander et al., 2021; Man et al., 2021).

At least three distinct BM niches have been described to date: endosteal, arteriolar, and sinusoidal. Each niche possesses distinct characteristics, cell types, and oxygen tension (Congrains et al., 2021; Dander et al., 2021).

The endosteal niche is formed by osteoblasts within a hypoxic zone in the endosteum (inner surface of the bone), and it negatively regulates proliferation of HSC through osteopontin secretion. Osteoblasts also produce CXCL12, which is involved in HSC retention and maintenance (Congrains et al., 2021; Dander et al., 2021; L. Ding & Morrison, 2013). Signaling pathways induced by the niche, such as Wnt, Notch and CXCL12/CXCR4 regulate cell cycling activity and self-renewal (Chiarini et al., 2016a; Purizaca et al., 2012).

Arteriolar niches are composed of different cell populations: stromal cells, endothelial cells, sympathetic nerves, and non-myelinating Schwann cells.

CXCL12-abundant reticular (CAR) perivascular stromal cells, an MSC subpopulation, have been recognized as important regulators of HSC maintenance and differentiation (Dander et al., 2021; Sugiyama et al., 2006). The sinusoidal niche contains a network of blood vessels called vascular sinuses with sinusoidal endothelial cells that promote HSC cell cycle activation through expression of stimulatory factors (e.g. FGF2, IGFBP2, DLL1, DHH30 and BMP4) (Itkin et al., 2016; Kobayashi et al., 2010). Expression of adhesion molecules such as E-selectin, P-selectin, VCAM-1, ICAM-1, PECAM-1, and vascular endothelial (VE)-cadherin by endothelial cells regulate homing and trafficking of lymphocytes (Doan & Chute, 2012; Smith & Calvi, 2013; Suárez-Álvarez et al., 2012) as described in more detail below.

The BM microenvironment plays an important role in the regulation of leukemia progression, survival, and chemotherapy response. Leukemic cells disrupt and destroy HSC-supportive microenvironments, reprogramming the equilibrium from a state that supports steady-state hematopoiesis to one favoring proliferation (Duarte et al., 2018; Sánchez-Aguilera & Méndez-Ferrer, 2017; Yamaguchi et al., 2021).

Oncogenes can activate inflammation-related gene cascades, thus contributing to a tumor-promoting microenvironment (Mantovani et al., 2019). B-ALL cells produce proinflammatory cytokines including TNFα, IL-1β, IL-12, and GM-CSF supporting the idea that cancer cells bestow a pro-inflammatory microenvironment within the BM. This pro-inflammatory state is mediated by hyperactivation of the NFκB and STAT3 pathways, maintaining the consecutive secretion of proinflammatory cytokines (Balandrán et al., 2017; Vilchis-Ordoñez et al., 2015). Furthermore, MSC isolated from the BM of B-ALL patients have increased nuclear translocation of the NF-κB transcription factor and consequently increased production of inflammatory intermediaries such as IL-1α, IL-6, IL-12p70 and TNF-α (Figure 2) (Balandrán et al., 2017).

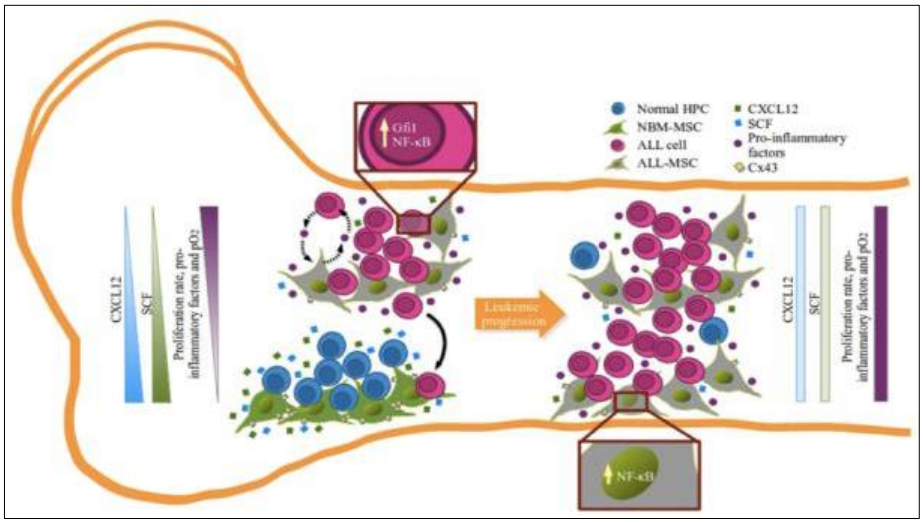

Figure 2. Leukemic B cells modify the bone marrow microenvironment.

Normal lymphopoiesis is supported by mesenchymal stromal cells (MSC), which produce high levels of CXCL12. However, during leukemogenesis, leukemic B cells hijack the microenvironment by reducing CXCL12 levels and increasing pro-inflammatory cytokines leading to leukemic cell proliferation and disruption of the balance of normal lymphopoiesis (Balandrán et al., 2017).

Indeed, direct leukemia-MSC contact via VCAM-1/VLA-4 interactions enhance leukemia survival by activating NF-kB signaling within the leukemic BM niche, suggesting a reciprocal NF-κB activation essential for promoting chemoresistance (Jacamo et al., 2014; Ma et al., 2020). Additionally, transcriptional profiles of MSC derived from primary patient samples showed two characteristics: a CXCL11-high immune-suppressive and leukemia-initiating cell (LIC)-like niche where LICs are maintained; and a CXCL12-low inflammatory and leukemia expansion (ILE)-like niche supporting leukemic burden (Balandrán et al., 2021).

Different studies on BM samples of pediatric B-ALL patients at disease diagnosis have demonstrated a dramatic decrease in CXCL12, which plays a crucial role in maintaining the hematopoietic stem cells pool. Loss of CXCL12 disrupts the CXCL12/CXCR4 axis, thus triggering the release of lymphatic

leukemic cells from the BM into blood circulation (Balandrán et al., 2017; van den Berk et al., 2014).

2.4 The CXCL12/CXCR4 axis regulates B-ALL cell migration

Chemokines are small 8-12 kDa proteins that bind to their corresponding G-protein-coupled receptors and regulate various cellular processes, such as formation of tissues, recruitment of immune cells, migration, invasion, and inflammatory microenvironment of tumors (Mousavi, 2020; Zhao et al., 2022). CXCL12 is a homeostatic chemokine that is also known as stromal cell-derived factor-1 (SDF-1). There are three isoforms of CXCL12: α, β, and γ. However, most studies focus on CXCL12-α, which possesses the highest binding affinity for the CXCL12 receptor CXCR4, followed by the β and γ isoforms (Laguri et al., 2007; Zhao et al., 2022).

CXCL12 is a chemokine constitutively expressed in many organs such as liver, brain, pituitary gland, kidney, lymph nodes (LN), colon, heart, and BM, but it is rapidly degraded in the blood. Many cell types produce CXCL12, including osteoblasts, endothelial cells and stromal cells within the BM as well as epithelial cells in extramedullary tissues. CXCL12 expression controls hematopoietic cell trafficking and adhesion during immune surveillance and development (Cojoc et al., 2013; Crazzolara et al., 2001; Mousavi, 2020).

Both CXCR4 and CXCR7 bind CXCL12 with high affinity. The expression of CXCR4 is highest in hematopoietic cells (normal $CD34^{+}$-hematopoietic progenitors, megakaryocytes, dendritic cells, monocytes, and B and T lymphocytes), but it is also widely present in endothelial stem cells, liver oval stem cells, neural stem cells, skeletal muscle satellite cells, primordial germ cells and embryonic stem cells (Cojoc et al., 2013; Zhao et al., 2022; Zhou et al., 2017). These cell populations not only have functional CXCR4 on their surface, but can also follow a CXCL12 gradient (Cojoc et al., 2013).

After binding CXCL12, CXCR4 activates several downstream signaling

pathways including Janus kinase/signal transducer and activator of transcription (JAK/STAT), Src kinase, p38 mitogen-activated protein kinase (p38MAPK), MEK/ERK, phosphatidylinositol 3-kinase (PI3K)/Akt, and protein kinase C (PKC). These result in regulation of gene transcription, cell survival, proliferation, adhesion, chemotaxis, and cell migration (Figure 3) (Chatterjee et al., 2014; Cheng et al., 2017; Shi et al., 2020).

The CXCL12/CXCR4 axis is involved in the development and maintenance of healthy tissues and organs; however, it also plays a critical role in hematopoietic disorders such as B-ALL (Chiarini et al., 2016). B leukemic lymphoblasts and related cell lines such as REH and Nalm6 display aberrant activation of key signaling pathways that control proliferation and the capacity to invade and spread (Chiarini et al., 2016). High expression of CXCR4 by leukemic cells and hyperactivation of the CXCL12/CXCR4 axis is involved in leukemia progression (Chiarini et al., 2016; Duarte et al., 2018; W. Shen et al., 2001; van den Berk et al., 2014). As CXCL12 is constitutively produced by different cells within the BM, a CXCL12 gradient drives the migration of circulating leukemic cells to the bone marrow during a process termed homing (Juarez et al., 2009), causing bone marrow infiltration and establishment within the BM (Chiarini et al., 2016b; Duarte et al., 2018; W. Shen et al., 2001; van den Berk et al., 2014). Moreover, CXCL12 can upregulate the expression of adhesion molecules such as very late antigen 4 (VLA-4), thus stimulating integrin-mediated adhesion of circulating cells on the vascular endothelium and promoting infiltration by leukemic blasts overexpressing CXCR4 into extramedullary tissues where CXCL12 is being secreted (Mousavi, 2020; Spiegel et al., 2008; Zhao et al., 2022).

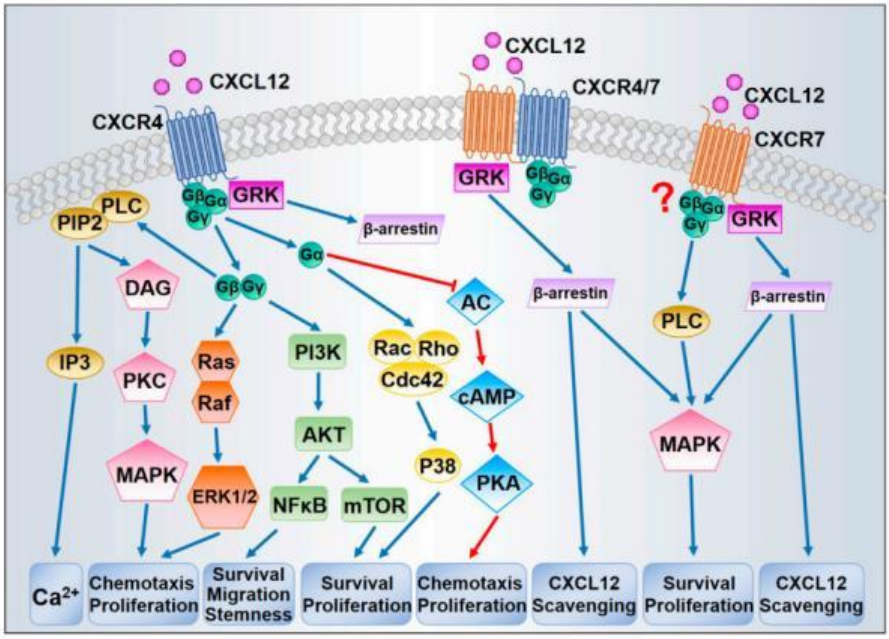

Figure 3. CXCL12/CXCR4 activates several signaling pathways.

When CXCL12 binds to CXCR4, it triggers downstream signaling through G proteins, which then activate MAPK, ERK1/2, and AKT, leading to cell survival and proliferation. Subsequently, β-arrestin recruitment causes CXCR4 internalization. CXCR7 can also induce β-arrestin recruitment, resulting in MAPK activation and CXCL12 scavenging (Shi et al., 2020).

2.5 Leukocyte homing and transendothelial migration

Migration of hematopoietic cells from the bloodstream to the bone marrow niche is known as homing, which follows similar steps of transendothelial migration of other leukocytes to sites of inflammation (Heazlewood et al., 2014).

Both homing and transendothelial migration rely on intracellular signaling and interaction between chemokines, chemokine receptors, adhesion molecules and proteases, promoting leukocyte adhesion to microvessels (Caocci et al., 2017). The sequence of adhesive interactions of leukocytes with endothelial cells is termed leukocyte extravasation cascade and involves different steps: tethering, rolling, slow rolling, firm adhesion, crawling, transmigratory cup formation on the apical endothelial surface and diapedesis (Figure 4) (Rutledge

& Muller, 2020; Schnoor et al., 2015; Vestweber, 2015).

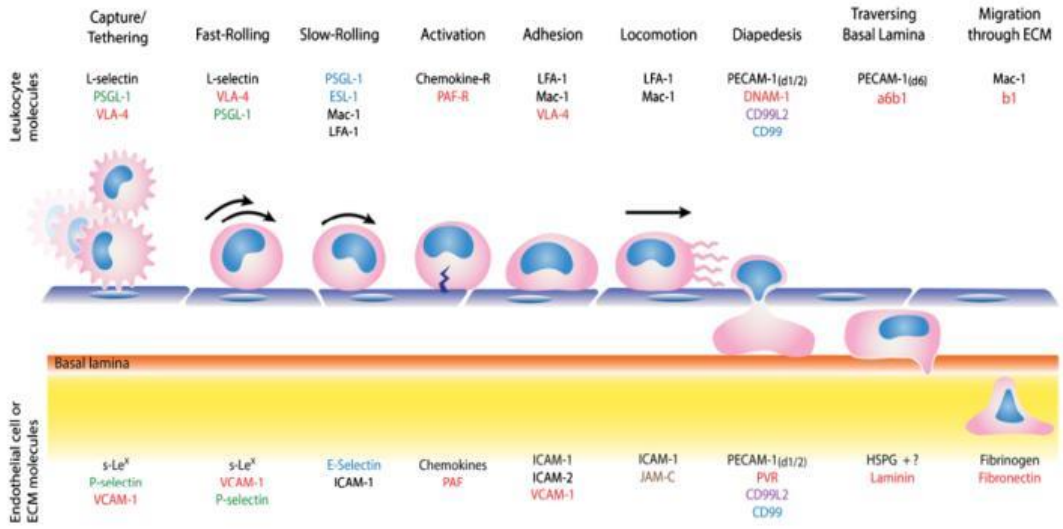

Figure 4. Leukocyte transendothelial migration cascade.

Cell adhesion receptors on activated endothelial cells mediate capture and rolling by binding to PSGL-1 and integrins on leukocytes. Transition from fast rolling to slow rolling enables leukocyte activation by recognition of chemokines and their receptors. Leukocytes adhere and crawl along the vessel wall to accomplish transmigration through the endothelial barrier. Diapedesis is mediated by sequential interactions between adhesion receptors expressed by the migrating leukocyte and the endothelium (Rutledge&Muller, 2020).

Within the BM, endothelial selectins (E- and P-selectin) as well as VCAM-1 are constitutively expressed by microvessels and are essential for cell movement (Caocci et al., 2017; Frenette et al., 1998). The interaction of leukocytes with CXCL12 is a critical chemoattractant mechanism (Heazlewood et al., 2014), which induces activation of VLA-4 ($\alpha_4\beta_1$ integrin) in leukocytes thus leading to firm adhesion (Figure 5) (Caocci et al., 2017; Mazo et al., 2011). CXCR4 triggers downstream signaling, resulting in phospholipase C (PLC) activation, increased intracellular Ca^{2+}, and activation of small GTPases such as Rap1 and Rho-A inducing actin remodeling. Leukocytes then crawl on the endothelium until they find the ideal spot for transmigration (Nitzsche et al., 2017), where they then pass through the endothelial cell cytoplasm (Sage &

Carman, 2009).

The extravasation cascade allows leukocytes to exit the blood stream into target tissues during immune surveillance and normal conditions. Likewise, leukemic cells need to transmigrate to infiltrate the BM and extramedullary organs (Gossai & Gordon, 2017; Infante & Ridley, 2013; Pramanik et al., 2013). B-ALL cells can infiltrate the central nervous system (CNS), lungs, testes, spleen, lymph nodes, liver and kidney (Crazzolara et al., 2001; Gossai & Gordon, 2017; Nies, Bodey, Thomas, Brecher, & Freireich, 1965; Spiegel et al., 2008), thus contributing to clinical manifestations of leukemia and disease progression (Chiarini et al., 2016b; Crazzolara et al., 2001).

Dynamic actin cytoskeletal remodeling in both transmigrating leukocytes and endothelial cells is required to accomplish transmigration and homing. Thus, actin-binding proteins (ABPs) such as cortactin are essential to regulate cell movements involved in these processes (Schnoor, 2015).

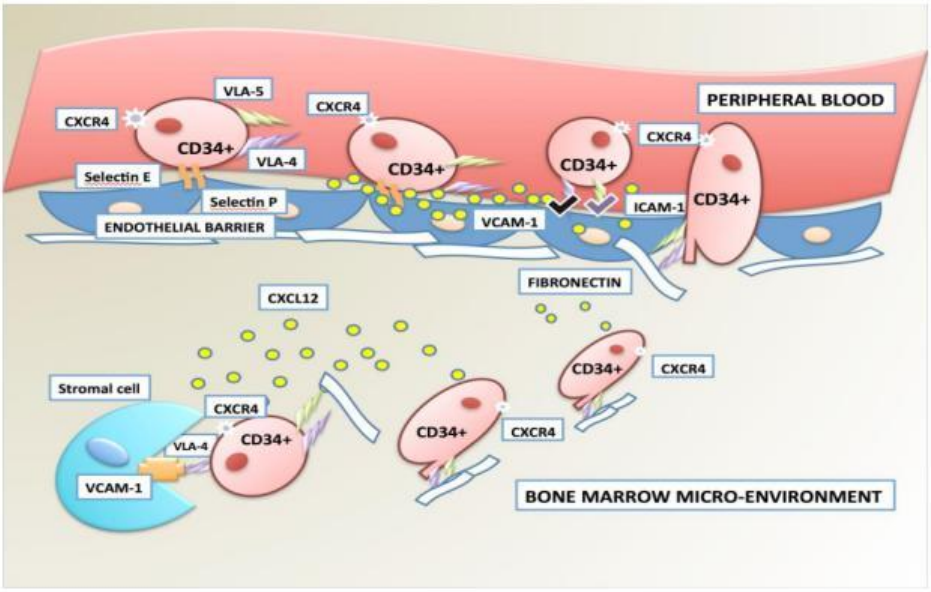

Figure 5. HSC homing into the bone marrow.

Endothelial cells in the BM microvessels express E- and P-selectin to promote slow rolling and adhesion of hematopoietic cells. Both cell types are further activated by CXCL12 binding to CXCR4. This results in stronger interaction between LFA1/ICAM-1 and VLA-4/VCAM-1 and firm arrest followed by transmigration. Molecules such as fibronectin in the extracellular matrix also favor hematopoietic cell retention in the BM. This mechanism is also exploited by B-ALL cells (Caocci et al., 2017).

2.6 Cortactin regulates migration of healthy and leukemic cells

Human cortactin is encoded by the *cttn* gene within the chromosome region 11q13 and generates a protein of 550 amino acids with several important domains (Figure 6) (Castellanos-Martínez et al., 2020; Schnoor et al., 2015; Schuuring et al., 1993; van Rossum et al., 2005). The N-terminal domain of cortactin includes an acidic region, which binds the Arp3 subunit of the Arp2/3 complex, an important nucleator of actin polymerization. Next is a 6.5 tandem repeat region responsible for F-actin binding. The C-terminal domain of cortactin regulates its activity, and consists of a helical region of unknown function, followed by a proline-serine-threonine-rich region (PST) and a Src homology 3 (SH3) domain. The SH3 domain mediates interactions with different actin cytoskeleton effectors or scaffolding proteins, including zonula occludens-1 (ZO-1), neural Wiskott-Aldrich syndrome protein (N-WASP), Nck1, and dynamin (Castellanos-Martínez et al., 2020; Cosen-Binker, 2006; Schnoor et al., 2017).

Three cortactin isoforms exist with repeat regions of different sizes that affect its ability to bind to F-actin (Lua & Low, 2005). Besides the WT isoform of 80 kDa, two splice variants have been reported: SV1-cortactin, lacking the 6th repeat (exon 11), and SV2-cortactin, lacking the 5th and 6th repeats (exon 10 and 11), generating proteins of 70 kDa and 60 kDa, respectively (Castellanos-Martínez et al., 2020; Schnoor et al., 2017; van Rossum et al., 2005).

Cortactin is an ABP colocalizing with actin-rich structures in the cell cortex and a linker between signal transduction and cytoskeletal organization (Cosen-Binker, 2006; Schnoor et al., 2017). Cortactin accumulates in lamellipodia at the leading edge of migrating cells, and in invadopodia where it triggers the secretion of extracellular matrix (ECM)-degrading proteinases essential for tumor cell invasion (Yin, Ma, & An, 2017).

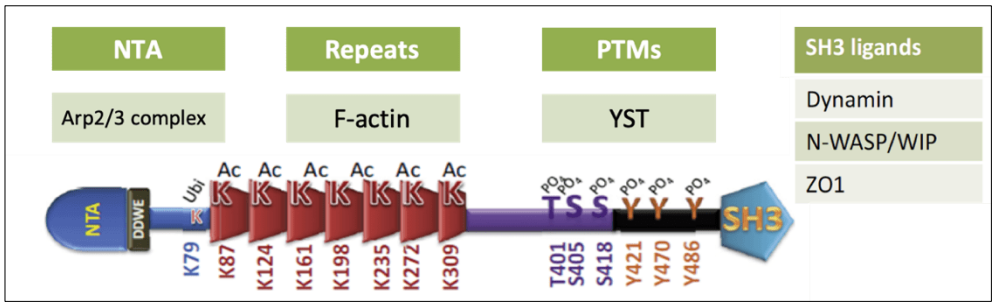

Figure 6. Cortactin protein domains.

Cortactin possesses an acidic region at the N-terminal domain (NTA), which interacts with the Arp3 subunit of the Arp2/3 complex. This is followed by a tandem repeat region prone to acetylation, where the 4th repeat is essential for F-actin binding. At the C-terminus, the proline-rich domain contains phosphorylation sites for several kinases. The SH3 domain mediates binding to many other cytoskeletal effector proteins (Modified from Schnoor, Stradal, & Rottner, 2017).

Cortactin is known to drive cancer progression. Overexpression of cortactin has been associated with invasive cancers, including melanoma, breast cancer, colorectal cancer, glioblastoma, and leukemia, making cortactin an important biomarker in different cancers (Gattazzo et al., 2014; MacGrath & Koleske, 2012; Schnoor et al., 2017; Velázquez-Avila et al., 2018; Yin et al., 2017).

In B cells derived from patients with chronic lymphoblastic leukemia (CLL), cortactin is overexpressed. Most of the patients overexpressed the wild-type isoform of cortactin of 80 kDa, which is absent in normal B-cells (Gattazzo et al., 2014). Cortactin overexpression also correlates with markers of poor prognosis, including ZAP-70 and MMP-9. Moreover, depletion of cortactin in CLL B cells reduced MMP-9 secretion, as well as the migratory capacity of the cells (Martini et al., 2017).

Recently, our group identified the expression of the 60 kDa isoform of cortactin (SV2) in the pre-B ALL cell line REH. Importantly, leukemic B cells from patients with relapse to bone marrow showed a positive correlation with high cortactin levels.

In REH cells, high cortactin levels correlated with CXCL12-dependent transendothelial migration, colonization of bone marrow organoids and organ infiltration in a mouse xenotransplantation model. Furthermore, cortactin-

depletion reduced organ invasion, strongly suggesting that cortactin drives the aggressiveness of leukemic B cells and enables them to infiltrate peripheral organs (Velázquez-Avila et al., 2018).

However, cortactin needs to be activated by post-translational modifications (PTM) to accomplish these functions efficiently.

2.6.1 Cortactin is activated by PTMs

In response to signaling pathways such as integrin- and cadherin-adhesion receptors as well as growth factor receptors, cortactin gets phosphorylated by the Src family kinases Fer, Fyn, Syk and Src, by the tyrosine kinases Abl and Arg, and serine/threonine kinases such as ERK, p21 activated kinase 1 (PAK1) and protein kinase D (PKD) (Figure 7) (Castellanos-Martínez et al., 2020; Kirkbride et al., 2011; MacGrath & Koleske, 2012; Schnoor et al., 2017).

Cortactin was first identified as a substrate of Src kinase with phosphorylation sites at tyrosines 421, 466, and 482 in mice (470 and 486 in humans) within the proline-rich domain. These phosphorylations induce activation of cortactin leading to extensive actin polymerization and cell migration (Huang et al., 1998; MacGrath & Koleske, 2012; Martinez-Quiles et al., 2004; Yin et al., 2017).

High levels of cortactin phosphorylation have been strongly associated with enhanced cell migration and cancer invasion, thus inhibition of kinases targeting cortactin has resulted in impairment of these processes (Castellanos-Martínez et al., 2020; Gattazzo et al., 2014; Hasan et al., 2019; Lua & Low, 2005).

Besides phosphorylation, cortactin activity can be regulated through acetylation by the histone acetyltransferases PCAF and p300, and deacetylation by histone deacetylase 6 (HDAC6) and sirtuin-1 (SIRT1) (Castellanos-Martínez et al., 2020; Schnoor et al., 2017; Zhang et al., 2007; Zhang et al., 2009). Acetylation sites of cortactin are within the tandem repeat region, which is essential for binding to F-actin. Acetylation of lysine residues neutralizes the charge of the protein, causing a reduction of the affinity of

cortactin for F-actin and a decrease in cell migration. HDAC6 overexpression leads to hypoacetylation of cortactin, potentiating cell migration capacity. Thus, cell migration is influenced by a HDAC6-dependent pathway (Kaluza et al., 2011; Luxton & Gundersen, 2007; MacGrath & Koleske, 2012; Nakane et al., 2012).

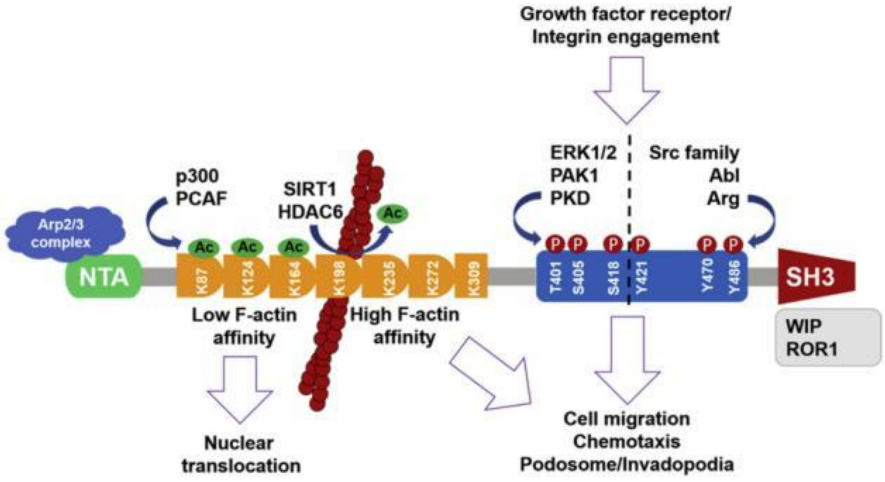

Figure 7. Post-translational modifications of cortactin and related functions.

Cortactin activity can be regulated by phosphorylation within the C-terminus, which enhances cell migration. In the tandem repeat region, several lysines can be modified by reversible acetylation, influencing cortactin affinity for F-actin and thus cell migration (Modified from Castellanos-Martínez et al., 2020).

2.7 HDAC6 participates in several cellular processes

To date, 18 mammalian histone deacetylases have been identified and categorized into four classes. Class I (HDAC1, HDAC2, HDAC3, and HDAC8), class II (HDAC4, HDAC5, HDAC6, HDAC7, HDAC9, and HDAC10) and class IV (HDAC11) are Zinc-dependent amidohydrolases and localized in both the nucleus and the cytoplasm of the cell. Class III HDACs (SIRT1–7) belong to the sirtuin family (homologous to the yeast Sir2 (Silent information regulator 2) family of proteins), which are NAD+-dependent enzymes localized in the nucleus (Glozak & Seto, 2007; Haberland et al., 2011; Park & Kim, 2020).

HDAC6 is the largest protein of the HDAC family containing 1215 amino acids. It harbors two homologous catalytic domains and a SE14 motif required for its cytoplasmic anchorage. HDAC6 also possesses an ubiquitin-binding zinc finger domain (ZnF-UBP domain) in the C-terminal region, which regulates ubiquitination-mediated degradation (Hard et al., 2010). Additionally, HDAC6 has a nuclear export sequence (NES) favoring its cytoplasmic localization (Figure 8) (Li et al., 2018; Milazzo et al., 2020; Safa, 2017). HDAC6 can also be found at the perinuclear region and at the leading-edge within migrating cells. HDAC6 associates with microtubules and localizes with $p150^{glued}$, a protein found in the dynein–dynactin microtubule motor complex, suggesting that HDAC6 may control microtubule-motor based cargo transport (Hubbert et al., 2002; Sakamoto & Aldana-Masangkay, 2011). Both catalytic domains of HDAC6 are needed for the overall activity of the enzyme. Catalytic domain 1 (CD1) preferentially deacetylates C- terminal acetyl-lysine substrates and CD2 exerts its activity on any acetyl-lysine (Hai & Christianson, 2016). The spatial arrangement of the two CD domains in HDAC6 is important for an efficient deacetylation reaction, as a significant loss of activity was found when inserting or deleting aminoacids in the linker region (Zhang et al., 2006).

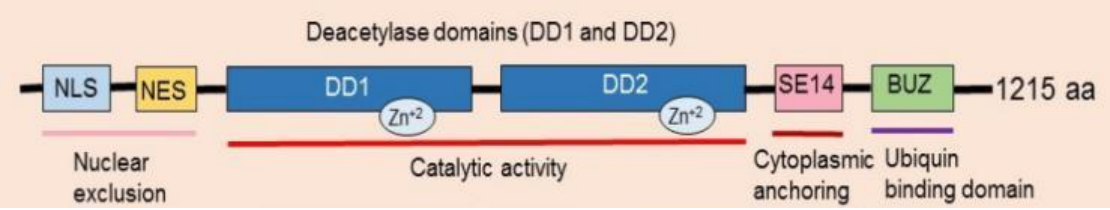

Figure 8. Structure of HDAC6.

HDAC6 possesses two deacetylase domains (DD) and a nuclear exclusion signal (NES) that favors its cytoplasmic localization improved by the SE14 (serine-glutamate tetradecapeptide) repeats which forms a unique structure required for cytoplasmic retention. HDAC6 N-terminal nuclear localization signal region (NLS) is target of acetylation, losing its interaction with the nuclear importin-α protein resulting in cytoplasmic maintenance of HDAC6. The ubiquitin-binding zinc finger (BUZ) domain is able to bind to ubiquitin and regulates proteosome-mediated degradation (Modified from Safa A., 2017; Yiu L., 2012; Bertos N., 2004).

HDAC6 displays a variable pattern of expression in healthy tissues. Highest levels of expression are found in breast, testis and skin, and lower levels in

blood cells, muscles, and pancreas, and low to absent levels in liver, spleen, and adipose tissues (Milazzo et al., 2020).

HDAC6 regulates multiple cellular processes via its deacetylase and ubiquitin binding ZnF-UBP domains. Through its deacetylase domains HDAC6 triggers cell migration by deacetylating cortactin and α-tubulin, important regulators of dynamic organization of the cytoskeleton during migration (Hubbert et al., 2002; Sakamoto & Aldana-Masangkay, 2011; Zhang et al., 2007). HDAC6 also mediates deacetylation of the chaperone heat-shock protein 90 (HSP90), which is required for its engagement with its targets to protect them from polyubiquitination and subsequent degradation (Kovacs et al., 2005; Liu et al., 2021).

In response to cell stress, the ubiquitin-binding ZnF-UBP domain of HDAC6 is crucial. HDAC6 can bind to polyubiquitinated misfolded proteins, recruiting them as cargos to dynein motors for transport along microtubules (Kawaguchi et al., 2003). Furthermore, HDAC6 recruits a cortactin-dependent actin-remodeling machinery to mediate autophagosome–lysosome fusion and autophagic degradation, which is activated as a compensatory mechanism when the ubiquitin–proteasome system is impaired in stressed cells (Lee et al., 2010). HDAC6 is also able to regulate apoptosis through deacetylation of Ku70. When Ku70 is in a deacetylated state, it binds to Bax, a pro-apoptotic protein, thus preventing Bax-induced cell death leading to cell survival (Gong et al., 2019; Subramanian et al., 2011).

Reversible acetylation occurs in a large number of non-histone proteins in both nuclear and cytoplasmic compartments (Choudhary et al., 2009; Glozak & Seto, 2007; Hofmann et al., 2011). However, the acetylation status of the whole proteome is impaired by dysregulated deacetylases in cancer, triggering tumor initiation and progression (Li & Seto, 2016; Parbin et al., 2014).

Aberrant expression of classical HDACs (class I, II, IV) has been associated with solid and hematological malignancies. HDAC6 substrates are involved in the regulation of cell cycle, apoptosis, migration and metastasis, thus high

HDACs levels correlate with tumor aggressiveness and poor outcomes (Li et al., 2020; Li & Seto, 2016).

2.7.1 HDAC6 promotes cell migration and cancer invasion

The microtubules (MTs) are regulators of cell motility and are composed of α- and β-tubulin subunits. MTs polymerize and depolymerize at high rates enabled by reversible acetylation of α-tubulin on K40. In the cytoplasm, HDAC6 associates with MTs and localizes with the microtubule motor complex containing p150 ^{glued} (Hubbert et al., 2002). Importantly, α-tubulin was the first identified non-histone protein substrate of HDAC6. HDAC6-mediated deacetylation of α-tubulin correlates with microtubule dynamics. Depolymerized tubulin is promptly deacetylated, whereas tubulin acetylation occurs only on stable or polymerized MTs. Microtubules growth occurs at the cell leading edge and microtubule shortening at the cell body and rear. MTs growth and shortening activate the small GTPase Rac-1 and RhoA signaling, respectively, to control actin dynamics and cell motility (Hubbert et al., 2002; Sakamoto & Aldana-Masangkay, 2011; Waterman-Storer & Salmon, 1999).

Additional to its participation in MTs-dependent migration, HDAC6 can also regulate actin-dependent cell migration through deacetylation of cortactin (Li et al., 2018; Zhang et al., 2007). After stimulation with growth factors and downstream integrin signaling, cortactin translocates to the cell periphery as a result of Rac1 activation (Weed et al., 1998). HDAC6 is also enriched at the membrane, where it needs to be phosphorylated by AURKA to be activated. NEDD9, a scaffold protein, brings cortactin, AURKA, and HDAC6 into a single complex, and once deacetylated by HDAC6, cortactin increases its ability to bind to F-actin and stabilize the branching mediated by the actin-nucleating complex Arp2/3, thus promoting cell movement (Kozyreva et al., 2014; Li et al., 2018; Van Helleputte et al., 2014; Zhang et al., 2007).

Cancer is characterized by uncontrolled proliferation of abnormal cells with high migratory and invasive capabilities (Friedl & Wolf, 2003; Sakamoto & Aldana-

Masangkay, 2011). HDAC6 overexpression has been identified in many types of cancer, tumor cell lines and mouse tumor models, where it contributes to cancer metastasis (Sakamoto & Aldana-Masangkay, 2011).

In breast cancer, estrogen mediates upregulation of HDAC6, which increases cell motility through deacetylation of both cortactin and tubulin, making it a useful biomarker to determine patient prognosis (Li et al., 2018; Saji et al., 2005). HDAC6 expression levels were higher in low-grade and high-grade ovarian carcinomas compared with benign lesions and immortalized ovarian surface epithelium cell lines (Bazzaro et al., 2008). Moreover, migration assays using ovarian cancer cell lines showed that high levels of HDAC6 and hypoacetylated cortactin triggered faster migration in comparison to those cell lines that expressed lower levels of HDAC6 with hyperacetylated cortactin (Zhang et al., 2007). In pancreatic cancer tissues, both HDAC6 mRNA and protein levels were highly increased, correlating also with increased cell motility (Li et al., 2014). HDAC6 expression was also upregulated in primary oral squamous cell lines and its level of expression correlated with primary tumor stage, with higher HDAC6 expression in more advanced stages (Sakuma et al., 2006; Tavares et al., 2022). Furthermore, overexpression of HDAC6 in neuroblastoma, bladder cancer, malignant melanoma, lung cancer, multiple myeloma and lymphoma have been reported (Li et al., 2018; Sakamoto & Aldana-Masangkay, 2011).

HDACs inhibitors have been shown to be effective therapeutic anticancer agents.

Pan-HDAC inhibitors are natural or synthetical products that possess different structural characteristics, such as cyclic peptides (Romidepsin, Apicidin), benzamides (Entinostat), aliphatic acids (Butyrate) and hydroximates (SAHA, Vorinostat, Trichostatin-A) (Li et al., 2018; Tan et al., 2010). However, despite the large number of existing pan-HDAC inhibitors, few compounds are able to selectively inhibit HDAC6 (Losson et al., 2020) (Table 1).

Table 1. Pan-HDAC inhibitors.

Classification	Examples	Specificity to HDAC
1. Aliphatic fatty acids	Butyrate	Classes I and IIa
	Valproic acid	Classes I and IIa
2. Hydroxamate	SAHA (vorinostat)	Pan inhibitor
	PXD101 (belinostat)	Pan inhibitor
	LBH589 (panobinostat)	Classes I and II
	ITF2357 (givinostat)	Pan inhibitor
	4SC-201 (resminostat)	Pan inhibitor
	PCI 24781 (abexinostat)	Classes I and II
	Tubacin	Class IIb
3. Benzamides	MS-275 (entinostat)	Class I
	MGCD0103 (mocetinostat)	Class I
	CI-994 (tacedinaline)	Class I
	MGCD-0103	Classes I and IV
4. Cyclic peptides	Depsipeptide/FK228 (romidepsin)	Class I
	Apicidin	Class I
5. Mercaptoketone	KD5170	Classes I and II

(Tandon N et al., 2016)

The first synthesized HDAC6-specific inhibitor was Tubacin, which inhibits α-tubulin deacetylation (Haggarty et al., 2003) and decreases migration of bladder cancer and Burkitt's lymphoma cells (Ding et al., 2014; Zuo et al., 2012). However, the complexity of its synthesis and lipophilicity eventually prevented its use *in vivo* (Haggarty et al., 2003). Later in 2010, Tubastatin-A was designed. Tubastatin-A is a tetrahydro-γ-carboline-capped selective HDAC6 inhibitor over other HDACs, that displays a phenyl-hydroxamate as a linker zinc binding group (Shen et al., 2020). Tubastatin-A was first tested in neuron cultures and found to induce tubulin acetylation but not histones (Butler et al., 2010), and recently has been used in gliobastoma and breast cancer, where it was able to reduce tumor cell migration and invasion (Kozyreva et al., 2014; Urdiciain et al., 2019). Since HDAC6 knock-out mice are viable, it is thought that selective inhibition could minimize the toxicity of current clinical HDAC inhibitors maintaining therapeutic effectiveness (Olaoye et al., 2021).

2.8 HDAC6 in leukemia

Few studies exist on HDAC6 in the context of leukemias. Importantly, HDAC6 was consistently overexpressed in primary acute myeloid leukemia (AML) blasts from patients (Bradbury et al., 2005). Moreover, HDAC6 overexpression in AML patient cells correlated with expansion of the hematopoietic stem and progenitor cell (HSPCs) population and increased chemotaxis efficacy (Pezzotta et al., 2022). In chronic myeloid leukemia (CML), HDAC6 deacetylates HSP90α, which targets BCR-ABL. In the acetylated form, HSP90α loses its chaperone function, leading to proteosome-mediated degradation of its targets. Pan-HDAC inhibitors (hydroxamic acid analogues LAQ824 and LBH589) and HDAC6 knockdown using siRNA in K562 cells inhibited HDAC6 activity and increased HSP90α acetylation leading to the ubiquitination and degradation of BCR-ABL (Krämer et al., 2014; Losson et al., 2020).

Regarding lymphoblastic leukemia, HDAC6 has been found upregulated in B-chronic lymphoblastic leukemia (B-CLL) patient cells and cell lines compared to normal controls. HDAC6 inhibition inhibited cell proliferation and sensitized B-CLL cells to apoptosis (Maharaj et al., 2018). However, there is no report yet on the role of HDAC6 in B-ALL.

Considering all the evidence about HDAC6 playing an important role in cell migration and survival, it is critical to determine whether HDAC6 also regulates transmigration and organ invasion of B-ALL cells.

3. JUSTIFICATION

Cortactin is overexpressed in leukemic B cells and triggers transendothelial migration, extramedullary infiltration, bone marrow colonization and relapse. Acetylation of cortactin regulates its affinity for F-actin and thus cell migration. However, it remains to be explored whether this modification modulates the aggressiveness of B-ALL cells. HDAC6 regulates cortactin deacetylation, migration, and proliferation; and its hyperactivation correlates with cell survival

and migration in solid tumors. Little is known about the role of HDAC6 in B-ALL. Thus, investigating the relevance of HDAC6-mediated cortactin deacetylation and the use of a pharmacological HDAC6 inhibitor to reduce migration of leukemic cells *in vitro* and *in vivo* may unveil a potential new therapeutic target for high-risk B-ALL patients to prevent disease relapse.

4. HYPOTHESIS

HDAC6-mediated deacetylation of cortactin is a critical event in leukemic B cells to favor transendothelial migration and organ infiltration.

5. GENERAL OBJECTIVE

To investigate the relevance of HDAC6 functions in leukemic B cells and analyze the effect of HDAC6 inhibition on the migratory capacity of leukemic B cells that is controlled by cortactin.

6. PARTICULAR OBJECTIVES

1) To analyze HDAC6 levels in leukemic B cells.
2) To evaluate whether pharmacological inhibition of HDAC6 alters the migratory behavior of leukemic B cells.
3) To unravel the molecular mechanism through which HDAC6 regulates leukemic B cell migration.
4) To test whether pharmacological inhibition of HDAC6 in immunodeficient mice reduces organ infiltration of leukemic B cells.
5) To evaluate HDAC6 levels and functions in patient-derived B-ALL samples and correlate them with available clinical data.

7. MATERIAL AND METHODS

7.1 MATERIAL

7.1.1 Culture media

Table 2. List of culture medium used.

Medium	Company, Catalogue number
Dulbecco Modified Eagle's Medium (DMEM) – high glucose	Sigma. Ref D5648-10X1L
Endothelial cell medium ECM	ScienCell. Ref 1001
RPMI 1640	Sigma. Ref R4130-10X1L
Minimum Essential Medium Eagle	Sigma. Ref M4655-1L

7.1.2 Plasmids

Table 3. List of plasmids used.

Plasmids	Reference
psPAX2	Addgene #12260
pMD2.G	Addgene #12259
pLentiCRISPRv2 puro	Addgene #98290

7.1.3 Antibodies

Table 4. List of antibodies used.

Antibody	Company, catalogue number

Alexa Fluor™ 488 goat anti-mouse IgG (H+L)	Invitrogen. Ref A11001
Alexa Fluor™ 647 goat anti-mouse IgG (H+L)	Invitrogen. Ref A21236
Anti- human acetyl-cortactin	Millipore. Ref 09-881
Anti-human acetyl-tubulin (Lys40) (D20G3) XP®	Cell Signaling Technology. Ref 5335
Anti-cortactin Alexa Fluor® 488/647 conjugated, clone 289H10	Kindly provided by Dr. Klemens Rottner, TU Braunshweig, Germany
Anti-human GAPDH Antibody (0411)	Santa Cruz. Ref sc-47724
Anti-human HDAC6 (D-11) Alexa Fluor® 647 conjugated	Santa Cruz. Ref sc-28386
Anti-human HDAC6	Cell Signaling Technology. Ref 4569
Anti-human cortactin, clone 289H10	Kindly provided by Dr. Klemens Rottner, TU Braunshweig, Germany
Anti-γ Tubulin Monoclonal Antibody (4D11)	ThermoFisher. Ref MA1-850
APC anti-human CD184 (CXCR4)	Biolegend. Ref 306510
APC anti-human CD29	Biolegend. Ref 303007
FITC anti-human CD34	Biolegend. Ref 304058
Goat anti-Mouse IgG-HRP (H+L) horse radish peroxidase conjugate	Invitrogen. Ref G21040

Human TruStain FcX™ (Fc Receptor Blocking Solution)	Biolegend. Ref 422301
Mouse anti-Rabbit igG-HRP (H+L) horse radish peroxidase conjugate	Santa Cruz. Ref sc-2357
PB-anti human CD45	Biolegend. Ref 304022
PE anti human CD19	Biolegend. Ref 302254
PE-anti mouse CD45	Biolegend. Ref 103106
PE/Cy7 anti-human CD49d	Biolegend. Ref 304313

7.1.4 Kits

Table 5. List of kits used.

Kits	**Company, catalogue number**
CellTrace™ Violet (CTV, DMSO)	Invitrogen. Ref C34557
DC™ Protein assay	Biorad. Ref 5000112
Mojo Sort™ Human CD19 Selection Kit	Biolegend. Ref 480106
MTT Cell Proliferation Assay	ATCC. Ref 30-1010K
Pacific Blue™ Annexin V Apoptosis Detection Kit with PI	Biolegend. Ref 640928
SuperSignal WestFemto	ThermoFisher. Ref 34095
Vybrant™ CFDA SE Cell Tracer Kit	Invitrogen. Ref V12883
Zombie NIR™ Fixable Viability Kit	Biolegend. Ref 423106

7.1.5 Reagents

Table 6. List of chemicals and reagents used.

Chemical	Company, catalogue number
30% Acrylamide/bis solution	Biorad. Ref 161-0153
Agarose	Cleaver Scientific Ltd #CSL-AG50
Alexa Fluor 488™ phalloidin	Invitrogen™ #A12379
Ammonium persulfate	Biorad. Ref 161-0700
Antibiotic/Antimycotic 100X	Corning. Ref 30-004-Cl
BD Pharm Lyse™	BD Biosciences #555899
Bovine Serum Albumin	Sigma. Ref A2153-100G
$CaCl_2$	J.T. Baker. Ref 1313-01
cOmplete™ protease inhibitor cocktail	Roche. Ref 11697498001
Dimethyl Sulfoxide (DMSO)	Sigma. Ref 8418-250ML
Ethanol BioUltra	Sigma. Ref 64-17-5
Ethylenediaminetetraacetic acid (EDTA)	Sigma. Ref E9884-500G
Ethyl alcohol	Sigma. Ref E703-1L
Fetal Bovine Serum	Biowest. Ref S1810
Glycerol	Sigma. Ref G6279-500ML
Glycine	J.T. Baker. Ref 4059-06
Imidazole	Sigma. Ref I2399

KCl	J.T. Baker. Ref 3040-01
$KH_2PO_4 \bullet 3H_2O$	Macron. Ref 7088-04
L-glutamine 100X	Gibco. Ref A2916801
Lymphoprep™	Stemcell. Ref 07851
MEM NEAA 100X	Gibco. Ref 11140-050
$MgSO_4 \bullet 7H_2O$	Merck. Ref A999986
$Na_2HPO_4 \bullet 7H_20$	J.T. Baker. Ref 3824-01
NaCl	J.T. Baker. Ref 3624-05
NaF	Sigma. Ref S7902
NaHCO3	Sigma. Ref S5761-1KG
Na_3VO_4	Sigma. Ref S6508
$Na_2HPO_4 \bullet 7H_20$	J.T. Baker. Ref 3824-01
Na-pyruvate 100X	Gibco. Ref 11360-070
Nitrocellulose membrane, pore 0.45 μm	Biorad. Ref 1620115
Nonidet™ P-40	Sigma. Ref 21-3277 SAJ
Paraformaldehyde	Sigma. Ref 158127-500G
Penicillin/streptomycin	Gibco
PhosSTOP phosphatase inhibitor	Roche. Ref 04-906-845-00
Polybrene® (Hexadimetrine bromide)	Sigma. Ref 107689
Ponceau S	Merck-Millipore. Ref 159270025

Puromycin	Sigma. Ref P8833
Recombinant Human SDF-1α (CXCL12)	Preprotech. Ref 300-28A
Recombinant Human VCAM-1-Fc (carrier-free)	Biolegend. Ref 553706
Rhodamine phalloidin	Invitrogen. Ref R415
Saponin	Sigma. Ref 84510-100
Skim milk	Svelty
Sodium dodecyl sulfate (SDS)	Biorad. Ref 1610302
Sodium pyruvate solution	Sigma. Ref S8636
TEMED	Biorad. Ref 161-0801
Tris•base	J.T. Baker. Ref 4109-06
Triton™ X-100	Sigma. Ref T9284-500ML
TrypLE™ Express	Gibco. Ref 12604-013
Trypsine-EDTA 0.25%	Sigma. Ref T4049-500ML
Tween 20®	Sigma. Ref P1379-500ML
Ultracomp eBeads™ Compensation Beads	Invitrogen. Ref 1943757
UltraPure DNase/RNase-Free Distilled Water	ThermoFisher. Ref 109977023
β-Mercaptoethanol	Sigma. Ref M3148-25ML

7.1.6 Buffers

Table 7. List of buffers used.

Blocking buffer	TBS-T 5% BSA or 5% milk
1X HBSS	8000 mg/L NaCl 400 mg/L KCl 40 mg/L Na_2HPO_4 60 mg/L KH_2PO_4 350 mg/L $NaHCO_3$ 1000 mg/L D-glucose pH 7.4
2X HBSS	16000 mg/L NaCl 800 mg/L KCl 80 mg/L Na_2HPO_4 120 mg/L KH_2PO_4 700 mg/L $NaHCO_3$ 2000 mg/L D-glucose 50 mM HEPES pH 7.4
HBSS $Ca^{++}Mg^{++}$	HBSS 1X 140 mg/L $CaCl_2$ 120 mg/L $MgSO_4$
5X Laemmli buffer	0.1875 M Tris-HCl pH 6.8 45% glycerol 2.5% SDS 1.78 M β-mercaptoethanol 0.00125% bromophenol blue
1X Mojo Sort isolation buffer	1X PBS 0.5% BSA 2 mM EDTA

	pH 7.2
1X PBS	138 mM NaCl 3 mM KCl 8.1 mM Na_2HPO_4 1.5 mM KH_2PO_4 pH 7.4
1X PBS-EDTA	1X PBS 5 mM EDTA
SDS lysis buffer	25 mM HEPES pH 7.5 2 mM EDTA 25 mM NaF 1 % SDS 1X Complete protease inhibitor cocktail
SDS-PAGE buffer	25 mM Tris 192 mM Glycine 0.1% SDS pH 8.3
1X TBS buffer	150 mM NaCl 10 mM Tris pH 8.0
TBS-T	TBS 1X 0.1% Tween20®
Transfer buffer	20% Methanol 25 mM Tris 192 mM Glycine 0.1% SDS pH 8.3

7.2 METHODS

7.2.1 Isolation of CD19^{+} B cells from human peripheral blood

Buffy coats from healthy donors were collected from the blood bank of Hospital Juarez (Mexico City, Mexico). The blood collection procedure was done according to international and institutional guidelines. Mononuclear cells (MNC) were isolated from the buffy coats by gradient centrifugation using Lymphoprep™. The buffy coats were mixed with sterile 1X PBS at a 3:1 ratio, then 35 mL of cell suspension was added on top of 15 mL of Lymphoprep™ in a 50 mL falcon tube. Cells were centrifuged at 700xg for 30 min at room temperature (RT). Then, the MNC layer was recovered from the interphase, washed with sterile 1X PBS and 10^{7} MNC resuspended in ice-cold 1X Mojo Sort™ isolation buffer were placed in a 5 mL (12x75 mm) polypropylene tube. to purify human B cells. Human CD19^{+} B cells were purified using the Mojo Sort™ Human CD19 Selection kit (Biolegend). 10 µL of the biotin anti-human CD19 antibody (clone SJ25C1) were added and incubated on ice for 15 min. Then, the Streptavidin Nanobeads were resuspend by vortexing and 10µL were added to the cells and incubated on ice for 15 min. 2.5 mL of Mojo Sort™ isolation buffer were added and the tube was placed in the magnet for 5 min. The unbound fraction was poured, and the cells bound to the walls of the tube were resuspended in 1 mL Mojo Sort™ Buffer. The Ethics, Research, and Biosafety Committees at Hospital Juarez (HJM-DIE-002- MA) approved all the procedures. All the samples were obtained after written informed consent from the donors.

7.2.2 B-ALL patients

BM aspirates and peripheral blood (PB) samples were obtained according to international and institutional guidelines from children and adolescents younger than 18 years that were newly diagnosed with B-ALL before starting any treatment, or upon relapse. All samples were collected after written informed consent from parents.

Patients were recruited and followed in the Hospital Infantil de Mexico “Federico Gomez” (Mexico City), the Centro de Investigación Biomédica de Oriente (CIBIOR, IMSS) (Atlixco, Mexico) and the IMIEM Hospital para el Niño (Toluca, Mexico). All procedures were approved by the Ethics, Research and Biosafety Committees of the hospitals and the bioethics committee of CINVESTAV. Clinical and laboratory data were obtained from patient records and institutional laboratory registers and correlated with our data.

Inclusion criteria

Patients younger than 18 years

Patients newly diagnosed with ALL without treatment

Patients newly diagnosed with ALL relapse

Normal control: PB $CD19^{+}$ cells from healthy consenting individuals, BM cells from patients not diagnosed with ALL

Exclusion criteria

Patients whose parents did not agree to participate

Samples stored at RT or at 4°C for more than 24 hours

Samples from patients in remission or under treatment

7. 2.3 Cell culture

The B-ALL cell line REH (pre-B leukemic cells, with the translocation 12:21 producing the *TEL/ETV6-AML1* fusion gene, from peripheral blood of a relapse case, (ATCC CRL-8286)) was cultured in RPMI 1640 (Sigma) medium supplemented with 10% FBS and 1% antibiotic/antimycotic. Primary B cells from healthy donors and B-ALL patients were cultured in the same media. The human BM stromal cell line HS-5 (ATCC CRL-11882) was cultured in DMEM (Gibco) medium supplemented with 10% FBS and 1% penicillin/streptomycin. Spheroids from these cells were maintained in the same medium. Primary MSC from B-ALL patients were cultured in DMEM medium supplemented as described above. REH cells were treated for different time points with the

HDAC6 inhibitor Tubastatin-A at 10 and 20 μM. Control cells were treated with equal volumes DMSO. After incubation, cells were washed with 1X PBS two times and used in the functional assays.

7.2.4 Generation of stable cortactin-depleted REH cells

$3.8x10^6$ HEK 293T cells were cultured in a 100 mm plate, and incubated at 37ºC, 5% CO_2 until they were at 70% confluency. Then, a mixture containing 200 µL DMEM (without FBS), 30 µL polyethyleneimine (PEI, 1 mg/mL), 3 µg psPAX2 plasmid, 1 µg pCMV-VSVG plasmid and 4 µg of cortactin pLentiCRISPRv2 plasmid (Table 2) were prepared and incubated for 15 min at RT. A mixture with the same components but the empty pLentiCRISPRv2 plasmid was used as control. HEK 293T cells were washed and 7 mL supplemented DMEM medium containing the described plasmid mixture was added. Cells were incubated for 6 hours at 37ºC, 5% CO_2. Afterwards, the medium was discarded and fresh medium added. After 48 hours, the cell culture supernatants were harvested and stored at 4ºC. 7 mL fresh supplemented DMEM medium were added to the transduced HEK 293T cells, and cultured at 37ºC, 5% CO_2. After 24 hours, cell culture supernatants were again harvested and mixed with the supernatant from the day before. Supernatants were centrifuged at 13,000 rpm for 2 hours at 4ºC to pellet the virus. The viral pellet was resuspended in 1 mL of RPMI medium supplemented with 10% FBS and 1% antibiotic/antimycotic.

Table 8. Sequences of sgRNA for the generation of stable cortactin knock-down cells.

Human	
CTTN#1	ATGACGCGGGGGCCGATGAC
CTTN#2	ATCGGCCCCCGCGTCATCCT
CTTN#4	GTCCATCGCCCAGGATGACG

After resuspending the viral pellet, 1 mL of the suspension was added to $5x10^5$ REH cells in 1 mL of RPMI medium supplemented with 10% FBS and 1% antibiotic/antimycotic with a final concentration of 8 µg/mL Polybrene® (hexadimethrine bromide) to increase transduction efficiency. Additionally, cells without the viral suspension were considered as a negative control for transduction. After 48 hours, the medium was changed to RPMI medium supplemented with 10% FBS and 1% antibiotic/antimycotic medium containing 2 µg/mL puromycin to eliminate non-transduced cells and incubated at 37°C, 5% CO_2. Cells were maintained in selection medium until all negative control cells died.

7.2.5 Isolation and propagation of HUVEC

To isolate human umbilical vein endothelial cells (HUVEC), umbilical cords of at least 25 cm were washed with water to remove excess of blood. Under sterile conditions, in the upper end of the cord vein a canule with a syringe containing 20 mL 1X PBS and 1% antibiotic solution was inserted and all content flushed. The syringe was removed, and ends were sealed with hemostatic clamps. 10 mL 0.25% trypsin-EDTA were added into the vein using a syringe and the cord was incubated at 37°C for 10 min in a water bath. The cord was massaged to facilitate the digestive process. Then, the clamp of the lower end was removed, and the content was recovered into a falcon tube and centrifuged at 1,500 rpm for 5 min. The cell pellet was resuspended in ECM medium (ScienCell) and plated in a 60 mm cell bind dish. To propagate and maintain HUVEC, the medium was aspirated, and cells were washed with 1X PBS three times. Then 1 mL of 0.25% trypsin-EDTA was added, and cells were incubated at 37°C for 5 min. 3 mL of serum-containing medium was added for trypsin inactivation, and the cell suspension was plated.

7. 2.6 Immunofluorescence microscopy

REH cells resuspended in 100 µL RPMI medium supplemented with 10% FBS and 1% antibiotic/antimycotic were placed on top of poly-L-Lysine coated slides

to allow adherence. After 15 min, the cells were fixed using 4% paraformaldehyde (PFA) at RT for 10 min and washed with 1X PBS three times. Cells were permeabilized with 0.1% Triton X-100 for 10 min at 4°C. Samples were blocked with 3% BSA in 1X PBS. Then, primary antibodies for HDAC6 and cortactin were incubated at 4°C overnight. Samples were washed three times with 1X PBS for 5 min. Cells were incubated with a species-specific secondary antibody coupled to Alexa-488 or Alexa-647 for 1 hour at RT in the dark. Samples were washed once with 1X PBS in the dark. Next, the cover slips were mounted using ProLong GOLD (Thermo Fisher Scientific) containing 0.5 µg/mL DAPI to stain nuclei. Cells were analyzed using a Leica SPE-8 confocal microscope.

7. 2.7 Western blotting

Cells were lysed in SDS buffer (25mM HEPES pH7.5, 150mM NaCl, 10mM $MgCl_2$, 1mM EDTA, 1% NP-40, 2% glycerol and complete protease inhibitor cocktail). Equal protein amounts were separated by 8% or 10% SDS-PAGE, transferred to nitrocellulose membranes (pore 0.45µm, Biorad) and blocked with either 5% skim milk or 5% BSA in TBS (150 mM NaCl,10 mM Tris, pH 8) with 0.1% Tween20. Membranes were incubated with primary anti-acetyl-cortactin (1:2000), anti-acetyl-tubulin (1:2000), anti-cortactin 289H10 (1:2000), anti-HDAC6 (1:4000) or anti-γ tubulin (1:4000, loading control) at 4°C overnight. Then, membranes were washed three times with TBS containing 0.1% Tween20 and incubated with species-specific peroxidase-conjugated secondary antibody (1:10,000 Santa Cruz) for 1 h at RT. The membranes were washed three times with TBS-T and developed using SuperSignal West Pico or Femto Chemiluminescent substrates (Thermo Scientific). Chemiluminescence signals were recorded using a Chemidoc imaging system (Bio Rad).

7. 2.8 Cell viability assay

REH cells were seeded at $3x10^4$ cells/well in a 96-well plate. Cells were treated with different concentrations of Tubastatin-A (50, 100 and 150 µM). Tubastatin-A was dissolved in DMSO and diluted to the final concentrations in RPMI medium. Control cells were treated with DMSO only. Following culture for 24 h with Tubastatin-A, 10 µL/well MTT solution (3-(4,5-dimethylthiazol-2-yl)-2,5-diphenyltetrazolium bromide) (5 mg/mL) was added and incubated for 4 h at 37°C. Subsequently, to solubilize crystals 100 µL of acidic propanol (50 mL of Triton X-100, 4 mL of HCl, 446 mL of isopropanol) was added to each well and stirred continuously at room temperature and darkness for 3 h. The absorbance of plates was determined at 560 nm using a spectrophotometer (Infinite F500 TECAN). The dose-response curve was used to calculate the concentration of the inhibitor resulting in 50% inhibition of cell viability (IC_{50}).

7. 2.9 Chemotaxis assay

$2.5x10^5$ patient-derived cells isolated from BM or PB were added in the top chamber of a Transwell filter (5 µm pore size) and 600 µL of complete medium containing 100 ng/mL of CXCL12 as chemoattractant was added to the bottom well. Cells were incubated for 4 h at 37°C to allow for chemotaxis. Subsequently, migrated cells were recovered from the bottom wells, and counted in a Neubauer chamber using trypan blue. Samples were analyzed in duplicates or triplicates depending on the number of viable cells.

7. 2.10 Filter-based transendothelial migration assay

$8x10^4$ HUVEC were grown to confluence on 5 µm pore transwell filters (Corning) pretreated with gelatin (Gibco, Thermo Scientific) for 30 min at 37°C. As a control to monitor monolayer formation, HUVEC were seeded in 96 well plates at the same density. Once the monolayer was formed (usually 48 h), $1.5x10^5$ REH cells untreated or previously treated with Tubastatin-A at 20 µM for 3 hours were washed twice with 1X PBS. Cells were resuspended in 100

µL RPMI medium and placed on top of the endothelial monolayer. 100 ng/mL of CXCL12 (Peprotech) as chemoattractant in 500 µl of fresh medium was added to the bottom well. Cells were allowed to transmigrate for 4 hours at 37°C. Transmigrated cells from the bottom chamber were collected and counted using a Neubauer chamber.

7. 2.11 In vitro spheroid competition colonization assay

HS-5 stromal cells were cultured in DMEM (Gibco) medium supplemented with 10% FBS and 1% antibiotic/antimycotic. To form spheroids in non-adhesion wells, suspensions of $2.5x10^4$ stromal cells were seeded in 96 well plates pre-coated with 100 µL 1% agarose to avoid adhesion to the plastic surface and incubated for 48 hours at 37°C, 5% CO_2 thus allowing for cell aggregation and formation of spheroids.

Untreated REH cells were stained with CFDA, meanwhile Tubastatin-A treated REH cells (20 µM for 3 h) were stained with CTV. $2.5x10^4$ stained REH cells were washed twice with 1X PBS and co-cultured with a spheroid for 24 hours. After this period, hematopoietic cells outside of spheroids were collected from supernatants, and spheroids with hematopoietic cells inside were collected separately after disaggregation of spheroids. To this end, spheroids were extensively washed with 1X PBS containing 5mM EDTA and enzymatic digestion was performed using TrypLE (Thermo Scientific) to dissociate attachment of MSC and REH cells by vigorous pipetting several times. The cell suspensions from inside and outside the spheroid were fixed and analyzed by flow cytometry.

For immunofluorescence, spheroids were recovered after co-culture with REH cells. Spheroids were washed with 1X PBS-5mM EDTA and fixed for 1 hour in 4% PFA at RT. Then, spheroids were washed again with 1X PBS, and with bidistilled water to remove salts. Spheroids were placed on slides, allowed to dry, and mounted using DABCO mounting medium without DAPI. Images were taken using a Leica SPE-DMI4000 confocal microscope. The number of cells in the spheroids was quantified using Imaris software.

7.2.12 Flow cytometry analysis of patient-derived cells

MNC were washed with 1 mL FACS buffer (1X PBS+1%FBS), blocked with anti-human FcRγ (1:1000) for 15 min at RT and then incubated with anti-human CD34 FITC (1:200; Biolegend), and anti-human CD19 phycoerytrin (1:200; Biolegend) in FACS buffer for 15 min at RT in the dark to identify $CD34^+$ progenitors, $CD34^+CD19^+$ pro-B and $CD34^-CD19^+$ pre-B cells. Then cells were fixed with 4% PFA for 20 min and permeabilized with FACS buffer containing 0.1% saponin (PermWash). Cells were incubated for 15 min at RT in the dark with either Alexa 647-labelled anti-human HDAC6 antibody (1:100) or Alexa 647-labelled anti-human cortactin antibody (1:100). Cells were resuspended in 100 μL FACS buffer and analyzed using a BD FASCanto II flow cytometer and FlowJo X software. $CD19^+$ B cells from healthy donors were used as non-malignant control cells.

7.2.13 Flow cytometry analysis of apoptosis

After Tubastatin-A treatment, REH cells were washed twice with FACS buffer and resuspended in 150 μL Annexin V binding Buffer (Biolegend). 1 μL of Pacific Blue™ Annexin V was added. Subsequently, 0.8 μL of propidium iodide was added. The cell suspension was gently vortexed and incubated for 15 min at RT in the dark. 100 μL of Annexin V binding buffer was added to each tube and analyzed by flow cytometry using an Aurora flow cytometer and FlowJo X software. REH cells with and without DMSO treatment were used as viability controls.

7.2.14 Flow cytometry analysis of CXCR4 and VLA-4

To analyze the effect of HDAC6 inhibition on CXCR4 dynamics, REH cells untreated or treated with Tubastatin-A at 10 or 20 μM for 24 h or 3 h were washed with 1X PBS+1%FBS. To analyze surface expression of CXCR4, cells were blocked with anti-human FcRγ (1:1000) and then incubated with APC-anti-human CXCR4 (1:200). To analyze total expression of CXCR4, cells were

washed, fixed with 4% PFA for 20 min and washed with Permwash to permeabilize. Then, cells were stained intracellularly with APC-anti-human CXCR4 (1:200), and washed with 1 mL FACS buffer, centrifuged for 5 min at 1500 rpm, and resuspended in 100 μL FACS buffer. To analyze VLA-4 levels, REH cells were washed and fixed with 4% PFA for 20 min. Subsequently, cells were washed with Permwash to permeabilize and stained intracellularly with APC-anti-human CD29 or PE/Cy7-anti-human CD49d. Cells were washed with 1 mL FACS buffer, centrifuged for 5 min at 1500 rpm, and resuspended in 100 μL FACS buffer. Samples were analyzed using a FACS Canto II flow cytometer and FlowJo X software.

7.2.15 Flow cytometry analysis of F-actin polymerization

To evaluate F-actin dynamics, REH cells untreated or treated with Tubastatin-A at 20 μM for 3h were stimulated with 100 ng/mL CXCL12 for 15, 30, 60, 180 and 360 seconds. Cells were directly transferred to 150 μL 4% PFA and incubated for 20 min at RT. Cells were then permeabilized with PermWash, and 1:400 Alexa Fluor™488-Phalloidin was used to stain F-actin for 30 min at RT. Acquisition was performed using a FACS Canto II cytometer, and data was analyzed using FlowJo X software.

7.2.16 Leukemic xenotransplantation assays

To analyze organ infiltration, $3x10^6$ REH cells were injected via the tail vein into non-irradiated male NSG mice (Jackson Laboratories, ME, USA). 50 mg/kg/day Tubastatin-A were intraperitoneally administered into mice three days per week for 3 weeks. An equivalent volume of DMSO was injected into control mice. Mice were kept in the animal facility of CINVESTAV and changes in body weight were monitored three times per week. Once disease was established in control mice (usually after 3 weeks, identified by weight loss, ruffled fur, hind limbs paralysis, lethargic, abnormal breathing, abnormal locomotion), mice were euthanized and BM, liver, spleen, brain, lung and testis

were harvested and mechanically disaggregated by careful slicing of tissue into pieces. Peripheral blood was obtained by cardiac puncture and erythrocytes were lysed using 1X BD Pharm lyse™ buffer according to the manufacturer's instructions. Single cell suspensions were analyzed for the presence of human $CD45^+$ leukemic B cells by flow cytometry. Data acquisition was performed using an Aurora cytometer, and analyzed using FlowJo X software.

7.2.17 Statistics

To perform statistical analysis, Prism V8.0.1(GraphPad) software was used. Differences between two groups were analyzed by Student's T-test, considering statistically significant values of $p<0.05$. Differences between more than two groups were analyzed by one-way ANOVA, whereas differences between more than two groups with different conditions were determined by two-way ANOVA considering statistically significant values of $p<0.05$. Multivariant statistical analysis was performed to correlate HDAC6 levels with clinical parameters. Mann–Whitney U-test was applied for clinical data.

8. RESULTS

8.1 The B-ALL cell line REH has higher HDAC6 levels compared to normal B cells

We previously reported that the B-ALL cell line REH overexpresses cortactin, which correlates with a high migratory capacity triggering organ infiltration in B-ALL (Velázquez-Avila et al., 2018). Cortactin regulates leukemic B cell migration and needs to be activated by deacetylation for efficient interaction with F-actin (Castellanos-Martínez et al., 2020). HDAC6 deacetylates cortactin and is also known to control cell migration and invasion in cancer (Sakamoto & Aldana-Masangkay, 2011). Considering these findings, we first analyzed HDAC6 protein levels by flow cytometry in REH cells compared to healthy CD19^{+} B cells (Fig. 9A) and found that leukemic cells contain significantly higher HDAC6 levels, suggesting that it could play an important role in B-ALL. Western blot analysis confirmed this finding and showed the expected molecular weight of HDAC6 at 160 kDa (Fig. 9B and 9C).

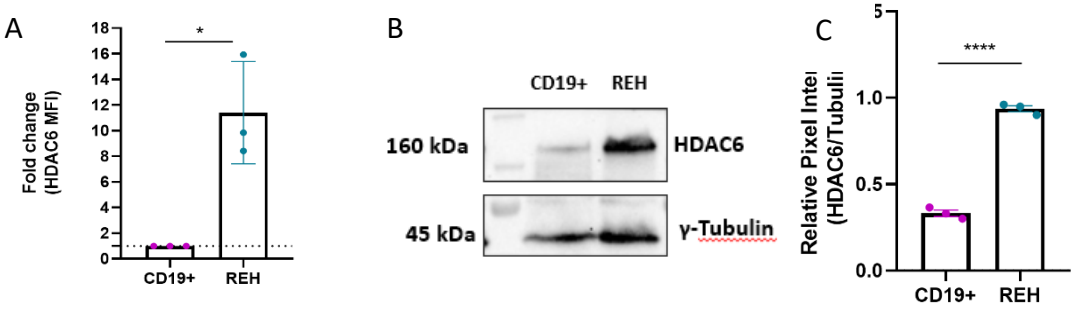

Figure 9. HDAC6 protein levels in the B-ALL cell line REH.
A) Flow cytometry of HDAC6 protein levels in the REH cells normalized to HDAC6 levels in CD19+ B cells as controls (set to 1). Data are presented as mean fluorescence intensity ± SD; n=3. *p<0.05. B) Representative Western blot of HDAC6 in CD19+ B cells and the B-ALL cell line REH showing the expected band at 160 kDa. C) Densitometric analysis of the relative pixel intensity was performed using Image J software. Unpaired, two-tailed Student's t-test was used to determine statistically significant difference ± SD; n=3. ****p≤0.0001

8.2 HDAC6 and cortactin co-localize in the cytosol and at the edge of REH cells

To identify the localization of HDAC6 in REH cells, we performed IF staining. Confocal images revealed that HDAC6 has primarily a cytoplasmic localization (Fig 2), which confirms what has been reported (Sakamoto & Aldana-Masangkay, 2011). IF staining for cortactin also showed its presence in the cytosol and at the cell periphery, suggesting that HDAC6 and cortactin are in close proximity. CXCL12 stimulation generates protrusions in REH cells, where an enrichment of both HDAC6 and cortactin in the polarized regions could be observed (Fig 10).

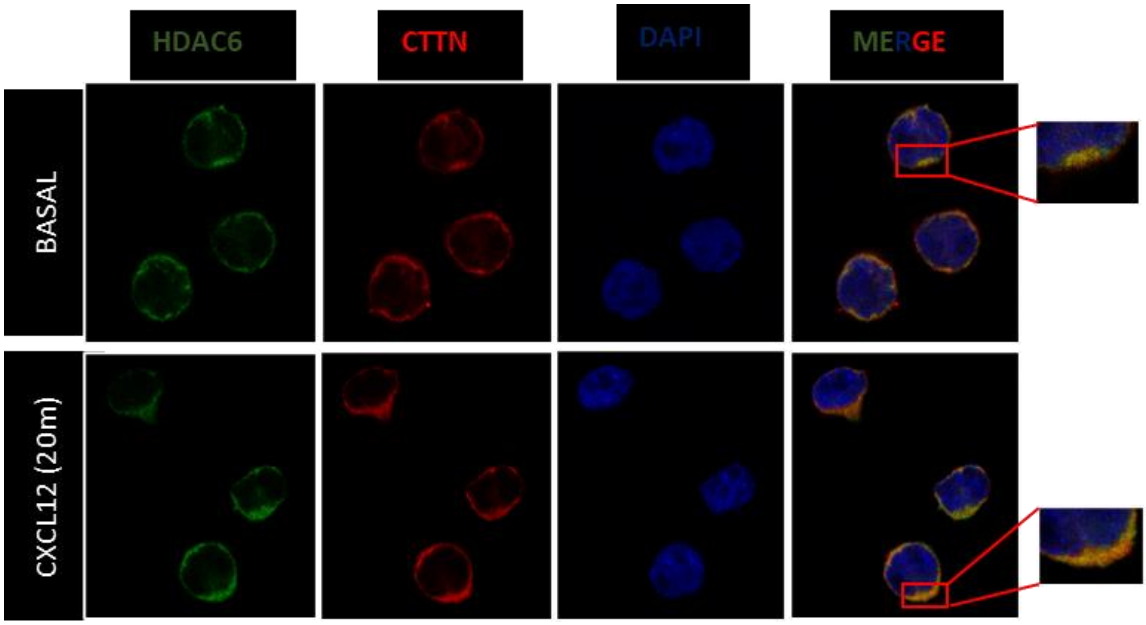

Figure 10. HDAC6 displays a cytoplasmic localization in REH cells.

Representative images of REH cells stained for HDAC6 (green), cortactin (red) and DAPI (nuclei, blue). Cells were visualized using a Leica TCS-SPE DMI4000 confocal with a 63x objective and a 1.5x digital zoom. Representative images of 2 independent experiments are shown. Magnifications show HDAC6 and cortactin presence at the cell periphery in co-localization.

8.3 Tubastatin-A kills REH cells only at high concentrations

To analyze the effect of HDAC6 inhibition on REH cell migration, we first determined the most suitable concentration of Tubastatin-A, a specific pharmacological HDAC6 inhibitor (Butler et al., 2010; S. Shen et al., 2020), by MTT assays. We found that the IC_{50} value of Tubastatin-A, which is the concentration inducing 50% of cell death, was 94 μM after 24 hours (Fig 11).

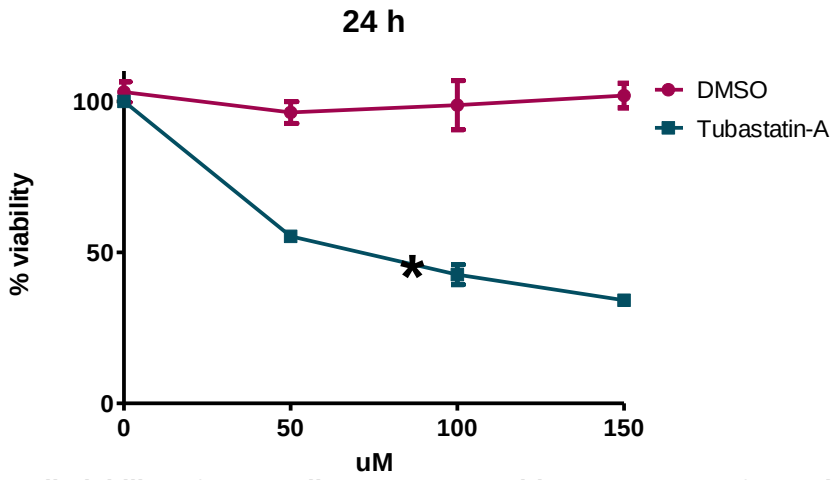

Figure 11. Cell viability of REH cells was assessed by MTT assay after Tubastatin-A treatment.

$3x10^4$ REH cells were plated into 96-well plates and then incubated with different concentrations of Tubastatin-A (50, 100 and 150 μM) for 24 h. Control cells were treated with DMSO. IC_{50} value is represented as * within the graph. Data are means ± SD of four independent experiments.

As we needed only viable REH cells in functional assays, we decided to select a lower incubation time and concentration of Tubastatin-A and analyzed apoptosis using flow cytometry as a control. Annexin V binds to phosphatidylserine (PS), which is normally only found on the intracellular leaflet of the plasma membrane in healthy cells, but during early apoptosis, membrane asymmetry is lost and PS translocates to the external leaflet. To distinguish between the necrotic and apoptotic cells, propidium iodide (PI) was

also used, which stains late-stage apoptotic cells and necrotic cells due to its passage into the nucleus where it can bind to DNA. Early apoptotic cells exclude PI (Biolegend, 2020). When we treated REH cells using a concentration of 20 µM of Tubastatin-A for 3 hours, the percentage of cells positive for PI and PB-Annexin V was neglectable and similar to what was observed in control REH cells treated with DMSO, meaning that the cells are not suffering apoptosis and are viable for functional assays (Figure 12).

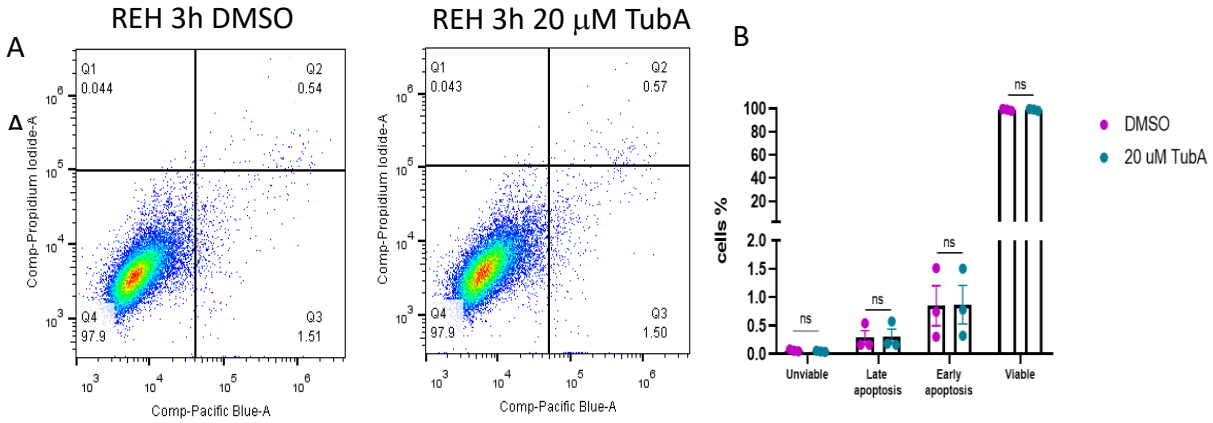

Figure 12. 20 µM of Tubastatin A for 3 h does not trigger apoptosis in REH cells.
A) Dot plots show apoptosis ratios of control REH cells treated with DMSO and REH cells treated with 20 µM of Tubastatin-A (TubA) using propidium iodide (PI) and Pacific Blue-annexin V. The Q1 quadrant represents dead cells (PI positive and annexin negative). The Q2 quadrant represents cells that are in late apoptosis or necrosis (both annexin and PI positive). The Q3 quadrant represents viable cells (both annexin and PI negative). The Q4 quadrant represents cells in early apoptosis (annexin positive and PI negative). Representative dot plots of 3 independent experiments are shown. B) Percentage of cells observed in each quadrant from A. ns, not significant.

8.4 HDAC6 deacetylates cortactin and tubulin in REH cells

Cortactin and α-tubulin are important proteins regulating cell migration (Daly, 2004; Kopf & Kiermaier, 2021) and have been reported as HDAC6 substrates in different cell lines (Hubbert et al., 2002; Zhang et al., 2007). Inhibition of HDAC6 with 20 µM of Tubastatin-A for 3 hours in REH cells revealed an increase in acetylation levels of both cortactin and α-tubulin, without changes in HDAC6 protein levels (Fig 13). These findings show HDAC6 is active at the

concentration and time used and that cortactin and tubulin are also HDAC6 targets in in REH cells. Furthermore, treatment conditions are appropriate to apply in functional assays.

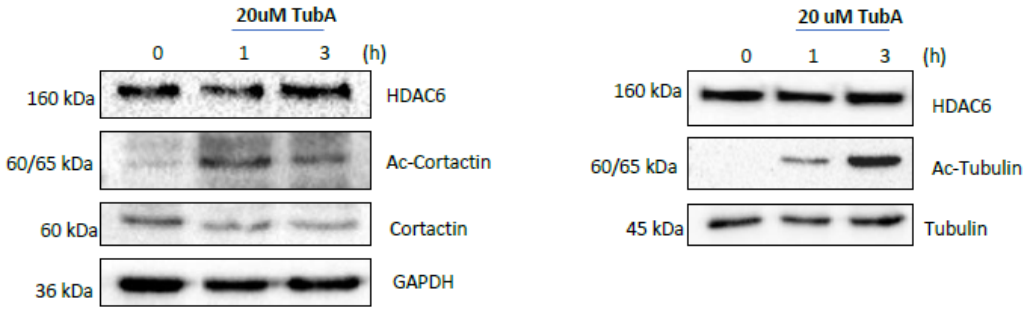

Figure 13. Tubastatin-A induces acetylation of cortactin and α-tubulin in REH cells.

Representative Western blots of HDAC6, acetyl-cortactin, cortactin and acetyl-tubulin after treatment with 20 μM of Tubastatin-A (TubA) in REH cells. GAPDH and γ-tubulin were used as loading control. Representative blots of 3 independent experiments are shown.

8.5 HDAC6 inhibition reduces migration of leukemic B cells by inhibition of F-actin polymerization

To evaluate whether HDAC6 has an important role in the migratory capacity of leukemic B cells, we pre-treated only REH cells with Tubastatin-A and performed transendothelial migration assays. We found that HDAC6 inhibition in REH cells significantly reduced their capacity to transmigrate across HUVEC monolayers in response to CXCL12, compared with DMSO pre-treated REH cells (Fig. 14A), suggesting that HDAC6 is needed to accomplish efficient transendothelial migration. Transmigration depends on F-actin dynamics. To investigate whether the reduced transmigration is due to altered F-actin dynamics, we performed actin polymerization assays. CXCL12 stimulation rapidly produced new actin filaments in control cells. However, actin polymerization in leukemic B cells under was significantly reduced by Tubastatin-A treatment at early time points in comparison with DMSO treated cells (Fig 14B).

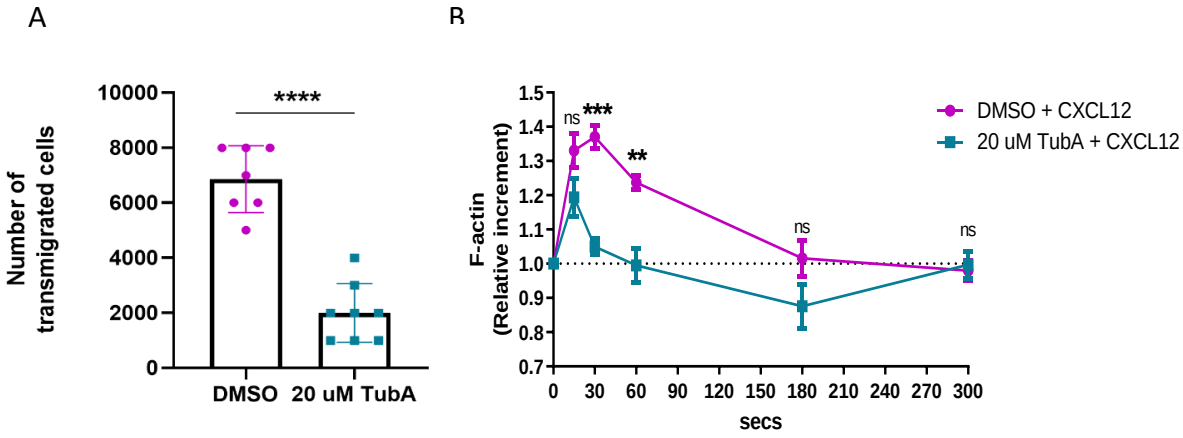

Figure 14. REH cell transendothelial migration and actin polymerization are reduced by HDAC6 inhibition.

*A) Transendothelial migration across HUVEC monolayers in response to CXCL12 (100 ng/mL) 4 h after treatment of REH cells with Tubastatin-A (TubA) 20 µM. Control REH cells were treated with equal volume of DMSO. Unpaired, two-tailed Student's t-test was used to determine statistically significant differences between experimental groups. Error bars in figures represent SD ****p<0.0001; n=3. B) Tubastatin-A pre-treated REH cells were stimulated with CXCL12 for the indicated time points. Cells were then immediately fixed at the indicated times and F-actin was stained using phalloidin. Data are presented as relative change to controls (time point 0 s set to 1) ± SD; n=3. Significance was determined using two-way ANOVA. ***p<0.001, **p<0.01, ns, not significant.*

8.6 HDAC6 inhibition in cortactin-depleted REH cells does not cause an additional effect on transendothelial migration

To analyze whether cortactin is a main target of HDAC6 through which it regulates transendothelial migration, we generated stable cortactin-depleted REH cells and subjected them to transmigration assays in the presence or absence of Tubastatin-A. Cortactin was depleted in REH cells with an efficiency of around 50% as confirmed by Western blot (Fig 15).

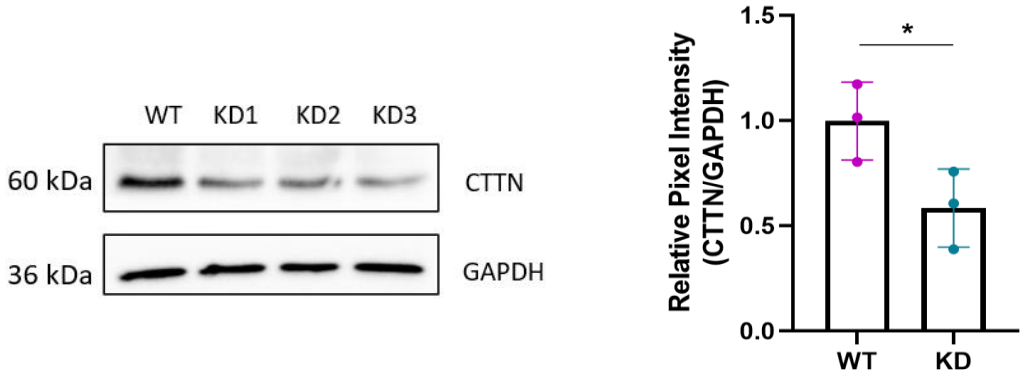

Figure 15. Generation of cortactin-depleted REH cells. Cortactin (CTTN)-depletion in REH cells was corroborated by western blot.

A) Representative blot of three independent experiments is shown. GAPDH was used as loading control. B) Relative pixel intensity of cortactin WT and KD REH cells after normalizing with GAPDH. The graph shows a reduction of around 50% on cortactin levels in KD cells compared to WT cells. Significance was determined using paired, two-tailed Student's t-test. Error bars in figures represent SD; *p<0.05.

HDAC6 inhibition in WT REH cells significantly impaired transmigration compared to DMSO pre-treated WT cells (Fig 16). Control cortactin-KD REH cells transmigrated significantly less in comparison to control WT REH cells. However, in cortactin-KD cells, HDAC6 inhibition did not further reduce transmigration in comparison to DMSO-treated KD cells or Tubastatin A-treated WT cells. Thus, the similar inhibition of transmigration in cortactin-depleted and Tubastatin-A treated WT REH cells, with no additional effect of HDAC6 inhibition in cortactin KD cells suggests that HDAC6 decreases transendothelial migration of REH cells mainly by acting on cortactin.

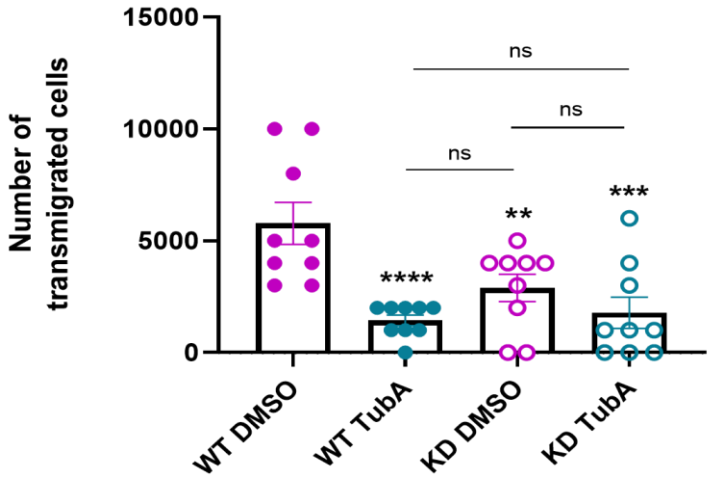

Figure 16. HDAC6 inhibition does not further reduce transendothelial migration of cortactin-KD REH cells.

Tubastatin-A (TubA)-treated (20 µM, 3 h) WT and cortactin-depleted REH were subjected to transendothelial migration assays using transwell filters and 100 ng/mL CXCL12 as chemoattractant for 4 h. Cells that migrated to the bottom chamber were stained with trypan blue and counted using a Neubauer chamber. Control WT and KD REH cells were treated with equal volume of DMSO. Data are presented as numbers of transmigrated cells ± SD; n=4. Significance was analyzed by two-way ANOVA using Graph Pad. ****p≤0.0001; ***p<0.001; **p<0.01. ns, not significant.

8.7 BM organoid colonization is impaired after HDAC6 inhibition in REH cells

The bone marrow microenvironment supports the growth and survival of normal and leukemic cells. CXCL12 is a chemokine constitutively produced by bone marrow mesenchymal stromal cells (MSC) to regulate the homing of circulating normal and leukemic cells to the bone marrow (Duarte et al., 2018). Thus, we wanted to know whether HDAC6 in REH cells is critical to accomplish colonization of MSC organoids resembling BM (Balandrán et al., 2017). We performed competition assays and flow cytometry analysis and found that REH cells pre-treated with Tubastatin-A were less able to colonize MSC organoids compared to DMSO treated REH cells (Fig. 17A), suggesting that HDAC6 is needed for an efficient colonization of BM-MSC organoids. Moreover, as control we analyzed whether the deacetylase activity of HDAC6 in REH cells was still inhibited after pre-treatment of Tubastatin-A and even maintained after

washing and 24 h co-culture with MSC organoids to allow colonization. We observed that after completion of colonization, ac-tubulin levels were similar to those observed immediately after Tubastatin-A treatment indicating that HDAC6 was indeed inhibited throughout the course of the experiment (Fig 17B).

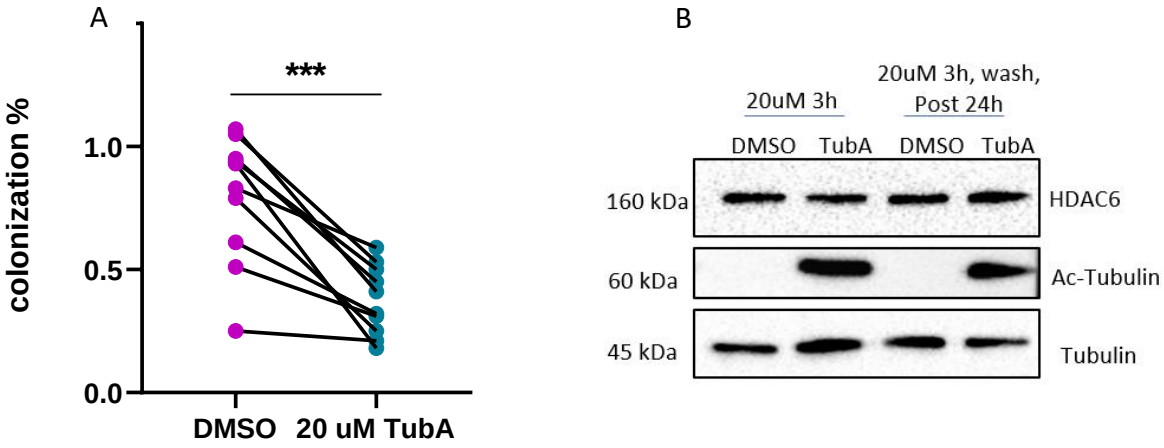

Figure 17. HDAC6 inhibition in REH cells diminishes their capacity to colonize MSC organoids.

A) MSC organoids were co-cultured for 24 h with REH cells. Prior co-culture, control REH cells were stained with CFDA, treated with DMSO and washed with 1X PBS. Tubastatin-A (TubA)-treated REH cells were stained with CTV and washed with 1X PBS. After co-culture, organoids were recovered, disaggregated, fixed, and analyzed using a BD FACS Canto II cytometer. Data are shown as colonization percentage of single cells. Significance was determined using paired, two-tailed Student's t-test. ***p<0.001; n=3. B) Representative Western blot of two independent experiments showing ac-tubulin levels in REH cells after 20 µM TubA treatment, washing with 1X PBS and 24h culture with fresh media. Tubulin was used as loading control.

Furthermore, we corroborated our results by confocal microscopy (Fig 18A). We recovered the complete organoids and confirmed that Tubastatin-A-treated REH cells were less able to colonize the organoids in comparison to DMSO-treated REH cells. We quantified the number of cells using IMARIS Software and found a significant reduced number of Tubastatin-A pre-treated REH cells inside the organoid in comparison to DMSO treated REH cells (Fig. 18B),

supporting the idea that HDAC6 is necessary for homing of B-ALL cells into the BM.

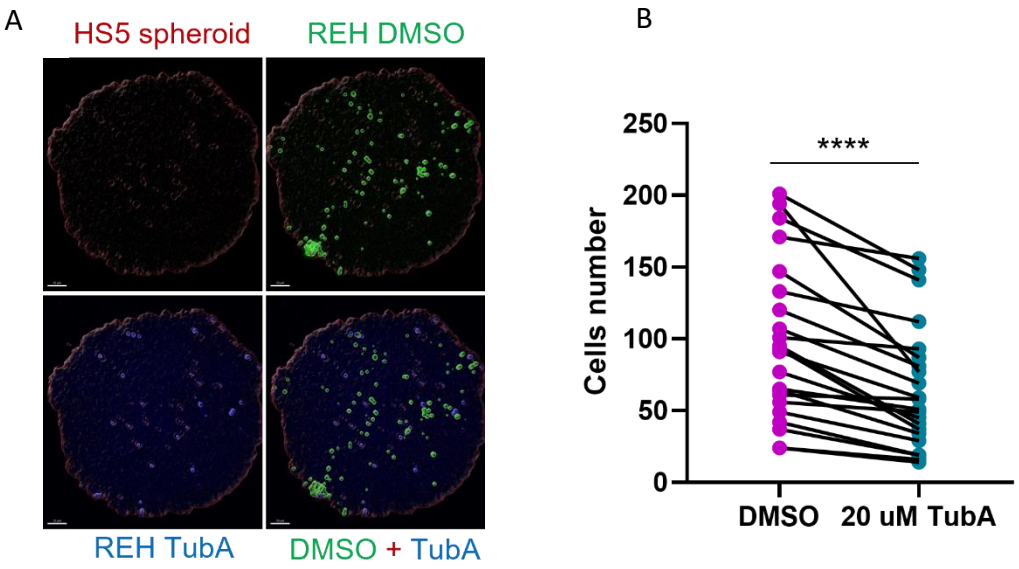

Figure 18. Confocal microscopy of MSC-organoid showed less presence of Tubastatin-A-treated cells.

A) MSC organoids were recovered after 24 h co-culture with REH cells, and analyzed using a Leica TCS-SPE DMI4000 confocal microscope. DMSO-treated cells were stained with CFDA (green) and TubA-treated cells with CTV (blue). Bar=50μm B) The number of REH cells inside the organoids was quantified using IMARIS Software. Significance was determined using paired, two-tailed Student's t-test. ****p≤0.0001; n=22 spheroids from 3 independent experiments.

8.8 HDAC6 inhibition causes a decrease in CXCR4 and VLA-4 levels in REH cells

As leukemic B cell transmigration and homing into the BM also depends on integrins and chemokine receptors, we analyzed CXCR4 and VLA-4 levels after HDAC6 inhibition. After 3 hours of treatment with Tubastatin-A, total CXCR4 levels were not changed compared to DMSO-treated control REH cells (Fig. 19A). Interestingly, we found significantly lower surface levels of CXCR4 in Tubastatin-A treated REH cells in comparison to DMSO-treated control REH cells. However, internalization of CXCR4 in response to CXCL12 occurred at similar rates in both cell types (Fig 19B). CXCR4 levels after 24 h of Tubastatin-

A treatment revealed that both surface and total levels of CXCR4 were significantly diminished compared to DMSO treated cells, therefore suggesting that HDAC6 may be involved in CXCR4 transport and degradation (Fig 19C).

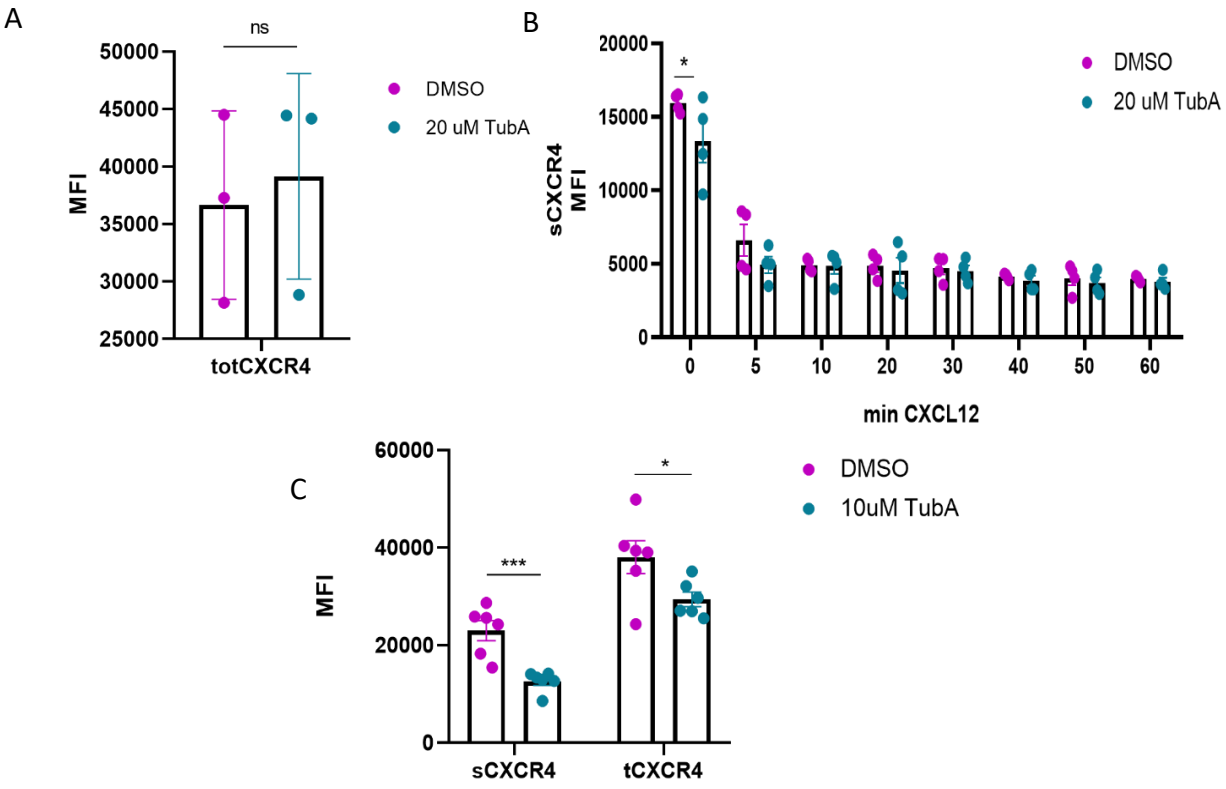

Figure 19.Tubastatin-A treatment diminishes surface and total CXCR4 levels in REH cells.

A) Total levels of CXCR4 were analyzed in permeabilized REH cells after 3 h treatment with 20 μM Tubastatin-A (TubA). n=3. ns, not significant. B) After 3 h treatment with 20 μM TubA, surface levels of CXCR4 were analyzed in non-permeabilized, untreated or CXCL12-stimulated cells. n=4. *p<0.05. C) Surface and total CXCR4 levels were determined after 24h treatment with 10 μM Tubastatin-A. In all experiments, DMSO-treated REH cells were used as control. Samples were analyzed using a BD FACS Canto II cytometer and analyzed by FlowJo X software. Data are presented as MFI ± SD. Significance was determined using unpaired, two-tailed Student's t-test and two-way ANOVA using Graph Pad. n=3. *p<0.05; ***p<0.001.

HDAC6 inhibition in REH cells for 3 h did not cause any changes in the surface levels of the VLA-4 integrin subunits (CD49d (integrin α_4) and CD29 (integrin β_1), in comparison to DMSO-treated cells (Fig 20A). However, after 24 h of Tubastatin-A treatment, we found a significant reduction of both CD49d and CD29 levels (Fig 20B), suggesting that HDAC6 may play a role in integrins transport.

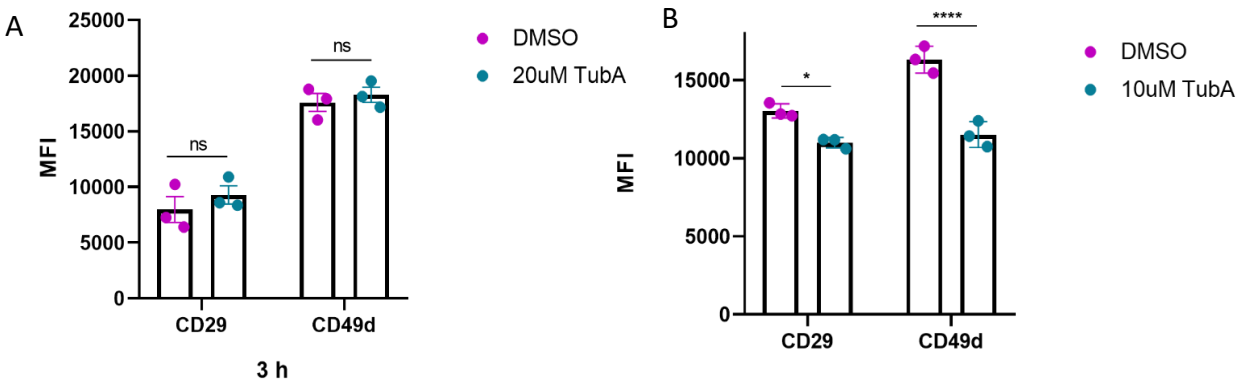

Figure 20. Tubastatin-A treatment for 24 h in REH cells causes a decrease in CD29 and CD49d subunit levels of VLA-4 in REH cells.

A) Surface CD29 and CD49d (VLA-4) levels were determined after 3 h treatment with 20 μM Tubastatin-A. n=3. ns, not significant. B) After 24h treatment with 10 μM Tubastatin-A, surface CD29 and CD49d levels were analyzed. In all experiments, DMSO treated REH cells were used as control. Samples were analyzed using a BD FACS Canto II cytometer and analyzed by FlowJo X software. Data are presented as MFI ± SD. Significance was determined using two-way ANOVA using Graph Pad. n=3. *p<0.05; ****p≤0.0001.

8.9 HDAC6 expression is higher in B cells derived from patients with B-ALL compared to normal B cells

Having shown the overexpression of HDAC6 in REH cells and its importance for migration, we wanted to investigate whether this was also true for primary patient-derived B-ALL cells. We investigated the expression of HDAC6 in a cohort of 22 pediatric B-ALL patients (Appendix 1). RNA-seq data revealed that HDAC6 expression was significantly higher in B-ALL patients compared with control patients (Fig 21A). Furthermore, we examined the protein levels of HDAC6 by flow cytometry in patient-derived bone marrow cells from a second

cohort of 49 B-ALL patients (Appendix 2). HDAC6 protein levels were also found to be higher in B-ALL cells compared with non-malignant $CD19^+$ B cells (Fig 21B). Remarkably, HDAC6 levels in B-ALL cells from relapse patients were increased threefold compared to cells from debut patients. Importantly, we followed 4 patients of our cohort since diagnosis, and found that their blasts at relapse increased HDAC6 levels in comparison to their blasts at debut (Fig 21C).

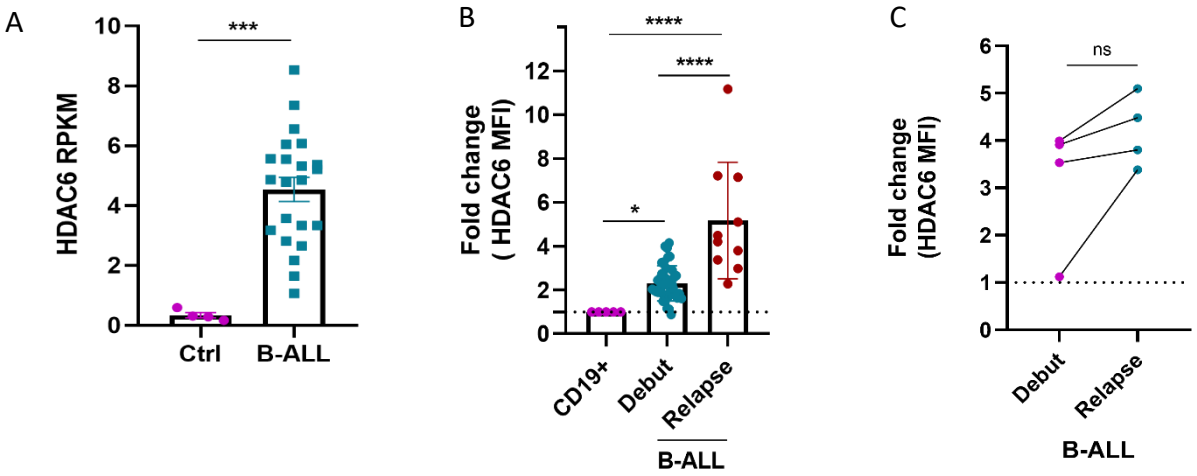

Figure 21. HDAC6 mRNA and protein levels are higher in primary leukemic B cells than in normal B cells.

A) HDAC6 RPKM expression values (reads per kilobase million) as determined by RNA-seq in a cohort of 22 B-ALL patients and 4 control patients. Each dot represents an individual. B) Flow cytometry of HDAC6 protein levels in newly diagnosed (n=39) and relapse (n=10) B-ALL patients normalized to HDAC6 levels in CD19+ B cells as controls (set to 1) (n=5). Each dot represents an individual. C) Flow cytometry of HDAC6 protein levels in 4 patients followed from debut to relapse. Each dot represents an individual. Data were normalized to HDAC6 levels in CD19+ B cells as controls (set to 1) (n=1). Flow cytometry data were analyzed by FlowJo X software and are presented as mean fluorescence intensity ± SD. One-way ANOVA was used to determine statistically significant differences between experimental groups using Graph Pad. Significance was calculated by comparing HDAC6 levels in B-ALL patient cells vs CD19+ B cells. *p<0.05; ***p<0.001; ****p≤0.0001; ns, not significant.

Correlation analysis of HDAC6 RPKM expression values with clinical parameters using non-parametric Mann-Whitney U test did not reveal any significative correlation (Table 9).

Table 9. Correlation analysis of HDAC6 RPKM expression.

Variable	P-value		HDAC6 RPKM (Reads per kilobase million)
Sex	0.1545	Female (n=6)	484.79
		Male (n=16)	311.02
Risk	0.4822	Standard (n=8)	414.16
		High (n=14)	326.55
Translocation	0.3002	Negative (n=18)	324.64
		Positive (n=4)	510.38
Hepatomegaly	0.8212	Negative (n=12)	368.48
		Positive (n=10)	381.73
Splenomegaly	0.4070	Negative (n=6)	402.02
		Positive (n=16)	301.13
Adenomegaly	0.7223	Negative (n=12)	344.35
		Positive (n=10)	375.28
Death	0.99	Negative (n=14)	373.50
		Positive (n=8)	376.25

To compare HDAC6 expression with available numeric variables, we used Pearson's correlation test. However, HDAC6 expression did not correlate with the percentage of BM blasts, platelets, leukocyte numbers or hemoglobin concentration (Fig 22).

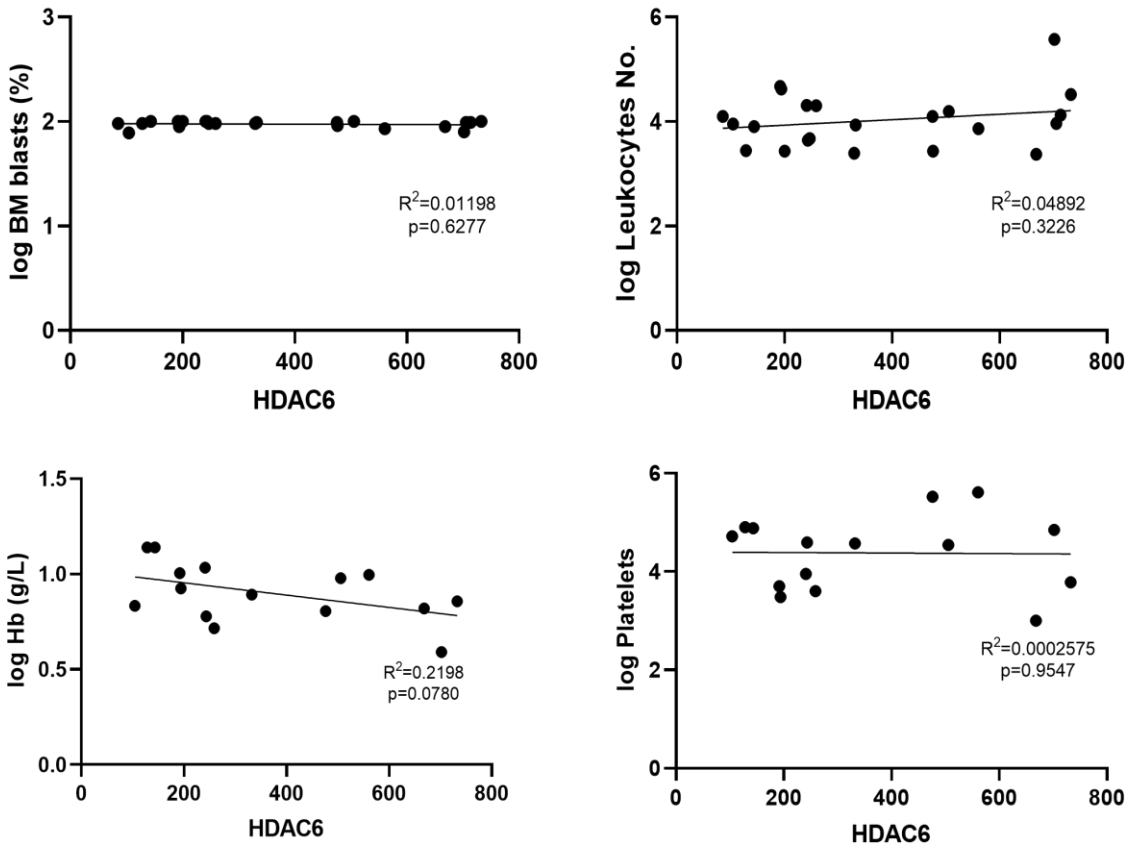

Figure 22. Correlation analysis of HDAC6 RPKM with patient data.

HDAC6 RPKM values in blasts from bone marrow of B-ALL patients (n=22) and control individuals (n=4) was determined by RNA-seq and then correlated with the indicated patient data. Y-axis is in logarithmic scale.

In order to correlate HDAC6 protein levels to clinical parameters, we analyzed clinical patient data and performed statistical analysis. We used non-parametric Mann-Whitney U test to categorize variables and analyze if they could be related with the increased HDAC6 levels. For each category, mean HDAC6 levels are displayed as fold increase (according to control $CD19^+$ B cells) (Table 10). Statistical analysis to identify whether HDAC6 levels associate to clinical features confirmed a significant correlation with relapse and translocations. However, HDAC6 upregulation was not related to sex, risk, immunophenotype, response to steroids, infections, neutropenia, thrombocytopenia, anemia, hepatomegaly, adenomegaly, splenomegaly or death. Importantly, Pearson's

correlation tests revealed increased leukocytes number and platelet numbers as significant correlation (Fig 23); but blasts percentage in BM and PB, lactate dehydrogenase (LDH) levels and hemoglobin levels were not significantly correlated to higher HDAC6 levels.

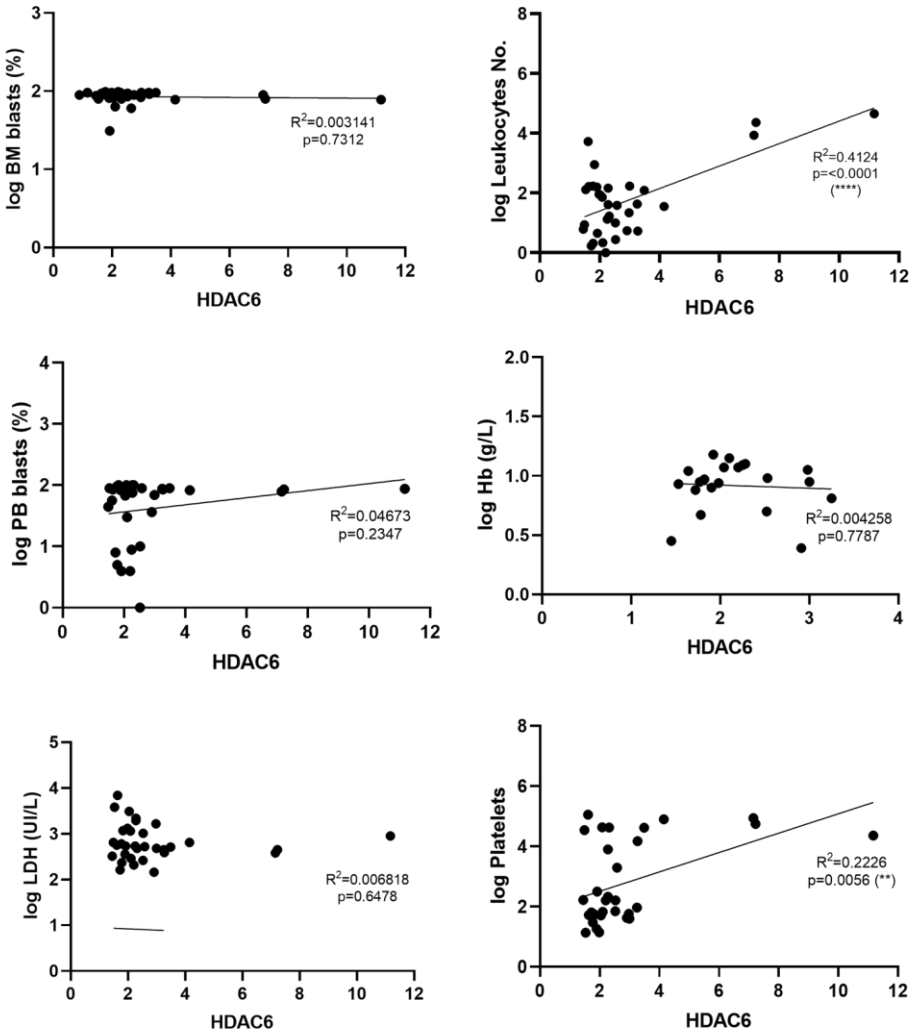

Figure 23. Correlation analysis of HDAC6 levels with patient data.

Fold increase levels of HDAC6 in progenitor and precursor B cells from bone marrow of B-ALL patients (n=49) was determined by flow cytometry (normalized to the mean fluorescence intensities from CD19+ B cells as controls (n=5), and then correlated with the indicated patient data. Y-axis is in logarithmic scale.

Table 10. Correlation analysis of HDAC6 protein levels.

Variable	P-value		HDAC6 levels (Fold increase of mean fluorescence intensity)
Sex	0.8150	Female (n=27)	3.18
		Male (n=22)	2.48
Risk	0.2528	Standard (n=12)	2.37
		High (n=26)	2.13
Immunophenotype	0.1007	Pre-B (n=14)	2.15
		Pro-B/Pre-B,Pro-B (n=35)	3
Translocation	**0.0034**	Negative (n=25)	**2.96**
		Positive (n=15)	**2.73**
Response to steroids	0.5687	Negative (n=4)	4.99
		Positive (n=31)	2.77
Infections	0.0787	Negative (n=29)	3.12
		Positive (n=9)	2.15
Anemia	0.7677	Negative (n=6)	2.31
		Positive (n=36)	2.96
Neutropenia	0.0683	Negative (n=14)	2.24
		Positive (n=13)	2.16
Thrombocytopenia	0.4788	Negative (n=10)	2.11
		Positive (n=32)	3.03
Hepatomegaly	0.5936	Negative (n=18)	2.20
		Positive (n=27)	3.04
Splenomegaly	0.6168	Negative (n=22)	2.20
		Positive (n=23)	3.17
Adenomegaly	0.2471	Negative (n=18)	2.26
		Positive (n=27)	2.98
Relapse	**≤0.0001**	Negative (n=39)	**2.21**
		Positive (n=10)	**6.16**
Death	0.5485	Negative (n=47)	2.73
		Positive (n=2)	2.07

8.10 Inhibition of HDAC6 in patient-derived leukemic B cells reduces their invasive capacity

Our previous results show that B-ALL patients have significantly increased HDAC6 levels compared to healthy B cells, suggesting that HDAC6 overexpression is a common characteristic in B-ALL, and more importantly, that HDAC6 upregulation is associated to relapse. Taking into account our previous findings that REH cells with high HDAC6 levels migrate more, we hypothesized that high HDAC6 levels in B-ALL cells from patients also trigger migration and organs invasion. To this end, we performed transmigration assays in response to CXCL12 across HUVEC monolayers with HDAC6 inhibition and found that leukemic blasts transmigrated less after Tubastatin-A treatment in comparison to DMSO-treated cells (Fig 24), which is in agreement with our findings in REH cells. Thus, HDAC6 is required in leukemic B cells to accomplish transmigration efficiently.

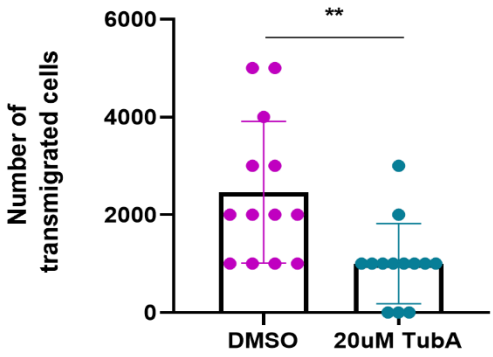

Figure 24. Patient-derived B-ALL cells transmigrate less after HDAC6 inhibition.

Transendothelial migration assays across HUVEC monolayers in response to CXCL12 (100 ng/mL) were performed for 4 h after treatment of REH cells with 20 μM Tubastatin-A (TubA) for 3 h. Control cells were treated with equal volume of DMSO. Unpaired, two-tailed Student's t-test was used to determine statistically significant differences between experimental groups. Error bars in figure represent SD; n=4. **p<0.01.

Furthermore, BM organoid colonization competition assays demonstrated that Tubastatin-A-treated B cells from patients colonized the organoids less efficiently than DMSO-treated cells (Fig 25A), which was also confirmed by IF (Fig 25B, 25C), similar to what we found using REH cells indicating that HDAC6 inhibition in leukemic B cells with high HDAC6 levels could reduce their invasiveness.

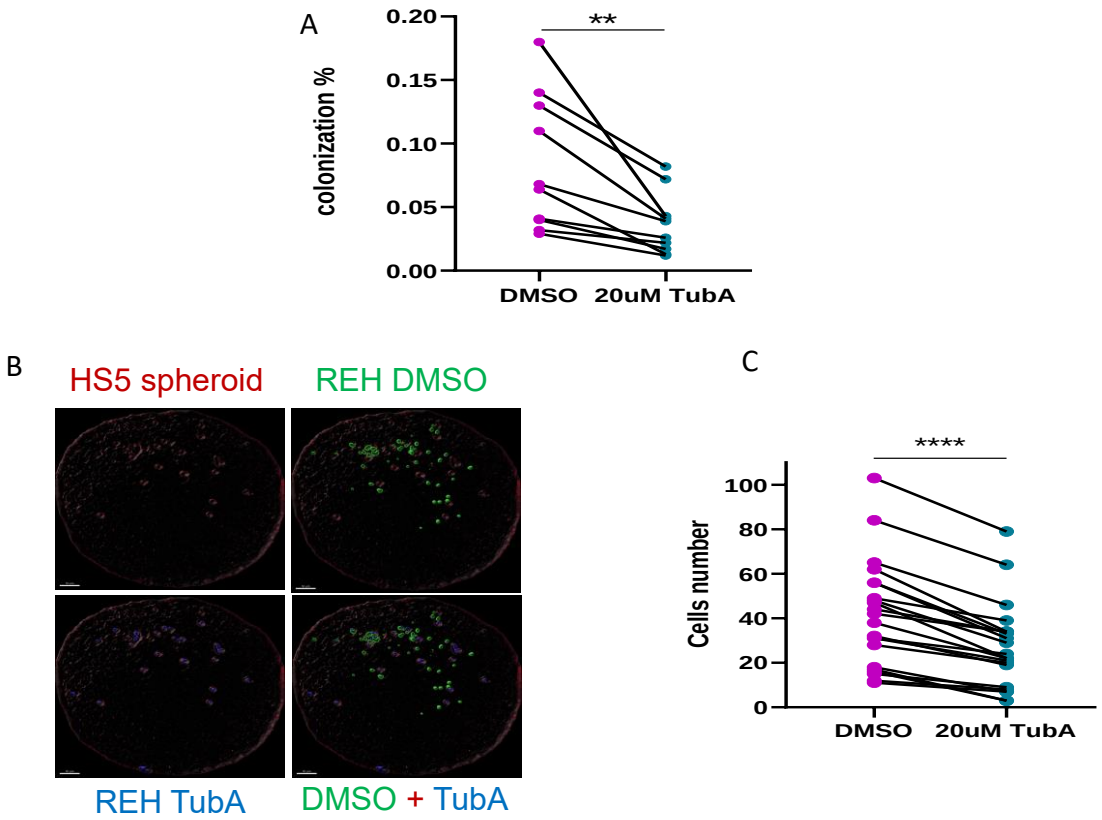

Figure 25. HDAC6 inhibition in patient-derived B-ALL cells reduces their ability to colonize MSC organoids.

A) MSC organoids were co-cultured for 24 h with patient-derived B-ALL cells. Prior co-culture, control cells were stained with CFDA, treated with DMSO, and washed with 1X PBS. Tubastatin-A (TubA, 20 μM, 3 h) treated cells were stained with CTV and washed with 1X PBS. After co-culture, organoids were recovered, disaggregated, fixed, and analyzed using a BD FACS Canto II cytometer. Data are shown as colonization percentage of single cells. Significance was determined using paired, two-tailed Student's t-test. **p<0.01; n=5. B) Whole MSC organoids were recovered after co-culture with patient-derived B-ALL cells, washed, fixed and analyzed using a Leica TCS-SPE DMI4000 confocal microscope. DMSO-treated cells were stained with CFDA (green) and TubA pre-treated cells with CTV (blue). Bar=50μm. C) Quantification of the number of cells inside the organoids was analyzed using IMARIS Software. Significance was determined using paired, two-tailed Student's t-test. ****p≤0.0001; n=22 spheroids from 3 independent experiments.

8.11 B-ALL patient cells isolated from BM possess higher HDAC6 levels than cells from PB, and bestow a migratory advantage

Next, we analyzed whether B-ALL cells isolated from BM or PB would exhibit different HDAC6 levels. We found that 9 of 12 patients from our cohort possessed higher HDAC6 levels in BM-derived blasts compared to blasts derived from PB (Fig 26A), suggesting that HDAC6 upregulation is triggered in the BM, which could potentiate leukemic B cells escape into blood circulation. Moreover, we found that relapse patients had higher HDAC6 levels in cells from both BM and PB in comparison to debut patients and control individuals (Fig. 26B).

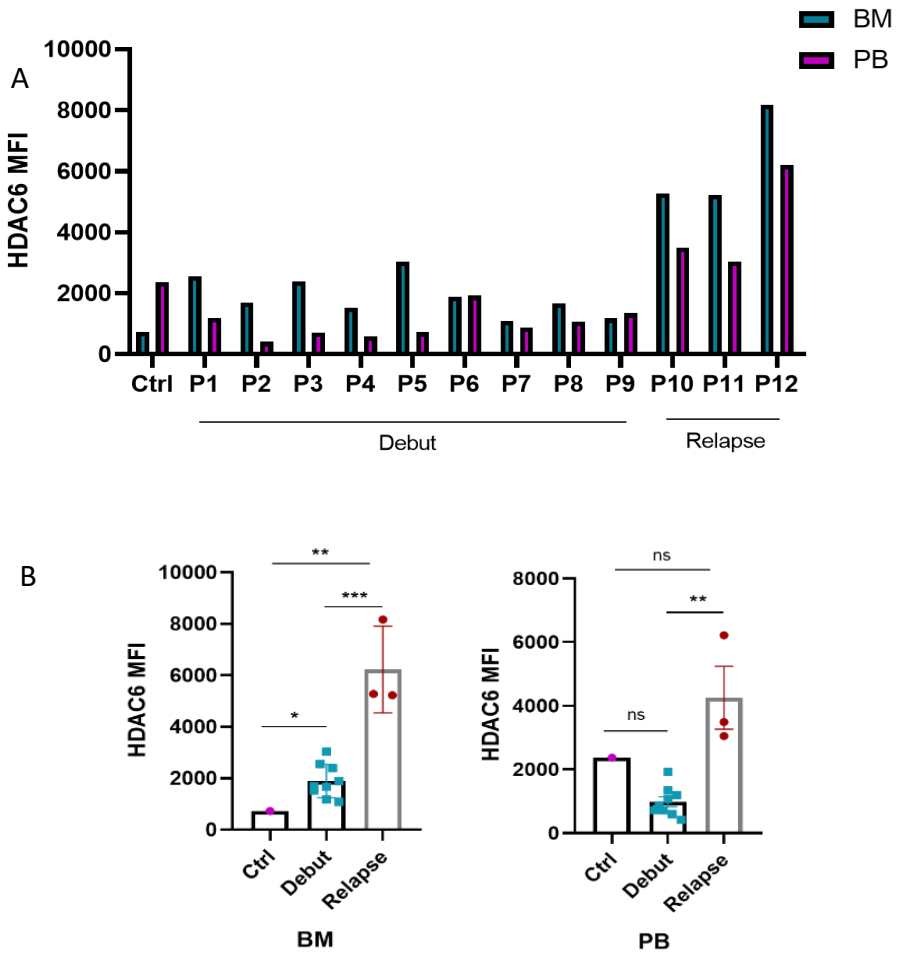

Figure 26. HDAC6 levels in patient-derived blasts from BM and PB correlate with migratory efficiency.

A) HDAC6 levels were analyzed by flow cytometry in patient-derived blasts isolated from BM and PB. Samples from 1 healthy individual, 9 newly diagnosed and 3 relapse patients were analyzed. Data were analyzed by FlowJo X software and are presented as MFI ± SD. B) Flow cytometry of HDAC6 protein levels in BM (left) and PB (right)-derived non-malignant cells (n=1), newly diagnosed (n=9) and relapse (n=3) B-ALL patients. Each dot represents an individual. Flow cytometry data were analyzed by FlowJo X software and are presented as mean fluorescence intensity ± SD. One-way ANOVA was used to determine statistically significant differences between experimental groups using Graph Pad. Significance was calculated by comparing HDAC6 levels in B-ALL patient cells vs CD19+ B cells. *p<0.05; **p<0.01; ***p<0.001; ns, not significant.

With the available patient cells we performed chemotaxis assays, and of note, we found that debut patient BM-derived blasts with highest HDAC6 levels (P5) were able to migrate more in response to CXCL12 in comparison to BM-derived blasts from debut patients with lower HDAC6 levels (P2, P4), demonstrating that HDAC6 indeed provides a migratory advantage (Fig. 27A). Additionally, chemotaxis assays comparing BM and PB blasts from 3 patients confirmed that migration efficiency correlated with HDAC6 levels (Fig. 27B).

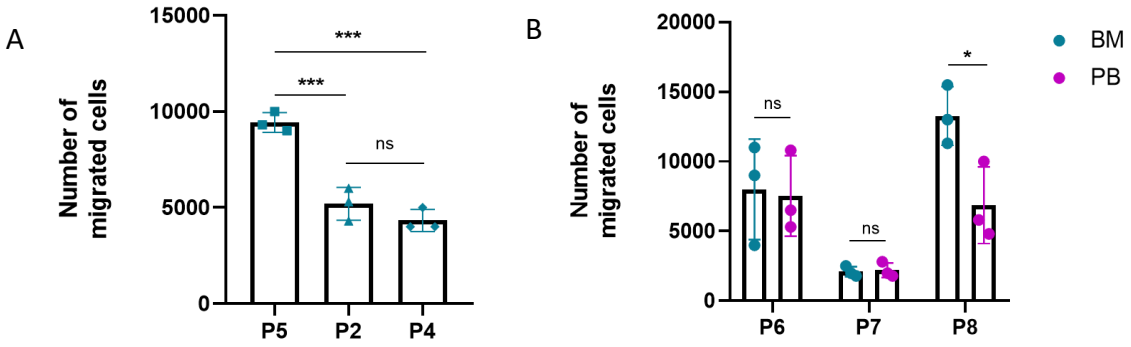

Figure 27. HDAC6 bestows a migratory efficiency in patient-derived blasts from BM and PB.

A) Chemotaxis assays were performed with patient-derived BM blasts and the number of migrated cells in response to CXCL12 after 4 h were counted. B) Chemotaxis assays in response to CXCL12 were performed with patient-derived BM and PB blasts. After 4 h, the number of migrated cells were counted. Experiments were performed by triplicate for each patient.

8.12 Direct contact with stromal cells leads to an increase of HDAC6 levels in leukemic B cells

The previous finding indicates that the BM microenvironment could be mediating HDAC6 upregulation. To corroborate this, we performed an adhesion assay, where REH cells were co-cultured for 24 h on top of MSC line HS5. Importantly, we found that REH cells that were strongly adhered to MSC presented a significant increase in HDAC6 levels compared to cells cultured alone. REH cells in the co-culture but not adhered to HS5 cells also showed an increase in HDAC6 levels (Fig. 28A). Furthermore, we analyzed HDAC6 levels in REH cells that were able to colonize BM-MSC organoids and found that leukemic B cells inside the organoid possessed higher HDAC6 levels compared to those cells that were not able to colonize (Fig. 28B).

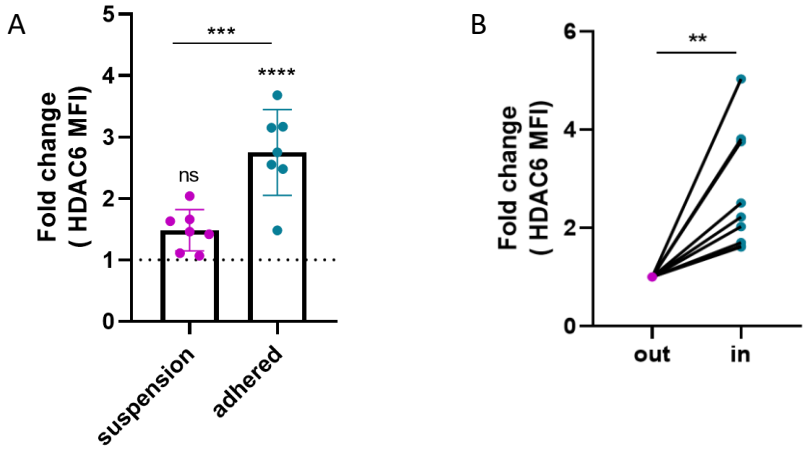

Figure 28. REH cells in contact with HS5 cells increase HDAC6 levels.

A) REH cells were stained with CFDA and added on top of a monolayer of HS5-MSC. After 24 h co-culture, REH cells in suspension were recovered and cells attached to HS5 cells were detached using TrypLE. HDAC6 levels were analyzed by flow cytometry and analyzed using FlowJo X software. Data are presented as fold change in comparison to REH cells cultured alone (dotted line, set to 1) ± SD. Significance was determined by one-way ANOVA using Graph Pad. n=3. B) HDAC6 levels in CFDA-stained REH cells were quantified after HS5-organoid co-cultures. Colonizing cells (in) expressed higher HDAC6 levels compared to non-colonizing cells (out). Data are presented as fold change in comparison to non-colonizing REH cells. Significance was determined by paired, two-tailed Student's t-test using Graph Pad. n=3. **p<0.01; ***p<0.001; ****p≤0.0001; ns, not significant.

These results were confirmed when analyzing B-ALL patient-derived cells. After adhesion to HS5-MSC, blasts from patients increased significantly HDAC6 levels, but cells in suspension did not show an increase (Fig. 29A). As well, patient-derived B-ALL cells that colonized BM-MSC organoids also significantly increased HDAC6 levels in comparison to cells that did not colonize the organoids. (Fig. 29B).

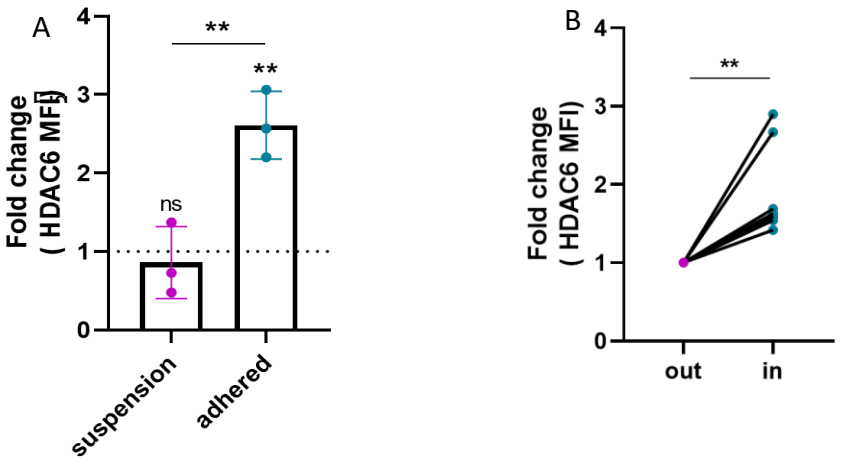

Figure 29. Patient-derived cells in contact with HS5 cells increase HDAC6 levels.

A) Patient-derived cells were stained with CFDA and co-cultured for 24 h with HS5-MSC. Cells in suspension and attached were recovered and HDAC6 levels were analyzed as described in Figure 28. Data are presented as fold change in comparison to patient cells cultured alone (dotted line, set to 1) ± SD. n=2. Significance was determined by one-way ANOVA using Graph Pad. B): HDAC6 levels were analyzed in CFDA-stained patient-derived cells in HS5-organoid colonizing (in) and non-colonizing cells (out). Data are presented as fold change in comparison to non-colonizing patient cells. n=3. Significance was determined by paired, two-tailed Student's t-test using Graph Pad. **p<0.01; ns, not significant.

Within the BM, the adhesion molecule VCAM-1 and the chemokine CXCL12 are expressed by MSCs and are important mediators of cell adhesion, retention, and mobilization, thus, we evaluated whether these molecules could be triggering HDAC6 upregulation in leukemic B cells. After culturing REH cells under the mentioned stimuli for 24 h, we quantified HDAC6 levels by flow cytometry, and found that both CXCL12 and adhesion to VCAM-1 slightly increase HDAC6 levels when comparing to non-stimulated REH cells. (Fig. 30).

Activin-A is a TGF-β family member produced by MSC which has recently been demonstrated to enhance the migratory properties of B-ALL cells. (Portale et al., 2019). When we analyzed HDAC6 levels in leukemic B cells after Activin-A stimulation, we also observed a modest increase (Fig. 30). However, none of these molecules led to an increase in HDAC6 levels as we observed in the 2D and 3D co-culture with MSC.

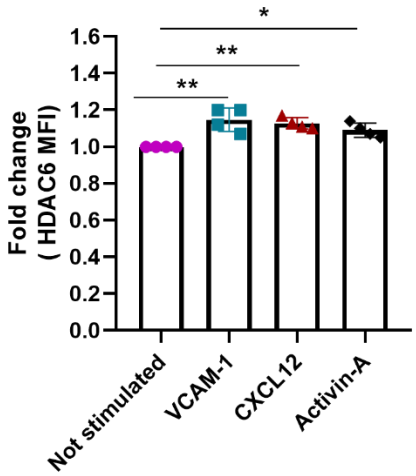

Figure 30. HDAC6 levels slightly increase in leukemic B cells after CXCL12, VCAM-1 and Activin-A stimulation.

REH cells were either seeded on top of VCAM-1-Fc (500 ng/mL) coated plates, cultured with CXCL12 (100 ng/mL) or with Activin-A (50 ng/mL). After 24 h, cells were recovered and HDAC6 levels were analyzed using a Cytek™Aurora cytometer and FlowJo X software. Data are presented as mean fluorescence intensity ± SD. n=4). Significance was determined by one-way ANOVA. *p<0.05; **p<0.01.

8.13 Tubastatin-A treatment in xenotransplanted mice inhibits leukemic B cell invasion and delays the signs of leukemia

Finally, we wanted to evaluate the potential clinical application of HDAC6 inhibition in a B-ALL model. To this end, we injected NSG male mice via the tail vein with 3 million REH cells and treated the mice with either vehicle or 50 mg/kg Tubastatin-A. The disease was established in all mice treated with DMSO after 24 days (weight loss, paralysis of posterior limbs, minor activity), whereas none of the Tubastatin-A-treated mice revealed any illness signs at the same time point. We sacrificed the mice and performed flow cytometry

analysis of the digested organs known to be targets for leukemic cells infiltration. Strikingly, Tubastatin-A strongly decreased the capacity of REH cells to engraft in the BM (Fig. 31A) and to invade the brain (Fig. 31D). These mice also showed a tendency to less percentage (but insignificant) of REH cells in PB (Fig. 31B), spleen (Fig. 31C) and lungs (Fig. 31F). Likewise, REH cells in the Tubastatin-A treated mice had significant decreased capacity to infiltrate the liver (Fig.31E) but did not present differences in testis (Fig. 31G).

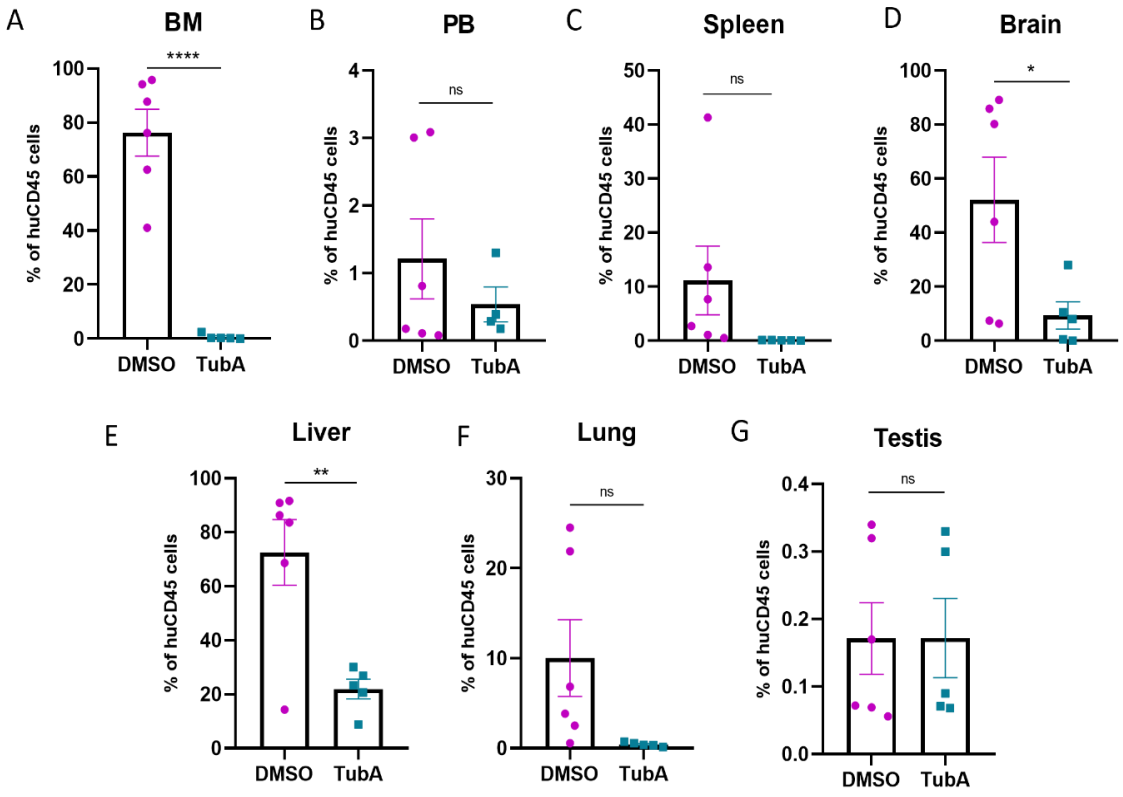

Figure 31. Tubastatin-A treatment in mice impaired leukemic B cells invasive capacity. REH-xenografted mice were treated by intraperitoneal injection with DMSO (n=6) or Tubastatin-A (50 mg/kg) (n=5) three days per week through 24 days. Bone marrow, brain, peripheral blood, spleen, lungs and testis were harvested and disaggregated. Cell suspensions were stained using anti-human APC-CD45 and anti-mouse FITC-CD45. Percentage of hCD45+ cells infiltrated in organs was analyzed from alive cells using a Cytek™Aurora cytometer. Data are represented as mean ± SEM. Significance was determined using unpaired, two-tailed Student's t-test. *p<0.05; **p<0.01; ****p≤0.0001; ns, not significant.

Importantly, populations of mCD45^{+} cells were mostly maintained in BM, lung, liver and testis of Tubastatin-A treated mice (Fig. 32A, 32B). Thus, our results highlight HDAC6 as a potential target for pharmacological inhibition to prevent organ infiltration in B-ALL patients.

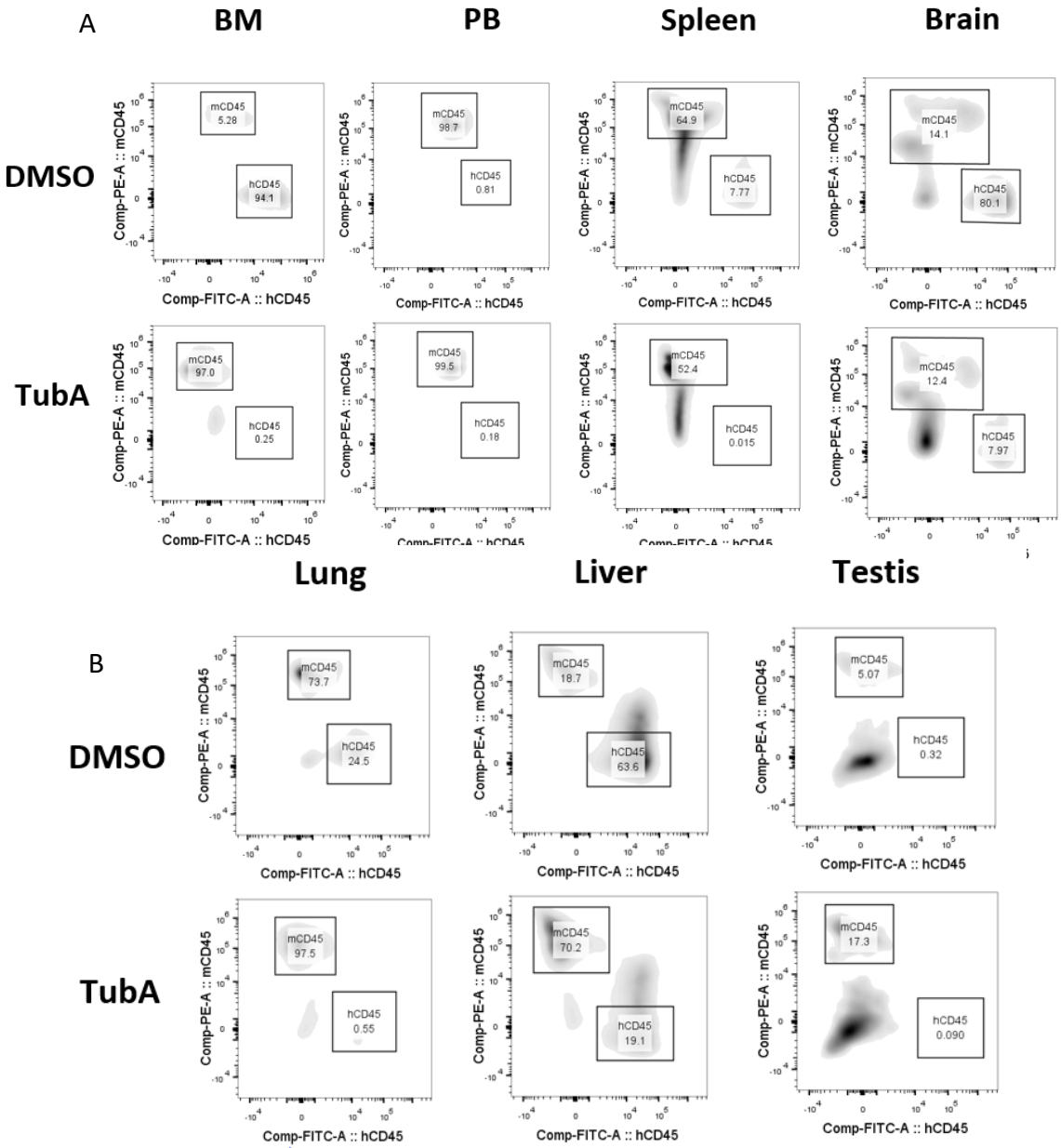

Figure 32. REH-xenografted mice were treated by intraperitoneal injection with DMSO or Tubastatin-A (50 mg/kg) three days per week through 24 days.
A, B) Representative density plots of each organ of DMSO and Tubastatin-A treated mice are shown. Percentage of hCD45 vs mCD45 positive cells are shown (of living cells).

9. DISCUSSION

HDAC6 overexpression has been detected in many solid tumors correlating with metastasis (Gao et al., 2007; Sakamoto & Aldana-Masangkay, 2011). In the context of leukemias, different studies revealed HDAC6 upregulation in B-CLL and AML (Bradbury et al., 2005; Maharaj et al., 2018; Pezzotta et al., 2022). Here, our investigation uncovered that the B-ALL cell line REH and patients with BM relapse exhibited higher HDAC6 levels in their leukemic B-cell precursors in comparison to healthy individuals. We also found that pharmacological inhibition of HDAC6 in a B-ALL xenotransplantation model strikingly reduced engraftment into the BM and organ infiltration of leukemic B cells, thus, we propose HDAC6 as a promising drug target in B-ALL.

In this project, we demonstrated that HDAC6 is localized in the cytoplasm of the pre-B ALL cell line REH. HDAC6 translocates to the cytoplasm due to the NES and SE14 motifs (Boyault et al., 2007), where it is able to participate in F-actin polymerization to modulate cell migration (Valenzuela-Fernández et al., 2008). In REH cells, HDAC6 co-localizes with cortactin. Cortactin stabilizes F-actin branches and is a substrate of HDAC6 (Zhang et al., 2007). High levels of cortactin were reported by our group in REH cells, where it correlated with increased migration and organ infiltration (Velázquez-Avila et al., 2018). Here, we found that in REH cells both HDAC6 and cortactin accumulate in the protrusions that are formed upon CXCL12 stimulation, suggesting that HDAC6 could be mediating cortactin activity by deacetylation to trigger cell migration as described before in epithelial cells (Zhang et al., 2007).

Few studies have investigated HDAC6 functions in leukemic cells. The AML cell lines HL60, K562 and KG1a had higher HDAC6 mRNA expression in comparison to $CD34^+$ mobilized peripheral blood cells (MPB), but protein levels and localization were not analyzed (Bradbury et al., 2005). The B-CLL cell lines OSU-CLL and Mec2 displayed more HDAC6 protein than normal healthy human primary B-cells (Maharaj et al., 2018). Importantly, we explored for the first time HDAC6 protein levels in the B-ALL cell line REH, which contained

higher HDAC6 levels compared to healthy $CD19^+$ B cells. This cell line was established from peripheral blood of a patient with BM relapse (Rosenfeld et al., 1977). Relapse can occur in the BM and in extramedullary sites, where leukemic cells can reach to get protection from systemic chemotherapy (Gaudichon et al., 2019), thus, we think that HDAC6 could be providing a migratory advantage.

HDACs induce multiple cellular and molecular processes through deacetylation of histone and nonhistone substrates, and dysregulation has been associated with cancer. Therefore, HDAC inhibitors have demonstrated promising therapeutic effects in solid and hematological cancer (Jenke et al., 2021). However, the lack of specificity of available pan-HDAC inhibitors led to global modification of acetylation levels in many substrates, which caused cytotoxic effects and adverse reactions in trial patients including thrombocytopenia, neutropenia, cardiac arrhythmia, and neurotoxicity (Bruserud et al., 2007). Therefore, those clinical trials had to be stopped. To overcome this problem, selective inhibitors for specific HDAC isoforms have been developed in the last few years, but only few specific HDAC6 inhibitors exist. Only tubacin has been examined before in the B ALL cell lines REH and Nalm-6, where an increase in acetyl-tubulin was reported. Moreover, tubacin treatment induced apoptosis and enhanced the effects of the chemotherapeutic agents vincristine, dexamethasone and L-asparaginase *in vitro* and *in vivo* (Aldana-Masangkay et al., 2011), suggesting that targeting HDAC6 could be an approach to treat B-ALL. In our project, we used for the first time Tubastatin-A to inhibit HDAC6 in B-acute lymphoblastic leukemic cells and observed increased acetylation levels of both cortactin and tubulin at dosages that did not induce cell death.

Post-translational modifications of cortactin and tubulin regulate cytoskeletal dynamics, thus their deacetylation by HDAC6 can control cell migration (Valenzuela-Fernández et al., 2008). Importantly, our TEM assays in response to CXCL12 revealed a significant impairment of REH cell migration upon HDAC6 inhibition with Tubastatin-A. These data resembled what we reported

with cortactin-knockdown REH cells. Cortactin knockdown leukemic cells were less able to accomplish TEM (Velázquez-Avila et al., 2018), which is in line with a previous report showing that cortactin needs to be deacetylated by HDAC6 to efficiently favor epithelial cells migration (Zhang et al., 2007). Our results also suggest that cortactin could be the main substrate through which HDAC6 regulates migration of B-ALL cells, because we did not find any differences in the transendothelial migration between cortactin knockdown cells and cortactin knockdown cells treated with Tubastatin-A. Our data using REH cells are also in line with another study showing that HDAC6 inhibition with Tubastatin-A reduced the ability of megakaryocytes to migrate towards CXCL12, due to reduced F-actin polymerization and increased cortactin acetylation (Messaoudi et al., 2017). Additionally, treatment with Trichostatin A (TSA), another HDAC6 inhibitor, in the T-ALL cell line CEM decreased their TEM capacity in response to CXCL12, which was also observed with HDAC6 knockdown lymphoblasts (Román Cabrero et al., 2006). Also, HDAC6 was found localized at protrusive structures at the leading edge of T lymphoblasts supporting the involvement of HDAC6 in the regulation of motility (Román Cabrero et al., 2006). Other HDAC6 inhibitors such as tubacin and niltubacin have been reported to inhibit CXCL12-induced motility of the Burkitt's lymphoma cell lines Raji and Namalwa by causing an increase in the acetylation level of tubulin (Ding et al., 2014). Thus, HDAC6 clearly controls migration of malignant T and B cells.

Cell migration is an essential process regulated by a variety of mechanisms including actin filament and microtubule dynamics (Yin et al., 2017). Microtubule growth occurs at the cell leading edge and microtubule shortening at the rear, and for an efficient turnover, depolymerized tubulin needs to be deacetylated by HDAC6 (Hubbert et al., 2002; Sakamoto & Aldana-Masangkay, 2011). This could be a mechanism through which HDAC6 inhibition affects TEM of REH cells. On the other hand, cortactin promotes actin filament formation by activating the Arp2/3 complex and stabilizing newly generated branched filaments that drive protrusions at the leading edge of migrating cells (Weaver et al., 2001). The tandem repeat region of cortactin is essential for F-actin

binding (Castellanos-Martínez et al., 2020). Of note, HDAC6 is able to deacetylate cortactin in the tandem repeat region to increase the affinity of cortactin for F-actin, with hyperacetylated cortactin having low affinity for F-actin leading to impaired cell migration (Zhang et al., 2007). In our investigation, we found that HDAC6 inhibition significantly affected F-actin polymerization induced by CXCL12, likely due to the observed increase in acetylated cortactin, suggesting that HDAC6-mediated deacetylation of cortactin is critical to stabilize new actin filaments in REH cells and potentiate migration.

Homing is the process where hematopoietic cells migrate into the BM (Caocci et al., 2017). CXCL12 is a chemokine required for optimal B-ALL *homing* (Juarez et al., 2009). Using a tridimensional organoid co-culture system consisting of bone marrow-stromal and leukemic B cells, we found that Tubastatin-A treatment of leukemic B cells strongly reduced their capacity to colonize the BM organoids, suggesting that HDAC6 deacetylase activity is needed for efficient BM homing. While HDAC6 has never been studied before in the context of lymphocyte homing, HDAC5 inhibition with LMK235 enhanced $CD34^+$ HSC homing. HDAC5 inhibition increased the acetylated levels of p65 in the CXCR4 promoter region leading to upregulation of CXCR4, which is the receptor for CXCL12 (Huang et al., 2018). These findings contrast with our data on HDAC6 inhibition. Possible explanations could be that HDAC5 is a nuclear protein and catalyzes the deacetylation of histones. As well, HDAC5 forms complexes with HDAC3 and HDAC4 and is involved in the regulation of apoptosis and glucose metabolism (Yang et al., 2021). Thus, HDAC5 and HDAC6 have different substrates affecting different signaling pathways in a specific manner.

High expression of CXCR4 and hyperactivation of the CXCL12/CXCR4 axis is involved in leukemic cell mobilization and disease progression (Chiarini et al., 2016b; Duarte et al., 2018; Shen et al., 2001; van den Berk et al., 2014). In our study, Tubastatin-A treatment for 24 hours reduced CXCR4 surface and total levels. Other reports have described that treatment with the pan-HDAC inhibitor

panobinostat reduced the mRNA and protein levels of CXCR4 in OCI-AML-3 and primary AML cells. CXCR4 is chaperoned by the heat shock protein 90 (HSP90) and panobinostat led to HSP90 hyperacetylation driving CXCR4 proteosomal degradation (Mandawat et al., 2010). Moreover, HDAC6 downregulation by siRNA in this cell line induced acetylation of HSP90 and interrupted its chaperone function, indicating that HSP90 is a HDAC6 substrate (Bali et al., 2005). Therefore, it would be important to study whether HSP90 is a substrate of HDAC6 in REH cells and verify the increase in HSP90 acetylation when using Tubastatin-A, which may explain the reduction in CXCR4 protein levels and provide better mechanistic understanding of HDAC6 functions in B-ALL.

In addition to CXCR4, HDAC6 could also be regulating cell surface levels of VLA-4 in REH cells, given our finding of reduced VLA-4 surface levels after 24 hours of Tubastatin-A treatment. Some studies reported HDAC6 association with endosomal compartments, where it controlled epidermal growth factor receptor (EGFR) trafficking through modulation of tubulin acetylation (Y. S. Gao et al., 2010). Additionally, HDAC6 is involved in IL-1β exocytosis in macrophages (Karnam et al., 2020) and regulates the movement and delivery of the lytic granules at the immune synapse in T cells (Núñez-Andrade et al., 2016). Thus, tubulin acetylation due to HDAC6 inhibition could be impairing microtubule-mediated vesicle transport in B-ALL cells, which needs to be unraveled in future studies. In agreement with our findings using Tubastatin-A in B-ALL cells, another group has shown that pan-HDAC inhibitors such as SAHA and VPA downregulate VLA-4 surface levels in HSC and AML cells, causing decreased adhesion to mesenchymal stromal cells (Mahlknecht & Schönbein, 2008). MPT0G413, a specific HDAC6 inhibitor, was also able to decrease the expression of VLA-4 in the multiple myeloma cells RPMI-8226 and NCI-H929 (Huang et al., 2019). As VLA-4 is essential for B-ALL cell survival and adhesion, positioning in BM niches and mobilization from the BM (Shalapour et al., 2011), HDAC6 inhibition could be affecting these important processes that control disease progression by reducing anchorage within the

BM and impairing VLA-4-mediated resistance to chemotherapy (Mahlknecht & Schönbein, 2008) .

Noteworthy, the exploited pharmacological approach here to inhibit HDAC6 blocks only the deacetylase activity of the enzyme (Weiss et al., 2007). However, HDAC6 still would be able to interact with binding partners, and thus, off-target effects may occur. Thus, it will be important to determine whether depletion of HDAC6 using a specific shRNA would yield the same results without potential off-target effects of Tubastatin-A.

HDAC6 overexpression has been described in AML patients, where it correlates with the expression of multidrug resistance genes such as the ATP Binding Cassette Subfamily C Member 1 (ABCC1) and the additional sex combs like-1 gene (ASXL1) (Pezzotta et al., 2022). Additionally, HDAC6 protein levels were higher in $CD19^{+}CD5^{+}$ cells from B-CLL patients compared to $CD19^{+}CD5^{-}$ cells from healthy donors, and also higher in $CD38^{+}$ patients than in $CD38^{-}$ patients. However, HDAC6 overexpression did not correlate with immunoglobulin heavy-chain variable (IGHV) region-mutated, the high risk factor ZAP70, or relapse (Maharaj et al., 2018). Similarly, in our study, we did not find a correlation between high HDAC6 protein levels and high risk debut patients. Usually, B-ALL patients are classified as standard risk or high risk based on age (Vrooman et al., 2018), which would not necessarily align with specific molecular characteristics. However, B-ALL cells from patients showed characteristic upregulation of both HDAC6 mRNA and protein in comparison to normal $CD19^{+}$ B cells, without any differences in $CD34^{+}CD19^{+}$ pro-B and $CD34^{-}CD19^{+}$ pre-B ALL patients. Strikingly, when we analyzed B-ALL cells from patients with relapse to the BM, our statistical analysis showed a positive correlation with highest HDAC6 levels in line with from our data using the cell line REH that is derived from a relapse patient. Of note, we were able to follow four patients from debut to relapse and found that leukemic B cells showed increased HDAC6 levels at relapse compared to debut. Three of these four relapsed patients exhibited higher HDAC6 levels at debut in comparison to

other non-relapsed patients from our cohort indicating that relapse could arise from HDAC6^{high} clones. High HDAC6 levels also correlated positively with whole white blood cell numbers and platelets. Importantly, platelets enhance adhesion of leukemic cells to other platelets and facilitate metastasis, therefore organ infiltration could also be related to high platelet levels (Zhang et al., 2022). Furthermore, HDAC6 is needed by patient-derived blasts to efficiently migrate because HDAC6 inhibition in patient-derived cells reduced their high migratory activity in TEM and BM-organoid colonization assays, similar to what we found using REH cells. Taken together, we think that HDAC6 drives organ infiltration, but it will be important to confirm whether those patients with the highest HDAC6 levels will always suffer infiltration to CNS or other organs.

We were also interested in investigating whether HDAC6 levels in PB-derived leukemic cells would be higher than in BM-derived cells, as those cells mobilized into the blood circulation are the ones that eventually extravasate into organs. However, we detected that BM-derived blasts from patients possessed the higher HDAC6 levels compared to PB-derived blasts. Surprisingly, PB-derived cells from relapse patients had higher HDAC6 levels than PB-cells derived from debut patients and control individuals, which could be providing a migratory advantage to colonize extramedullary organs that may evade clinical detection.

Communication of leukemic cells with MSC in the BM is an important mediator of disease progression in leukemia and other hematological diseases (Yamaguchi et al., 2021). Importantly, it has been demonstrated that adhesion of mantle cell lymphoma (MCL) and other non-Hodgkin lymphoma cells to HS5-MSC triggers and sustains c-myc activation and miR-548m downregulation, leading to HDAC6 upregulation (Lwin et al., 2013). When we performed co-culture assays in a 2D- and 3D-model using HS5-MSC with either REH cells or patient-derived blasts, we observed that HDAC6 levels were significantly increased in leukemic B cells adhered to the stroma and inside the BM-organoids. Thus, it will be important to analyze whether c-myc activation is

being exploited in the B-ALL niche to drive HDAC6 upregulation in leukemic B cells. We therefore hypothesize that BM-MSC interactions (via VLA-4 and CXCR4) induce the synthesis of HDAC6 in B-ALL cells and that, within leukemic B cells population, this sub-population is prone to mobilization and migration.

Survival of B-ALL cells is also promoted by their interaction with BM-MSC, where the VLA-4 integrin subunits alpha-4 and beta-1 mediate homing of leukemic B cells to the BM, retention and chemoresistance (Härzschel et al., 2020; Shabnam et al., 2011; Shishido et al., 2014). Other studies have shown that imatinib-insensitive CML stem cells ($CD34^{+}CD38^{-}$) overexpress HDAC6 compared to CML cells (Losson et al., 2020), and that the pan-HDAC inhibitor SAHA sensitizes CML stem cells to the therapeutic effect of imatinib (Bamodu et al., 2018). Therefore, our findings using Tubastatin-A support the idea that HDAC6 inhibition could also enhance the sensitivity of leukemic B cells to chemotherapy and overcome resistance induced by interactions with the bone marrow microenvironment. Additionally, it would be relevant to investigate the role of HDAC6 in B-ALL leukemia stem cells.

Finally, we tested whether targeting HDAC6 could reduce organ infiltration in a xenotransplantation model of B-ALL. We found that Tubastatin-A treatment in mice significantly reduced leukemic B cell engraftment in the BM and infiltration of different extramedullary organs, processes that usually lead to fatal disease outcomes.

The minimal leukemic B cell engraftment in the BM could also explain the reduction in organ infiltration, as leukemic B cells must engraft first in the BM before starting to proliferate and then exit to peripheral blood. Tubastatin-A has been investigated by others in *in vivo* models, such as breast cancer (Hsieh et al., 2019; Kozyreva et al., 2014), ovarian cancer (Depetter et al., 2019) and squamous cell carcinoma (Zhang & Gan, 2017), where it minimized the degree of metastasis in agreement with our results.

To date, five compounds that inhibit HDACs have been approved by the United States Food and Drug Administration: vorinostat (pan-HDACi), romidepsin (class I HDACi), panobinostat (pan-HDACi), belinostat (pan-HDACi), and tucidinostat (class I and II HDACi). Principally, these HDAC inhibitors have been clinically successful in hematological malignancies, such as T-cell lymphomas and multiple myeloma (Bondarev et al., 2021). Tubastatin-A has been tested only in preclinical investigations by others and us. However, although showing promising results, this compound has demonstrated reduced bioavailability and has not been optimized for oral delivery, thus difficulting evaluation in clinical trials. Currently, among HDAC6 inhibitors, only ricolinostat (ACY-1215) is being tested in phase I and II clinical trials for multiple myeloma and non-Hodgkin lymphomas as monotherapy and in combination with other drugs. Synergistic activity was observed when ricolinostat was used in combination with dexamethasone and the proteasome inhibitors bortezomib and carfilzomib, demonstrating a low toxicity profile (Cosenza & Pozzi, 2018). Whether pan-HDAC or HDAC6 inhibitors could be used for treatment alone or applied in combination therapy for those B-ALL patients displaying high HDAC6 levels and organ infiltration will be important to unravel in future clinical studies. It will also be relevant to determine whether the approved HDAC6 inhibitor ricolinostat could be used to treat B-ALL.

Taken together, our findings highlight HDAC6 as a biomarker for relapse prediction and as a promising drug target to impair cell migration and organ infiltration in B-ALL.

10. CONCLUSION

Pharmacological inhibition of HDAC6 robustly reduced the abilities of leukemic B cells to transmigrate, engraft in the BM and infiltrate extramedullary organs, likely through the regulation of cortactin acetylation and actin polymerization. HDAC6 levels were higher in B-ALL patients than in healthy individuals, with highest amounts positively correlating with relapse, thus demonstrating the pathological relevance of HDAC6 as a biomarker for relapse prediction in B-ALL. We propose HDAC6 as new therapeutic target for B-ALL patients to prevent organ infiltration during relapse and improve the clinical outcome of patients at high risk of suffering relapse.

11. PERSPECTIVES

-To generate HDAC6 knockdown REH cells to confirm our data using Tubastatin-A and control off-target effects of HDAC6 inhibitors *in vitro* and *in vivo*.
-To confirm whether Tubastatin-A-mediated CXCR4 downregulation is regulated by the acetylation of the chaperone HSP90.
-To test whether HDAC6 is needed for microtubule-mediated vesicle transport in B-ALL cells.
-To investigate the mechanism that triggers HDAC6 upregulation in B-ALL cells in the BM.
-To validate HDAC6 RNAseq data from B-ALL patients by performing qRT-PCR in patient-derived cells.
-To analyze acetyl-cortactin and acetyl-tubulin status in B-ALL cells from patients, and correlate them with HDAC6 levels.
-To unravel whether those patients with the highest HDAC6 levels at debut suffer relapse and organ infiltration.
-To explore whether HDAC6 inhibitors can sensitize chemotherapy-resistant B-ALL cells.
-To initiate clinical trials and test whether HDAC6 inhibitors could be used as sole treatment or in combination therapy in B-ALL patients.

12. REFERENCES

Aldana-Masangkay, G. I., Rodriguez-Gonzalez, A., Lin, T., Ikeda, A. K., Hsieh, Y.-T., Kim, Y.-M., Lomenick, B., Okemoto, K., Landaw, E. M., Wang, D., Mazitschek, R., Bradner, J. E., & Sakamoto, K. M. (2011). Tubacin suppresses proliferation and induces apoptosis of acute lymphoblastic leukemia cells. *Leukemia & Lymphoma*, *52*(8), 1544–1555. https://doi.org/10.3109/10428194.2011.570821

Balandrán, J. C., Dávila-Velderrain, J., Sandoval-Cabrera, A., Zamora-Herrera, G., Terán-Cerqueda, V., García-Stivalet, L. A., Limón-Flores, J. A., Armenta-Castro, E., Rodríguez-Martínez, A., Leon-Chavez, B. A., Vallejo-Ruiz, V., Hassane, D. C., Pérez-Tapia, S. M., Ortiz-Navarrete, V., Guzman, M. L., & Pelayo, R. (2021). Patient-Derived Bone Marrow Spheroids Reveal Leukemia-Initiating Cells Supported by Mesenchymal Hypoxic Niches in Pediatric B-ALL. *Frontiers in Immunology*, *12*. https://doi.org/10.3389/fimmu.2021.746492

Balandrán, J. C., Purizaca, J., Enciso, J., Dozal, D., Sandoval, A., Jiménez-Hernández, E., Alemán-Lazarini, L., Perez-Koldenkova, V., del Prado, H. Q. N., de los Ríos, J. R., Mayani, H., Ortiz-Navarrete, V., Guzman, M. L., & Pelayo, R. (2017). Pro-inflammatory-related loss of CXCL12 niche promotes acute lymphoblastic leukemic progression at the expense of normal lymphopoiesis. *Frontiers in Immunology*, *7*(JAN), 1–14. https://doi.org/10.3389/fimmu.2016.00666

Balandrán, J. C., Vadillo, E., Dozal, D., Reyes-López, A., Sandoval-Cabrera, A., Laffont-Ortiz, M. D., Prieto-Chávez, J. L., Vilchis-Ordoñez, A., Quintela-Nuñez del Prado, H., Mayani, H., Núñez-Enríquez, J. C., Mejía-Aranguré, J. M., López-Martínez, B., Jiménez-Hernández, E., & Pelayo, R. (2016). Analysis of Normal Hematopoietic Stem and Progenitor Cell Contents in Childhood Acute Leukemia Bone Marrow. *Archives of Medical Research*, *47*(8), 629–643. https://doi.org/10.1016/j.arcmed.2016.12.004

Bali, P., Pranpat, M., Bradner, J., Balasis, M., Fiskus, W., Guo, F., Rocha, K., Kumaraswamy, S., Boyapalle, S., Atadja, P., Seto, E., & Bhalla, K. (2005). Inhibition of Histone Deacetylase 6 Acetylates and Disrupts the Chaperone Function of Heat Shock Protein 90: A NOVEL BASIS FOR ANTILEUKEMIA ACTIVITY OF HISTONE DEACETYLASE INHIBITORS*. *Journal of Biological Chemistry*, *280*(29), 26729–26734. https://doi.org/https://doi.org/10.1074/jbc.C500186200

Bamodu, O. A., Kuo, K. T., Yuan, L. P., Cheng, W. H., Lee, W. H., Ho, Y. S., Chao, T. Y., & Yeh, C. T. (2018). HDAC inhibitor suppresses proliferation and tumorigenicity of drug-resistant chronic myeloid leukemia stem cells through regulation of hsa-miR-196a targeting BCR/ABL1. *Experimental Cell Research*, *370*(2), 519–530. https://doi.org/10.1016/j.yexcr.2018.07.017

Bazzaro, M., Lin, Z., Santillan, A., Lee, M. K., Wang, M. C., Chan, K. C., Bristow, R. E., Mazitschek, R., Bradner, J., & Roden, R. B. S. (2008). Ubiquitin proteasome system stress underlies synergistic killing of ovarian cancer cells by bortezomib and a novel HDAC6 inhibitor. *Clinical Cancer Research*, *14*(22), 7340–7347. https://doi.org/10.1158/1078-0432.CCR-08-0642

Bhojwani, D., & Pui, C. H. (2013). Relapsed childhood acute lymphoblastic leukaemia. *The Lancet Oncology*, *14*(6), e205–e217. https://doi.org/10.1016/S1470-2045(12)70580-6

Biolegend. (2020). *Pacific Blue™ Annexin V Apoptosis Detection Kit with PI*. www.biolegend.com

Bondarev, A. D., Attwood, M. M., Jonsson, J., Chubarev, V. N., Tarasov, V. V., & Schiöth, H. B. (2021). Recent developments of HDAC inhibitors: Emerging indications and novel molecules. In *British Journal of Clinical Pharmacology* (Vol. 87, Issue 12, pp. 4577–4597). John Wiley and Sons Inc. https://doi.org/10.1111/bcp.14889

Boyault, C., Sadoul, K., Pabion, M., & Khochbin, S. (2007). HDAC6, at the crossroads between cytoskeleton and cell signaling by acetylation and ubiquitination. In *Oncogene* (Vol. 26, Issue 37, pp. 5468–5476). https://doi.org/10.1038/sj.onc.1210614

Bradbury, C. A., Khanim, F. L., Hayden, R., Bunce, C. M., White, D. A., Drayson, M. T., Craddock, C., & Turner, B. M. (2005). Histone deacetylases in acute myeloid leukaemia show a distinctive pattern of expression that changes selectively in response to deacetylase inhibitors. *Leukemia*, *19*(10), 1751–1759. https://doi.org/10.1038/sj.leu.2403910

Bruserud, Ø., Stapnes, C., Ersvaer, E., Gjertsen, B. T., & Ryningen, A. (2007). Histone deacetylase inhibitors in cancer treatment: a review of the clinical toxicity and the modulation of gene expression in cancer cell. *Current Pharmaceutical Biotechnology*, *8*(6), 388—400. https://doi.org/10.2174/138920107783018417

Butler, K. V., Kalin, J., Brochier, C., Vistoli, G., Langley, B., & Kozikowski, A. P. (2010). Rational design and simple chemistry yield a superior, neuroprotective HDAC6 inhibitor, tubastatin A. *Journal of the American Chemical Society*. https://doi.org/10.1021/ja102758v

Caocci, G., Greco, M., & La Nasa, G. (2017). Bone marrow homing and engraftment defects of human hematopoietic stem and progenitor cells. In *Mediterranean Journal of Hematology and Infectious Diseases* (Vol. 9, Issue 1). Universita Cattolica del Sacro Cuore. https://doi.org/10.4084/MJHID.2017.032

Castellanos-Martínez, R., Jiménez-Camacho, K. E., & Schnoor, M. (2020). Cortactin Expression in Hematopoietic Cells. *The American Journal of Pathology*, *190*(5), 958–967. https://doi.org/10.1016/j.ajpath.2019.12.011

Chatterjee, S., Behnam Azad, B., & Nimmagadda, S. (2014). The intricate role of CXCR4 in cancer. In *Advances in Cancer Research* (1st ed., Vol. 124). Elsevier Inc. https://doi.org/10.1016/B978-0-12-411638-2.00002-1

Cheng, Y., Qu, J., Che, X., Xu, L., Song, N., Ma, Y., Gong, J., Qu, X., & Liu, Y. (2017). CXCL12/SDF-1α induces migration via SRC-mediated CXCR4-EGFR cross-talk in gastric cancer cells. *Oncology Letters*, *14*(2), 2103–2110. https://doi.org/10.3892/ol.2017.6389

Chiaretti, S., Zini, G., & Bassan, R. (2014). Diagnosis and subclassification of acute lymphoblastic leukemia. *Mediterranean Journal of Hematology and Infectious Diseases*, *6*(1). https://doi.org/10.4084/mjhid.2014.073

Chiarini, F., Lonetti, A., Evangelisti, C., Buontempo, F., Orsini, E., Evangelisti, C., Cappellini, A., Neri, L. M., McCubrey, J. A., & Martelli, A. M. (2016a). Advances

in understanding the acute lymphoblastic leukemia bone marrow microenvironment: From biology to therapeutic targeting. *Biochimica et Biophysica Acta - Molecular Cell Research*, *1863*(3), 449–463. https://doi.org/10.1016/j.bbamcr.2015.08.015

Chiarini, F., Lonetti, A., Evangelisti, C., Buontempo, F., Orsini, E., Evangelisti, C., Cappellini, A., Neri, L. M., McCubrey, J. A., & Martelli, A. M. (2016b). Advances in understanding the acute lymphoblastic leukemia bone marrow microenvironment: From biology to therapeutic targeting. *Biochimica et Biophysica Acta - Molecular Cell Research*, *1863*(3), 449–463. https://doi.org/10.1016/j.bbamcr.2015.08.015

Choudhary, C., Choudhary, C., Kumar, C., Gnad, F., Nielsen, M. L., Rehman, M., Walther, T. C., Olsen, J. V, & Mann, M. (2009). Lysine Acetylation Targets Protein Complexes and Co-Regulates Major (suppli).pdf. *Science*, *325*(August), 834–840. https://doi.org/10.1126/science.1175371

Cobaleda, C., & Sánchez-García, I. (2009). B-cell acute lymphoblastic leukaemia: Towards understanding its cellular origin. *BioEssays*, *31*(6), 600–609. https://doi.org/10.1002/bies.200800234

Cojoc, M., Peitzsch, C., Trautmann, F., Polishchuk, L., Telegeev, G. D., & Dubrovska, A. (2013). Emerging targets in cancer management: Role of the CXCL12/CXCR4 axis. In *OncoTargets and Therapy* (Vol. 6, pp. 1347–1361). https://doi.org/10.2147/OTT.S36109

Congrains, A., Bianco, J., Rosa, R. G., Mancuso, R. I., & Saad, S. T. O. (2021). 3D Scaffolds to Model the Hematopoietic Stem Cell Niche: Applications and Perspectives. *Materials*, *14*(3). https://doi.org/10.3390/ma14030569

Cooper, S. L., & Brown, P. A. (2015). Treatment of pediatric acute lymphoblastic leukemia. In *Pediatric Clinics of North America* (Vol. 62, Issue 1, pp. 61–73). W.B. Saunders. https://doi.org/10.1016/j.pcl.2014.09.006

Cosen-Binker, L. I. (2006). Cortactin: The Gray Eminence of the Cytoskeleton. *Physiology*, *21*(5), 352–361. https://doi.org/10.1152/physiol.00012.2006

Cosenza, M., & Pozzi, S. (2018). The therapeutic strategy of HDAC6 inhibitors in lymphoproliferative disease. In *International Journal of Molecular Sciences* (Vol. 19, Issue 8). MDPI AG. https://doi.org/10.3390/ijms19082337

Crazzolara, R., Kreczy, a, Mann, G., Heitger, a, Eibl, G., Fink, F. M., Möhle, R., & Meister, B. (2001). High expression of the chemokine receptor CXCR4 predicts extramedullary organ infiltration in childhood acute lymphoblastic leukaemia. *British Journal of Haematology*, *115*(3), 545–553. https://doi.org/10.1046/j.1365-2141.2001.03164.x

Daly, R. J. (2004). Cortactin signalling and dynamic actin networks. In *Biochemical Journal*. https://doi.org/10.1042/BJ20040737

Dander, E., Palmi, C., D'Amico, G., & Cazzaniga, G. (2021). The Bone Marrow Niche in B-Cell Acute Lymphoblastic Leukemia: The Role of Microenvironment from Pre-Leukemia to Overt Leukemia. *International Journal of Molecular Sciences*, *22*(9). https://doi.org/10.3390/ijms22094426

Depetter, Y., Geurs, S., De Vreese, R., Goethals, S., Vandoorn, E., Laevens, A., Steenbrugge, J., Meyer, E., de Tullio, P., Bracke, M., D'hooghe, M., & De Wever, O. (2019). Selective pharmacological inhibitors of HDAC6 reveal

biochemical activity but functional tolerance in cancer models. *International Journal of Cancer*, *145*(3), 735–747. https://doi.org/10.1002/ijc.32169

Ding, L., & Morrison, S. J. (2013). Haematopoietic stem cells and early lymphoid progenitors occupy distinct bone marrow niches. *Nature*, *495*(7440), 231–235. https://doi.org/10.1038/nature11885

Ding, N., Ping, L., Feng, L., Zheng, X., Song, Y., & Jun, Z. (2014a). Histone deacetylase 6 activity is critical for the metastasis of Burkitt s lymphoma cells. *Cancer Cell International*, *14*(1). https://doi.org/10.1186/s12935-014-0139-z

Ding, N., Ping, L., Feng, L., Zheng, X., Song, Y., & Jun, Z. (2014b). Histone deacetylase 6 activity is critical for the metastasis of Burkitt s lymphoma cells. *Cancer Cell International*, *14*(1). https://doi.org/10.1186/s12935-014-0139-z

Doan, P. L., & Chute, J. P. (2012). The vascular niche: Home for normal and malignant hematopoietic stem cells. *Leukemia*, *26*(1), 54–62. https://doi.org/10.1038/leu.2011.236

Dobson, S. M., García-Prat, L., Vanner, R. J., Wintersinger, J., Waanders, E., Gu, Z., McLeod, J., Gan, O. I., Grandal, I., Payne-Turner, D., Edmonson, M. N., Ma, X., Fan, Y., Voisin, V., Chan-Seng-Yue, M., Xie, S. Z., Hosseini, M., Abelson, S., Gupta, P., … Dick, J. E. (2020). Relapse-fated latent diagnosis subclones in acute B lineage leukemia are drug tolerant and possess distinct metabolic programs. *Cancer Discovery*, *10*(4), 568–587. https://doi.org/10.1158/2159-8290.CD-19-1059

Duarte, D., Hawkins, E. D., & Lo Celso, C. (2018). The interplay of leukemia cells and the bone marrow microenvironment. *Blood*, *131*(14), blood-2017-12-784132. https://doi.org/10.1182/blood-2017-12-784132

Ebinger, S., Özdemir, E. Z., Ziegenhain, C., Tiedt, S., Castro Alves, C., Grunert, M., Dworzak, M., Lutz, C., Turati, V. A., Enver, T., Horny, H. P., Sotlar, K., Parekh, S., Spiekermann, K., Hiddemann, W., Schepers, A., Polzer, B., Kirsch, S., Hoffmann, M., … Jeremias, I. (2016a). Characterization of Rare, Dormant, and Therapy-Resistant Cells in Acute Lymphoblastic Leukemia. *Cancer Cell*, *30*(6), 849–862. https://doi.org/10.1016/j.ccell.2016.11.002

Ebinger, S., Özdemir, E. Z., Ziegenhain, C., Tiedt, S., Castro Alves, C., Grunert, M., Dworzak, M., Lutz, C., Turati, V. A., Enver, T., Horny, H. P., Sotlar, K., Parekh, S., Spiekermann, K., Hiddemann, W., Schepers, A., Polzer, B., Kirsch, S., Hoffmann, M., … Jeremias, I. (2016b). Characterization of Rare, Dormant, and Therapy-Resistant Cells in Acute Lymphoblastic Leukemia. *Cancer Cell*, *30*(6), 849–862. https://doi.org/10.1016/j.ccell.2016.11.002

Force, L. M., Abdollahpour, I., Advani, S. M., Agius, D., Ahmadian, E., Alahdab, F., Alam, T., Alebel, A., Alipour, V., Allen, C. A., Almasi-Hashiani, A., Alvarez, E. M., Amini, S., Amoako, Y. A., Anber, N. H., Arabloo, J., Artaman, A., Atique, S., Awasthi, A., … Bhakta, N. (2019). The global burden of childhood and adolescent cancer in 2017: an analysis of the Global Burden of Disease Study 2017. *The Lancet Oncology*, *20*(9), 1211–1225. https://doi.org/10.1016/S1470-2045(19)30339-0

Frenette, P. S., Subbarao, S., Mazo, I. B., von Andrian, U. H., & Wagner, D. D. (1998). Endothelial selectins and vascular cell adhesion molecule-1 promote hematopoietic progenitor homing to bone marrow. *Proceedings of the National*

Academy of Sciences, *95*(24), 14423–14428. https://doi.org/10.1073/pnas.95.24.14423

Friedl, P., & Wolf, K. (2003). Tumour-cell invasion and migration: diversity and escape mechanisms. *Nature Reviews Cancer*, *3*(5), 362–374. https://doi.org/10.1038/nrc1075

Frishman-Levy, L., Shemesh, A., Bar-Sinai, A., Ma, C., Ni, Z., Frenkel, S., Muench, V., Bruckmueller, H., Vokuhl, C., Debatin, K. M., Eckert, C., Stanulla, M., Schrappe, M., Campbell, K. S., Loewenthal, R., Schewe, D. M., Hochman, J., Meyer, L. H., Kaufman, D., … Izraeli, S. (2015). Central nervous system acute lymphoblastic leukemia: Role of natural killer cells. *Blood*, *125*(22), 3420–3431. https://doi.org/10.1182/blood-2014-08-595108

Gattazzo, C., Martini, V., Frezzato, F., Trimarco, V., Tibaldi, E., Castelli, M., Facco, M., Zonta, F., Brunati, A. M., Zambello, R., Semenzato, G., & Trentin, L. (2014). Cortactin, another player in the Lyn signaling pathway, is over-expressed and alternatively spliced in leukemic cells from patients with B-cell chronic lymphocytic leukemia. *Haematologica*, *99*(6), 1069–1077. https://doi.org/10.3324/haematol.2013.090183

Gaudichon, J., Jakobczyk, H., Debaize, L., Cousin, E., Galibert, M. D., Troadec, M. B., & Gandemer, V. (2019). Mechanisms of extramedullary relapse in acute lymphoblastic leukemia: Reconciling biological concepts and clinical issues. In *Blood Reviews* (Vol. 36, pp. 40–56). Churchill Livingstone. https://doi.org/10.1016/j.blre.2019.04.003

Gaynon, P. S. (2005). Childhood acute lymphoblastic leukaemia and relapse. *British Journal of Haematology*, *131*(5), 579–587. https://doi.org/10.1111/j.1365-2141.2005.05773.x

Glozak, M. A., & Seto, E. (2007). Histone deacetylases and cancer. In *Oncogene* (Vol. 26, Issue 37, pp. 5420–5432). https://doi.org/10.1038/sj.onc.1210610

Gong, P., Wang, Y., & Jing, Y. (2019). Apoptosis Induction byHistone Deacetylase Inhibitors in Cancer Cells: Role of Ku70. *International Journal of Molecular Sciences*, *20*(7). https://doi.org/10.3390/ijms20071601

Gossai, N. P., & Gordon, P. M. (2017). The Role of the Central Nervous System Microenvironment in Pediatric Acute Lymphoblastic Leukemia. *Frontiers in Pediatrics*, *5*(April), 1–8. https://doi.org/10.3389/fped.2017.00090

Greaves, M. (2018). A causal mechanism for childhood acute lymphoblastic leukaemia. *Nature Reviews Cancer*, 1. https://doi.org/10.1038/s41568-018-0015-6

Greaves, M. F., & Wiemels, J. (2003). Origins of chromosome translocations in childhood leukaemia. *Nature Reviews Cancer*, *3*, 639.

Haberland, M., Montgomery, R. L., & Olson, E. N. (2011). Physiology : Implications for Disease and Therapy. *Nature Reviews. Genetics*, *10*(1), 32–42. https://doi.org/10.1038/nrg2485.The

Haggarty, S. J., Koeller, K. M., Wong, J. C., Grozinger, C. M., & Schreiber, S. L. (2003). *Domain-selective small-molecule inhibitor of histone deacetylase 6 (HDAC6)-mediated tubulin deacetylation*. www.pnas.orgcgidoi10.1073pnas.0430973100

Hai, Y., & Christianson, D. W. (2016). Histone deacetylase 6 structure and molecular basis of catalysis and inhibition. *Nature Chemical Biology*, *12*(9), 741–747. https://doi.org/10.1038/nchembio.2134

Hard, R. L., Liu, J., Shen, J., Zhou, P., & Pei, D. (2010). HDAC6 and Ubp-M BUZ domains recognize specific C-terminal sequences of proteins. *Biochemistry*, *49*(50), 10737–10746. https://doi.org/10.1021/bi101014s

Härzschel, A., Zucchetto, A., Gattei, V., & Hartmann, T. N. (2020). VLA-4 Expression and Activation in B Cell Malignancies: Functional and Clinical Aspects. In *International Journal of Molecular Sciences* (Vol. 21, Issue 6). MDPI. https://doi.org/10.3390/ijms21062206

Hasan, M. K., Rassenti, L., Widhopf, G. F., Yu, J., & Kipps, T. J. (2019). Wnt5a causes ROR1 to complex and activate cortactin to enhance migration of chronic lymphocytic leukemia cells. *Leukemia*, *33*(3), 653–661. https://doi.org/10.1038/s41375-018-0306-7

Heazlewood, S. Y., Oteiza, A., Cao, H., & Nilsson, S. K. (2014). Analyzing hematopoietic stem cell homing, lodgment, and engraftment to better understand the bone marrow niche. *Annals of the New York Academy of Sciences*, *1310*(1), 119–128. https://doi.org/10.1111/nyas.12329

Hofmann, F. B., Board, E., Beavo, J. A., Barrett, J. E., Ganten, D., Geppetti, P., Michel, M. C., Page, C. P., & Rosenthal, W. (2011). *Histone Deacetylases: the Biology and Clinical Implication* (Vol. 206). https://doi.org/10.1007/978-3-642-21631-2

Hsieh, Y.-L., Tu, H.-J., Pan, S.-L., Liou, J.-P., & Yang, C.-R. (2019). Anti-metastatic activity of MPT0G211, a novel HDAC6 inhibitor, in human breast cancer cells in vitro and in vivo. *Biochimica et Biophysica Acta (BBA) - Molecular Cell Research*, *1866*(6), 992–1003. https://doi.org/https://doi.org/10.1016/j.bbamcr.2019.03.003

Huang, C., Liu, J., Haudenschild, C. C., & Zhan, X. (1998). The role of tyrosine phosphorylation of cortactin in the locomotion of endothelial cells. *Journal of Biological Chemistry*, *273*(40), 25770–25776. https://doi.org/10.1074/jbc.273.40.25770

Huang, F. L., Liao, E. C., Li, C. L., Yen, C. Y., & Yu, S. J. (2020). Pathogenesis of pediatric B-cell acute lymphoblastic leukemia: Molecular pathways and disease treatments (Review). *Oncology Letters*, *20*(1), 448–454. https://doi.org/10.3892/ol.2020.11583

Huang, X., Guo, B., Liu, S., Wan, J., & Broxmeyer, H. E. (2018). Neutralizing negative epigenetic regulation by HDAC5 enhances human haematopoietic stem cell homing and engraftment. *Nature Communications*, *9*(1). https://doi.org/10.1038/s41467-018-05178-5

Hubbert, C., Guardiola, A., Shao, R., Kawaguchi, Y., Ito, A., Nixon, A., Yoshida, M., Wang, X.-F., & Yao, T.-P. (2002). HDAC6 is a microtubule-associated deacetylase. *Nature*, *417*(6887), 455–458. https://doi.org/10.1038/417455a

Infante, E., & Ridley, A. J. (2013). Roles of Rho GTPases in leucocyte and leukaemia cell transendothelial migration. In *Philosophical Transactions of the Royal Society B: Biological Sciences* (Vol. 368, Issue 1629). https://doi.org/10.1098/rstb.2013.0013

Itkin, T., Gur-Cohen, S., Spencer, J. A., Schajnovitz, A., Ramasamy, S. K., Kusumbe, A. P., Ledergor, G., Jung, Y., Milo, I., Poulos, M. G., Kalinkovich, A., Ludin, A., Kollet, O., Shakhar, G., Butler, J. M., Rafii, S., Adams, R. H., Scadden, D. T., Lin, C. P., & Lapidot, T. (2016). Distinct bone marrow blood vessels differentially regulate haematopoiesis. *Nature*, *532*(7599), 323–328. https://doi.org/10.1038/nature17624

Jabbour, E. J., Faderl, S., & Kantarjian, H. M. (2005). Adult acute lymphoblastic leukemia. *Mayo Clinic Proceedings*, *80*(11), 1517–1527. https://doi.org/10.4065/80.11.1517

Jacamo, R., Chen, Y., Wang, Z., Ma, W., Zhang, M., Spaeth, E. L., Wang, Y., Battula, V. L., Mak, P. Y., Schallmoser, K., Ruvolo, P., Schober, W. D., Shpall, E. J., Nguyen, M. H., Strunk, D., Bueso-Ramos, C. E., Konoplev, S., Davis, R. E., Konopleva, M., & Andreeff, M. (2014). *Reciprocal leukemia-stroma VCAM-1/VLA-4-dependent activation of NF-kB mediates chemoresistance Key Points*. https://doi.org/10.1182/blood-2013-06

Jenke, R., Reßing, N., Hansen, F. K., Aigner, A., & Büch, T. (2021). Anticancer Therapy with HDAC Inhibitors: Mechanism-Based Combination Strategies and Future Perspectives. *Cancers*, *13*(4). https://doi.org/10.3390/cancers13040634

Juarez, J. G., Thien, M., Dela Pena, A., Baraz, R., Bradstock, K. F., & Bendall, L. J. (2009). CXCR4 mediates the homing of B cell progenitor acute lymphoblastic leukaemia cells to the bone marrow via activation of p38MAPK. *British Journal of Haematology*, *145*(4), 491–499. https://doi.org/https://doi.org/10.1111/j.1365-2141.2009.07648.x

Kaluza, D., Kroll, J., Gesierich, S., Yao, T. P., Boon, R. A., Hergenreider, E., Tjwa, M., Rössig, L., Seto, E., Augustin, H. G., Zeiher, A. M., Dimmeler, S., & Urbich, C. (2011). Class IIb HDAC6 regulates endothelial cell migration and angiogenesis by deacetylation of cortactin. *EMBO Journal*, *30*(20), 4142–4156. https://doi.org/10.1038/emboj.2011.298

Kawaguchi, Y., Kovacs, J. J., McLaurin, A., Vance, J. M., Ito, A., & Yao, T.-P. (2003). The Deacetylase HDAC6 Regulates Aggresome Formation and Cell Viability in Response to Misfolded Protein Stress. *Cell*, *115*(6), 727–738. https://doi.org/10.1016/S0092-8674(03)00939-5

Kirkbride, K. C., Sung, B. H., Sinha, S., & Weaver, A. M. (2011). Cortactin: A multifunctional regulator of cellular invasiveness. *Cell Adhesion and Migration*, *5*(2), 187–198. https://doi.org/10.4161/cam.5.2.14773

Kobayashi, H., Butler, J. M., O'Donnell, R., Kobayashi, M., Ding, B.-S., Bonner, B., Chiu, V. K., Nolan, D. J., Shido, K., Benjamin, L., & Rafii, S. (2010). Angiocrine factors from Akt-activated endothelial cells balance self-renewal and differentiation of haematopoietic stem cells. *Nature Cell Biology*, *12*(11), 1046–1056. https://doi.org/10.1038/ncb2108

Kopf, A., & Kiermaier, E. (2021). Dynamic Microtubule Arrays in Leukocytes and Their Role in Cell Migration and Immune Synapse Formation. In *Frontiers in Cell and Developmental Biology* (Vol. 9). Frontiers Media S.A. https://doi.org/10.3389/fcell.2021.635511

Kovacs, J. J., Murphy, P. J. M., Gaillard, S., Zhao, X., Wu, J.-T., Nicchitta, C. V, Yoshida, M., Toft, D. O., Pratt, W. B., & Yao, T.-P. (2005). HDAC6 Regulates

Hsp90 Acetylation and Chaperone-Dependent Activation of Glucocorticoid Receptor. *Molecular Cell*, *18*(5), 601–607. https://doi.org/https://doi.org/10.1016/j.molcel.2005.04.021

Kozyreva, V. K., McLaughlin, S. L., Livengood, R. H., Calkins, R. A., Kelley, L. C., Rajulapati, A., Ice, R. J., Smolkin, M. B., Weed, S. A., & Pugacheva, E. N. (2014). NEDD9 Regulates Actin Dynamics through Cortactin Deacetylation in an AURKA/HDAC6-Dependent Manner. *Molecular Cancer Research*, *12*(5), 681–693. https://doi.org/10.1158/1541-7786.MCR-13-0654

Krämer, O. H., Mahboobi, S., & Sellmer, A. (2014). Drugging the HDAC6-HSP90 interplay in malignant cells. In *Trends in Pharmacological Sciences* (Vol. 35, Issue 10, pp. 501–509). Elsevier Ltd. https://doi.org/10.1016/j.tips.2014.08.001

Kruse, A., Abdel-Azim, N., Kim, H. N., Ruan, Y., Phan, V., Ogana, H., Wang, W., Lee, R., Gang, E. J., Khazal, S., & Kim, Y. M. (2020). Minimal residual disease detection in acute lymphoblastic leukemia. In *International Journal of Molecular Sciences* (Vol. 21, Issue 3). MDPI AG. https://doi.org/10.3390/ijms21031054

Kulis, J., Sędek, Ł., Słota, Ł., Perkowski, B., & Szczepański, T. (2022). Commonly Assessed Markers in Childhood BCP-ALL Diagnostic Panels and Their Association with Genetic Aberrations and Outcome Prediction. In *Genes* (Vol. 13, Issue 8). MDPI. https://doi.org/10.3390/genes13081374

Laguri, C., Sadir, R., Rueda, P., Baleux, F., Gans, P., Arenzana-Seisdedos, F., & Lortat-Jacob, H. (2007). The novel CXCL12γ isoform encodes an unstructured cationic domain which regulates bioactivity and interaction with both glycosaminoglycans and CXCR4. *PLoS ONE*, *2*(10). https://doi.org/10.1371/journal.pone.0001110

Lam, C. G., Howard, S. C., Bouffet, E., & Pritchard-Jones, K. (2019). Science and health for all children with cancer. *Science*, *363*(6432), 1182–1186. https://doi.org/10.1126/science.aaw4892

Lancet, T. (2019). *Global Health Metrics R2 www.thelancet.com Vol 393 Figure 1: Composition of DALYs by YLLs and YLDs for*. www.thelancet.com

Lee, J.-Y., Koga, H., Kawaguchi, Y., Tang, W., Wong, E., Gao, Y.-S., Pandey, U. B., Kaushik, S., Tresse, E., Lu, J., Taylor, J. P., Cuervo, A. M., & Yao, T.-P. (2010). HDAC6 controls autophagosome maturation essential for ubiquitin-selective quality-control autophagy. *The EMBO Journal*, *29*(5), 969–980. https://doi.org/https://doi.org/10.1038/emboj.2009.405

Li, D., Sun, X., Zhang, L., Yan, B., Xie, S., Liu, R., Liu, M., & Zhou, J. (2014). Histone deacetylase 6 and cytoplasmic linker protein 170 function together to regulate the motility of pancreatic cancer cells. *Protein and Cell*, *5*(3), 214–223. https://doi.org/10.1007/s13238-013-0010-3

Li, G., Tian, Y., & Zhu, W. G. (2020). The Roles of Histone Deacetylases and Their Inhibitors in Cancer Therapy. In *Frontiers in Cell and Developmental Biology* (Vol. 8). Frontiers Media S.A. https://doi.org/10.3389/fcell.2020.576946

Li, T., Zhang, C., Hassan, S., Liu, X., Song, F., Chen, K., Zhang, W., & Yang, J. (2018). Histone deacetylase 6 in cancer. In *Journal of Hematology and Oncology*. https://doi.org/10.1186/s13045-018-0654-9

Li, Y., & Seto, E. (2016). HDACs and HDAC Inhibitors in Cancer. *Cold Spring Harb Perspect Med*, *3*(6), 1–10.

Liu, P., Xiao, J., Wang, Y., Song, X., Huang, L., Ren, Z., Kitazato, K., & Wang, Y. (2021). Posttranslational modification and beyond: interplay between histone deacetylase 6 and heat-shock protein 90. *Molecular Medicine*, *27*(1), 110. https://doi.org/10.1186/s10020-021-00375-3

Locatelli, F., Schrappe, M., Bernardo, M. E., & Rutella, S. (2012). How i treat relapsed childhood acute lymphoblastic leukemia. *Blood*, *120*(14), 2807–2816. https://doi.org/10.1182/blood-2012-02-265884

Loghavi, S., Kutok, J. L., & Jorgensen, J. L. (2015). B-acute lymphoblastic leukemia/lymphoblastic lymphoma. *American Journal of Clinical Pathology*, *144*(3), 393–410. https://doi.org/10.1309/AJCPAN7BH5DNYWZB

Losson, H., Schnekenburger, M., Dicato, M., & Diederich, M. (2020). HDAC6—an emerging target against chronic myeloid leukemia? In *Cancers* (Vol. 12, Issue 2). MDPI AG. https://doi.org/10.3390/cancers12020318

Lua, B. L., & Low, B. C. (2005). Cortactin phosphorylation as a switch for actin cytoskeletal network and cell dynamics control. *FEBS Letters*, *579*(3), 577–585. https://doi.org/10.1016/j.febslet.2004.12.055

Luxton, G. W. G., & Gundersen, G. G. (2007). HDAC6-Pack: Cortactin Acetylation Joins the Brew. In *Developmental Cell* (Vol. 13, Issue 2, pp. 161–162). https://doi.org/10.1016/j.devcel.2007.07.014

Lwin, T., Zhao, X., Cheng, F., Zhang, X., Huang, A., Shah, B., Zhang, Y., Moscinski, L. C., Choi, Y. S., Kozikowski, A. P., Bradner, J. E., Dalton, W. S., Sotomayor, E., & Tao, J. (2013). A microenvironment-mediated c-Myc/miR-548m/HDAC6 amplification loop in non-Hodgkin B cell lymphomas. *Journal of Clinical Investigation*, *123*(11), 4612–4626. https://doi.org/10.1172/JCI64210

Ma, C., Witkowski, M. T., Harris, J., Dolgalev, I., Sreeram, S., Qian, W., Tong, J., Chen, X., Aifantis, I., & Chen, W. (2020). Leukemia-on-a-chip: Dissecting the chemoresistance mechanisms in B cell acute lymphoblastic leukemia bone marrow niche. *Science Advances*, *6*(44), eaba5536. https://doi.org/10.1126/sciadv.aba5536

MacGrath, S. M., & Koleske, A. J. (2012). Cortactin in cell migration and cancer at a glance. *Journal of Cell Science*, *125*(7), 1621–1626. https://doi.org/10.1242/jcs.093781

Maharaj, K., Powers, J. J., Achille, A., Deng, S., Fonseca, R., Pabon-Saldana, M., Quayle, S. N., Jones, S. S., Villagra, A., Sotomayor, E. M., Sahakian, E., & Pinilla-Ibarz, J. (2018). Silencing of HDAC6 as a therapeutic target in chronic lymphocytic leukemia. *Blood Advances*, *2*(21), 3012–3024. https://doi.org/10.1182/bloodadvances.2018020065

Mahlknecht, U., & Schönbein, C. (2008). Histone deacetylase inhibitor treatment downregulates VLA-4 adhesion in hematopoietic stem cells and acute myeloid leukemia blast cells. *Haematologica*, *93*(3), 443–446. https://doi.org/10.3324/haematol.11796

Man, Y., Yao, X., Yang, T., & Wang, Y. (2021). Hematopoietic Stem Cell Niche During Homeostasis, Malignancy, and Bone Marrow Transplantation. *Frontiers in Cell and Developmental Biology*, *9*. https://doi.org/10.3389/fcell.2021.621214

Mansell, E., Zareian, N., Malouf, C., Kapeni, C., Brown, N., Badie, C., Baird, D., Lane, J., Ottersbach, K., Blair, A., & Case, C. P. (2019). DNA damage signalling

from the placenta to foetal blood as a potential mechanism for childhood leukaemia initiation. *Scientific Reports*, *9*(1). https://doi.org/10.1038/s41598-019-39552-0

Mantovani, A., Ponzetta, A., Inforzato, A., & Jaillon, S. (2019). Innate immunity, inflammation and tumour progression: double-edged swords. *Journal of Internal Medicine*, *285*(5), 524–532. https://doi.org/https://doi.org/10.1111/joim.12886

Martinez-Quiles, N., Ho, H.-Y. H., Kirschner, M. W., Ramesh, N., & Geha, R. S. (2004). Erk/Src Phosphorylation of Cortactin Acts as a Switch On-Switch Off Mechanism That Controls Its Ability To Activate N-WASP. *Molecular and Cellular Biology*, *24*(12), 5269–5280. https://doi.org/10.1128/MCB.24.12.5269-5280.2004

Martini, V., Frezzato, F., Trimarco, V., Pizzi, M., Chiodin, G., Severin, F., Scomazzon, E., Saraggi, D., Martinello, L., Visentin, A., Brunati, A. M., Semenzato, G., Gattazzo, C., Frezzato, F., Trimarco, V., Pizzi, M., Chiodin, G., Severin, F., Scomazzon, E., … Trentin, L. (2017). Cortactin, a Lyn substrate, is a checkpoint molecule at the intersection of BCR and CXCR4 signalling pathway in chronic lymphocytic leukaemia cells. *British Journal of Haematology*, *178*(1), 81–93. https://doi.org/10.1111/bjh.14642

Mazo, I. B., Massberg, S., & von Andrian, U. H. (2011). Hematopoietic stem and progenitor cell trafficking. *Trends in Immunology*, *32*(10), 493–503. https://doi.org/10.1016/j.it.2011.06.011

Mejía-Aranguré, J. M., Núñez-Enríquez, J. C., Flores-Lujano, J., Aldebarán Duarte-Rodríguez, D., Jiménez-Hernández, E., Alfonso Martín-Trejo, J., Allende-López, A., Gabriel Peñaloza-González, J., Luisa Pérez-Saldivar, M., Medina-Sanson, A., Refugio Torres-Nava, J., Anastacia Solís-Labastida, K., Victoria Flores-Villegas, L., Martha Espinosa-Elizondo, R., Amador-Sánchez, R., Margarita Velázquez-Aviña, M., Elizabeth Merino-Pasaye, L., Nancy Núñez-Villegas, N., Itamar González-Ávila, A., … Arellano-Galindo, J. (2022). *Persistently high incidence rates of childhood acute leukemias from 2010 to 2017 in Mexico City: A population study from the MIGICCL*.

Messaoudi, K., Ali, A., Ishaq, R., Palazzo, A., Sliwa, D., Bluteau, O., Souquère, S., Muller, D., Diop, K. M., Rameau, P., Lapierre, V., Marolleau, J. P., Matthias, P., Godin, I., Pierron, G., Thomas, S. G., Watson, S. P., Droin, N., Vainchenker, W., … Debili, N. (2017). Critical role of the HDAC6-cortactin axis in human megakaryocyte maturation leading to a proplatelet-formation defect. *Nature Communications*, *8*(1786), 1–17. https://doi.org/10.1038/s41467-017-01690-2

Milazzo, G., Mercatelli, D., Di Muzio, G., Triboli, L., De Rosa, P., Perini, G., & Giorgi, F. M. (2020). Histone deacetylases (HDACs): Evolution, specificity, role in transcriptional complexes, and pharmacological actionability. In *Genes* (Vol. 11, Issue 5). MDPI AG. https://doi.org/10.3390/genes11050556

Mousavi, A. (2020). CXCL12/CXCR4 signal transduction in diseases and its molecular approaches in targeted-therapy. *Immunology Letters*, *217*, 91–115. https://doi.org/https://doi.org/10.1016/j.imlet.2019.11.007

Mullighan, C. G., Phillips, L. A., Su, X., Ma, J., Miller, C. B., Shurtleff, S. A., & Downing, J. R. (2008). Genomic Analysis of the Clonal Origins of Relapsed

Acute Lymphoblastic Leukemia. *Science*, *322*(5906), 1377–1380. https://doi.org/10.1126/science.1164266

Nakane, K., Fujita, Y., Terazawa, R., Atsumi, Y., Kato, T., Nozawa, Y., Deguchi, T., & Ito, M. (2012). Inhibition of cortactin and SIRT1 expression attenuates migration and invasion of prostate cancer DU145 cells. *International Journal of Urology*, *19*(1), 71–79. https://doi.org/10.1111/j.1442-2042.2011.02888.x

Nguyen, K., Devidas, M., Cheng, S. C., La, M., Raetz, E. A., Carroll, W. L., Winick, N. J., Hunger, S. P., Gaynon, P. S., & Loh, M. L. (2008). Factors influencing survival after relapse from acute lymphoblastic leukemia: A Children's Oncology Group study. *Leukemia*, *22*(12), 2142–2150. https://doi.org/10.1038/leu.2008.251

Olaoye, O. O., Watson, P. R., Nawar, N., Geletu, M., Sedighi, A., Bukhari, S., Raouf, Y. S., Manaswiyoungkul, P., Erdogan, F., Abdeldayem, A., Cabral, A. D., Hassan, M. M., Toutah, K., Shouksmith, A. E., Gawel, J. M., Israelian, J., Radu, T. B., Kachhiyapatel, N., De Araujo, E. D., … Gunning, P. T. (2021). Unique Molecular Interaction with the Histone Deacetylase 6 Catalytic Tunnel: Crystallographic and Biological Characterization of a Model Chemotype. *Journal of Medicinal Chemistry*, *64*(5), 2691–2704. https://doi.org/10.1021/acs.jmedchem.0c01922

Parbin, S., Kar, S., Shilpi, A., Sengupta, D., Deb, M., Rath, S. K., & Patra, S. K. (2014). Histone Deacetylases: A Saga of Perturbed Acetylation Homeostasis in Cancer. *Journal of Histochemistry and Cytochemistry*, *62*(1), 11–33. https://doi.org/10.1369/0022155413506582

Park, S. Y., & Kim, J. S. (2020). A short guide to histone deacetylases including recent progress on class II enzymes. In *Experimental and Molecular Medicine* (Vol. 52, Issue 2, pp. 204–212). Springer Nature. https://doi.org/10.1038/s12276-020-0382-4

Paul, S., Kantarjian, H., & Jabbour, E. J. (2016). Adult Acute Lymphoblastic Leukemia. *Mayo Clinic Proceedings*, *91*(11), 1645–1666. https://doi.org/10.1016/j.mayocp.2016.09.010

Pérez-Saldivar, M. L., Fajardo-Guti?rrez, A., Bern?ldez-R?os, R., Mart?nez-Avalos, A., Medina-Sanson, A., Espinosa-Hern?ndez, L., Flores-Chapa, J. D. D., Amador-S?nchez, R., Pe?aloza-Gonz?lez, J. G., ?lvarez-Rodr?guez, F. J., Bolea-Murga, V., Flores-Lujano, J., Rodr?guez-Zepeda, M. D. C., Rivera-Luna, R., Dorantes-Acosta, E. M., Jim?nez-Hern?ndez, E., Alvarado-Ibarra, M., Vel?zquez-Avi?a, M. M., Torres-Nava, J. R., … Mejia-Arangure, J. M. (2011). Childhood acute leukemias are frequent in Mexico City: Descriptive epidemiology. *BMC Cancer*, *11*. https://doi.org/10.1186/1471-2407-11-335

Pezzotta, A., Gentile, I., Genovese, D., Totaro, M. G., Battaglia, C., Leung, A. Y. H., Fumagalli, M., Parma, M., Cazzaniga, G., Fazio, G., Alcalay, M., Marozzi, A., & Pistocchi, A. (2022). HDAC6 inhibition decreases leukemic stem cell expansion driven by Hedgehog hyperactivation by restoring primary ciliogenesis. *Pharmacological Research*, *183*. https://doi.org/10.1016/j.phrs.2022.106378

Pramanik, R., Sheng, X., Ichihara, B., Heisterkamp, N., & Mittelman, S. D. (2013). Adipose tissue attracts and protects acute lymphoblastic leukemia cells from

chemotherapy. *Leukemia Research*, *37*(5), 503–509. https://doi.org/10.1016/j.leukres.2012.12.013

Pui, C. H., & Howard, S. C. (2008). Current management and challenges of malignant disease in the CNS in paediatric leukaemia. *The Lancet Oncology*, *9*(3), 257–268. https://doi.org/10.1016/S1470-2045(08)70070-6

Pui, C.-H., & Jeha, S. (2007). New therapeutic strategies for the treatment of acute lymphoblastic leukaemia. *Nature Reviews Drug Discovery*, *6*, 149.

Pui, C.-H., Robison, L., & Look, T. (2008). Acute Lymphoblastic Leukaemia. *The Lancet Oncology*, *371*, 1030–1043. https://doi.org/10.1007/978-1-61779-074-4_8

Purizaca, J., Meza, I., & Pelayo, R. (2012). Early Lymphoid Development and Microenvironmental Cues in B-cell Acute Lymphoblastic Leukemia. *Archives of Medical Research*, *43*(2), 89–101. https://doi.org/10.1016/j.arcmed.2012.03.005

Rahmani, M., Talebi, M., Hagh, M. F., Feizi, A. A. H., & Solali, S. (2018). Aberrant DNA methylation of key genes and Acute Lymphoblastic Leukemia. *Biomedicine & Pharmacotherapy*, *97*, 1493–1500. https://doi.org/https://doi.org/10.1016/j.biopha.2017.11.033

Román Cabrero, J., Serrador, J. M., Barreiro, O., Mittelbrunn, M., Naranjo-Suárez, S., Martín-Có freces, N., Vicente-Manzanares, M., Mazitschek, R., Bradner, J. E., Valenzuela-Fernández, A., & Sánchez-Madrid, F. (2006). Lymphocyte Chemotaxis Is Regulated by Histone Deacetylase 6, Independently of Its Deacetylase Activity □ V. *Molecular Biology of the Cell*, *17*, 3435–3445. https://doi.org/10.1091/mbc.E06

Rose, G., Reinhard, H., & Kahwash, S. B. (2020). *Is this a blast? An illustrated practical review on peripheral blood smear examination in the paediatric patient*.

Rosenfeld, C., Goutner, A., Choquet, C., Venuat, A. M., Kayibanda, B., Pico, J. L., & Greaves, M. F. (1977). Phenotypic characterisation of a unique non-T, non-B acute lymphoblastic leukaemia cell line. *Nature*, *267*(5614), 841–843. https://doi.org/10.1038/267841a0

Rudin, S., Marable, M., & Huang, R. S. (2017). The Promise of Pharmacogenomics in Reducing Toxicity During Acute Lymphoblastic Leukemia Maintenance Treatment. *Genomics, Proteomics & Bioinformatics*, *15*(2), 82–93. https://doi.org/https://doi.org/10.1016/j.gpb.2016.11.003

Rutledge, N. S., & Muller, W. A. (2020). Understanding Molecules that Mediate Leukocyte Extravasation. In *Current Pathobiology Reports* (Vol. 8, Issue 2, pp. 25–35). Springer. https://doi.org/10.1007/s40139-020-00207-9

Safa, A. R. (2017). *Role of histone deacetylase 6 (HDAC6) in cancers*. http://www.alliedacademies.org/journal-pharmacology-therapeutic-research/

Sage, P., & Carman, C. (2009). Settings and mechanisms for trans-cellular diapedesis Peter. *Front. Biosci*, *100*(2), 130–134. https://doi.org/10.1016/j.pestbp.2011.02.012.Investigations

Saji, S., Kawakami, M., Hayashi, S., Yoshida, N., Hirose, M., Horiguchi, S., Itoh, A., Funata, N., Schreiber, S. L., Yoshida, M., & Toi, M. (2005). Significance of HDAC6 regulation via estrogen signaling for cell motility and prognosis in

estrogen receptor-positive breast cancer. *Oncogene*, *24*(28), 4531–4539. https://doi.org/10.1038/sj.onc.1208646

Sakamoto, K. M., & Aldana-Masangkay, G. I. (2011). The role of HDAC6 in cancer. In *Journal of Biomedicine and Biotechnology* (Vol. 2011). https://doi.org/10.1155/2011/875824

Sakuma, T., Uzawa, K., Onda, T., Shiiba, M., Yokoe, H., Shibahara, T., & Tanzawa, H. (2006). *Aberrant expression of histone deacetylase 6 in oral squamous cell carcinoma*.

Sánchez-Aguilera, A., & Méndez-Ferrer, S. (2017). The hematopoietic stem-cell niche in health and leukemia. In *Cellular and Molecular Life Sciences* (Vol. 74, Issue 4, pp. 579–590). Birkhauser Verlag AG. https://doi.org/10.1007/s00018-016-2306-y

Schnoor, M. (2015). Endothelial Actin-Binding Proteins and Actin Dynamics in Leukocyte Transendothelial Migration. *The Journal of Immunology*, *194*(8), 3535–3541. https://doi.org/10.4049/jimmunol.1403250

Schnoor, M., Alcaide, P., Voisin, M. B., & Van Buul, J. D. (2015a). Crossing the Vascular Wall: Common and Unique Mechanisms Exploited by Different Leukocyte Subsets during Extravasation. *Mediators of Inflammation*, *2015*(Figure 1). https://doi.org/10.1155/2015/946509

Schnoor, M., Alcaide, P., Voisin, M. B., & Van Buul, J. D. (2015b). Crossing the Vascular Wall: Common and Unique Mechanisms Exploited by Different Leukocyte Subsets during Extravasation. *Mediators of Inflammation*, *2015*(Figure 1). https://doi.org/10.1155/2015/946509

Schnoor, M., Stradal, T. E., & Rottner, K. (2017). Cortactin: Cell Functions of A Multifaceted Actin-Binding Protein. *Trends in Cell Biology*, *28*(2), 79–98. https://doi.org/10.1016/j.tcb.2017.10.009

Schuuring, E., Verhoeven, E., Litvinov, S., & Michalides, R. J. (1993). The product of the EMS1 gene, amplified and overexpressed in human carcinomas, is homologous to a v-src substrate and is located in cell-substratum contact sites. *Molecular and Cellular Biology*, *13*(5), 2891–2898. https://doi.org/10.1128/mcb.13.5.2891

Shabnam Shalapour, Jana Hof, Renate Kirschner-Schwabe, Lorenz Bastian, Cornelia Eckert, Javier Prada, Günter Henze, Arend von Stackelberg, & Karl Seeger. (2011). High VLA-4 expression is associated with adverse outcome and distinct gene expression changes in childhood B-cell precursor acute lymphoblastic leukemia at first relapse. *Haematologica*, *96*(11), 1627–1635. https://doi.org/10.3324/haematol.2011.047993

Shalapour, S., Hof, J., Kirschner-Schwabe, R., Bastian, L., Eckert, C., Prada, J., Henze, G., von Stackelberg, A., & Seeger, K. (2011). High VLA-4 expression is associated with adverse outcome and distinct gene expression changes in childhood B-cell precursor acute lymphoblastic leukemia at first relapse. *Haematologica*, *96*(11), 1627–1635. https://doi.org/10.3324/haematol.2011.047993

Shen, S., Svoboda, M., Zhang, G., Cavasin, M. A., Motlova, L., McKinsey, T. A., Eubanks, J. H., Bařinka, C., & Kozikowski, A. P. (2020). Structural and in Vivo Characterization of Tubastatin A, a Widely Used Histone Deacetylase 6

Inhibitor. *ACS Medicinal Chemistry Letters*, *11*(5), 706–712. https://doi.org/10.1021/acsmedchemlett.9b00560

Shen, W., Bendall, L. J., Gottlieb, D. J., & Bradstock, K. F. (2001). The chemokine receptor CXCR4 enhances integrin-mediated in vitro adhesion and facilitates engraftment of leukemic precursor-B cells in the bone marrow. *Experimental Hematology*, *29*(12), 1439–1447. https://doi.org/10.1016/S0301-472X(01)00741-X

Shi, Y., Riese, D. J., & Shen, J. (2020). The Role of the CXCL12/CXCR4/CXCR7 Chemokine Axis in Cancer. *Frontiers in Pharmacology*, *11*. https://doi.org/10.3389/fphar.2020.574667

Shishido, S., Bönig, H., & Kim, Y.-M. (2014). Role of Integrin Alpha4 in Drug Resistance of Leukemia. *Frontiers in Oncology*, *4*. https://doi.org/10.3389/fonc.2014.00099

Siegel, R. L., Miller, K. D., Wagle, N. S., & Jemal, A. (2023). Cancer statistics, 2023. *CA: A Cancer Journal for Clinicians*, *73*(1), 17–48. https://doi.org/https://doi.org/10.3322/caac.21763

Smith, J. N. P., & Calvi, L. M. (2013). Concise review: Current concepts in bone marrow microenvironmental regulation of hematopoietic stem and progenitor cells. *Stem Cells (Dayton, Ohio)*, *31*(6), 1044–1050. https://doi.org/10.1002/stem.1370

Spiegel, A., Kollet, O., Peled, A., Abel, L., Nagler, A., Bielorai, B., Rechavi, G., Vormoor, J., & Lapidot, T. (2008). result of altered CXCR4 expression and signaling Unique SDF-1 – induced activation of human precursor-B ALL cells as a result of altered CXCR4 expression and signaling. *Blood*, *103*(8), 2900–2907. https://doi.org/10.1182/blood-2003-06-1891

Suárez-Álvarez, B., López-Vázquez, A., & López-Larrea, C. (2012). Mobilization and homing of hematopoietic stem cells. *Advances in Experimental Medicine and Biology*, *741*, 152–170. https://doi.org/10.1007/978-1-4614-2098-9_11

Subramanian, C., Jarzembowski, J. A., Opipari, A. W., Castle, V. P., & Kwok, R. P. S. (2011). HDAC6 deacetylates Ku70 and regulates Ku70-Bax binding in neuroblastoma. *Neoplasia*, *13*(8), 726–734. https://doi.org/10.1593/neo.11558

Sugiyama, T., Kohara, H., Noda, M., & Nagasawa, T. (2006). Maintenance of the Hematopoietic Stem Cell Pool by CXCL12-CXCR4 Chemokine Signaling in Bone Marrow Stromal Cell Niches. *Immunity*, *25*(6), 977–988. https://doi.org/10.1016/j.immuni.2006.10.016

Tan, J., Cang, S., Ma, Y., Petrillo, R. L., & Liu, D. (2010). *Novel histone deacetylase inhibitors in clinical trials as anti-cancer agents*. http://www.jhoonline.org/content/3/1/5

Tavares, M. O., Milan, T. M., Bighetti-Trevisan, R. L., Leopoldino, A. M., & de Almeida, L. O. (2022). Pharmacological inhibition of HDAC6 overcomes cisplatin chemoresistance by targeting cancer stem cells in oral squamous cell carcinoma. *Journal of Oral Pathology & Medicine*, *51*(6), 529–537. https://doi.org/https://doi.org/10.1111/jop.13326

Terwilliger, T., & Abdul-Hay, M. (2017). Acute lymphoblastic leukemia: a comprehensive review and 2017 update. *Blood Cancer Journal*, *7*(6), e577. https://doi.org/10.1038/bcj.2017.53

Urdiciain, A., Erausquin, E., Meléndez, B., Rey, J. A., Idoate, M. A., & Castresana, J. S. (2019). Tubastatin A, an inhibitor of HDAC6, enhances temozolomide-induced apoptosis and reverses the malignant phenotype of glioblastoma cells. *International Journal of Oncology*, *54*(5), 1797–1808. https://doi.org/10.3892/ijo.2019.4739

Valenzuela-Fernández, A., Cabrero, J. R., Serrador, J. M., & Sánchez-Madrid, F. (2008). HDAC6: a key regulator of cytoskeleton, cell migration and cell-cell interactions. In *Trends in Cell Biology* (Vol. 18, Issue 6, pp. 291–297). https://doi.org/10.1016/j.tcb.2008.04.003

van den Berk, L. C. J., van der Veer, A., Willemse, M. E., Theeuwes, M. J. G. A., Luijendijk, M. W., Tong, W. H., van der Sluis, I. M., Pieters, R., & den Boer, M. L. (2014). Disturbed CXCR4/CXCL12 axis in paediatric precursor B-cell acute lymphoblastic leukaemia. *British Journal of Haematology*, *166*(2), 240–249. https://doi.org/https://doi.org/10.1111/bjh.12883

Van Helleputte, L., Benoy, V., & Van Den Bosch, L. (2014). The role of histone deacetylase 6 (HDAC6) in neurodegeneration. *Research and Reports in Biology*, 1. https://doi.org/10.2147/rrb.s35470

van Rossum, A. G. S. H., Schuuring-Scholtes, E., van Buuren-van Seggelen, V., Kluin, P. M., & Schuuring, E. (2005). Comparative genome analysis of cortactin and HS1: The significance of the F-actin binding repeat domain. *BMC Genomics*, *6*, 1–14. https://doi.org/10.1186/1471-2164-6-15

Velázquez-Avila, M., Balandrán, J. C., Ramírez-Ramírez, D., Velázquez-Avila, M., Sandoval, A., Felipe-López, A., Nava, P., Alvarado-Moreno, J. A., Dozal, D., Prieto-Chávez, J. L., Schaks, M., Rottner, K., Dorantes-Acosta, E., López-Martínez, B., Schnoor, M., & Pelayo, R. (2018). High cortactin expression in B-cell acute lymphoblastic leukemia is associated with increased transendothelial migration and bone marrow relapse. *Leukemia*, *1*, 1337–1348. https://doi.org/10.1038/s41375-018-0333-4

Vestweber, D. (2015). How leukocytes cross the vascular endothelium. *Nature Reviews Immunology*, *15*(11), 692–704. https://doi.org/10.1038/nri3908

Vilchis-Ordoñez, A., Contreras-Quiroz, A., Vadillo, E., Dorantes-Acosta, E., Reyes-López, A., Quintela-Nuñez Del Prado, H. M., Venegas-Vázquez, J., Mayani, H., Ortiz-Navarrete, V., López-Martínez, B., & Pelayo, R. (2015). Bone marrow cells in acute lymphoblastic leukemia create a proinflammatory microenvironment influencing normal hematopoietic differentiation fates. *BioMed Research International*, *2015*. https://doi.org/10.1155/2015/386165

Vrooman, L. M., Blonquist, T. M., Harris, M. H., Stevenson, K. E., Place, A. E., Hunt, S. K., O'Brien, J. E., Asselin, B. L., Athale, U. H., Clavell, L. A., Cole, P. D., Kelly, K. M., Laverdiere, C., Leclerc, J. M., Michon, B., Schorin, M. A., Sulis, M. L., Welch, J. J. G., Neuberg, D. S., … Silverman, L. B. (2018). Refining risk classification in childhood b acute lymphoblastic leukemia: Results of DFCI ALL consortium protocol 05-001. *Blood Advances*, *2*(12), 1449–1458. https://doi.org/10.1182/bloodadvances.2018016584

Waterman-Storer, C. M., & Salmon, E. D. (1999). Positive feedback interactions between microtubule and actin dynamics during cell motility. *Current Opinion in Cell Biology*, *11*(1), 61–67. https://doi.org/https://doi.org/10.1016/S0955-0674(99)80008-8

Weaver, A. M., Karginov, A. V., Kinley, A. W., Weed, S. A., Li, Y., Parsons, J. T., & Cooper, J. A. (2001). Cortactin promotes and stabilizes Arp2/3-induced actin filament network formation. *Current Biology*, *11*(5), 370–374. https://doi.org/10.1016/S0960-9822(01)00098-7

Weed, S. A., Du, Y., & Parsons, J. T. (1998). Translocation of cortactin to the cell periphery is mediated by the small GTPase Rac1. *Journal of Cell Science*, *111*(16), 2433–2443.

Weiss, W. A., Taylor, S. S., & Shokat, K. M. (2007). Recognizing and exploiting differences between RNAi and small-molecule inhibitors. In *Nature Chemical Biology* (Vol. 3, Issue 12, pp. 739–744). Nature Publishing Group. https://doi.org/10.1038/nchembio1207-739

World Health Organization. (2021). *CureAll framework: WHO global initiative for childhood cancer: increasing access, advancing quality, saving lives*. World Health Organization.

Yamaguchi, T., Kawamoto, E., Gaowa, A., Park, E. J., & Shimaoka, M. (2021). Remodeling of bone marrow niches and roles of exosomes in Leukemia. In *International Journal of Molecular Sciences* (Vol. 22, Issue 4, pp. 1–15). MDPI AG. https://doi.org/10.3390/ijms22041881

Yang, J., Gong, C., Ke, Q., Fang, Z., Chen, X., Ye, M., & Xu, X. (2021). Insights Into the Function and Clinical Application of HDAC5 in Cancer Management. In *Frontiers in Oncology* (Vol. 11). Frontiers Media S.A. https://doi.org/10.3389/fonc.2021.661620

Yin, M., Ma, W., & An, L. (2017). Cortactin in cancer cell migration and invasion. *Oncotarget*, *8*(50), 88232–88243. https://doi.org/10.18632/oncotarget.21088

Zapata-Tarrés, M., Carlos Balandrán, J., Rivera-Luna, R., & Pelayo, R. (2021). Childhood Acute Leukemias in Developing Nations: Successes and Challenges. *Current Oncology Reports*, *23*(56). https://doi.org/10.1007/s11912-021-01043-9/Published

Zhang, G., & Gan, Y. H. (2017). Synergistic antitumor effects of the combined treatment with an HDAC6 inhibitor and a COX-2 inhibitor through activation of PTEN. *Oncology Reports*, *38*(5), 2657–2666. https://doi.org/10.3892/or.2017.5981

Zhang, X., Yuan, Z., Zhang, Y., Yong, S., Salas-Burgos, A., Koomen, J., Olashaw, N., Parsons, J. T., Yang, X. J., Dent, S. R., Yao, T. P., Lane, W. S., & Seto, E. (2007). HDAC6 Modulates Cell Motility by Altering the Acetylation Level of Cortactin. *Molecular Cell*, *27*(2), 197–213. https://doi.org/10.1016/j.molcel.2007.05.033

Zhang, Y., Gilquin, B., Khochbin, S., & Matthias, P. (2006). Two Catalytic Domains Are Required for Protein Deacetylation*. *Journal of Biological Chemistry*, *281*(5), 2401–2404. https://doi.org/https://doi.org/10.1074/jbc.C500241200

Zhang, Y., Zhang, M., Dong, H., Yong, S., Li, X., Olashaw, N., Kruk, P. A., Cheng, J. Q., Bai, W., Chen, J., Nicosia, S. V., & Zhang, X. (2009). Deacetylation of cortactin by SIRT1 promotes cell migration. *Oncogene*, *28*(3), 445–460. https://doi.org/10.1038/onc.2008.388

Zhao, R., Liu, J., Li, Z., Zhang, W., Wang, F., & Zhang, B. (2022). Recent Advances in CXCL12/CXCR4 Antagonists and Nano-Based Drug Delivery Systems for

Cancer Therapy. In *Pharmaceutics* (Vol. 14, Issue 8). MDPI. https://doi.org/10.3390/pharmaceutics14081541

Zhou, W., Guo, S., Liu, M., Burow, M. E., & Wang, G. (2017). Targeting CXCL12/CXCR4 Axis in Tumor Immunotherapy. *Current Medicinal Chemistry*, *26*(17), 3026–3041. https://doi.org/10.2174/0929867324666170830111531

Zuo, Q., Wu, W., Li, X., Zhao, L., & Chen, W. (2012). HDAC6 and SIRT2 promote bladder cancer cell migration and invasion by targeting cortactin. *Oncology Reports*, *27*(3), 819–824. https://doi.org/10.3892/or.2011.1553

13. APPENDIX 1

Patient	Age	Type	Sex	Risk	Immunophenotype	BM blasts %	Translocations	Response to steroids	Leukocytes (x10^3)	PB blasts %	Hemoglobine (g/dL)
P1	10Y 8M	Debut	M	High	PreB	100	BCR-ABL1	ND	15630	ND	9.5
P2	17Y 4M	Debut	M	High	PreB	98	Negative	ND	12570	ND	ND
P3	9Y 4M	Debut	F	High	PreB	95	Negative	ND	2430	ND	ND
P4	3Y 9M	Debut	M	High	PreB	100	Negative	ND	4400	ND	6
P5	4Y	Debut	F	Standard	PreB	98	TEL-AML1	ND	9200	ND	ND
P6	14Y 8M	Debut	M	High	PreB	96	Negative	ND	12460	ND	ND
P7	4Y 8M	Debut	M	Standard	PreB	98	Negative	ND	13300	ND	ND
P8	9Y 10M	Debut	F	Standard	PreB	78	Negative	ND	9000	ND	6.8
P9	12Y 7M	Debut	M	High	PreB	96	Negative	ND	4700	ND	ND
P10	1Y 8M	Debut	F	Standard	PreB	100	Negative	ND	32780	ND	7.2
P11	2Y 3M	Debut	M	High	PreB	100	Negative	ND	2710	ND	ND
P12	13Y	Debut	M	High	PreB	100	Negative	ND	8000	ND	13.8
P13	4Y 7M	Debut	F	Standard	PreB	89	Negative	ND	42100	ND	8.4
P14	7Y 9M	Debut	F	High	PreB	80	MLL-AFF1	ND	371000	ND	3.9
P15	4Y 4M	Debut	F	High	PreB	100	Negative	ND	20220	ND	10.8
P16	12Y 8M	Debut	M	High	PreB	85	Negative	ND	7200	ND	9.9
P17	4Y 6M	Debut	M	Standard	PreB	92	Negative	ND	2700	ND	6.4
P18	6Y	Debut	F	High	PreB	90	Negative	ND	2360	ND	6.6
P19	7Y 3M	Debut	F	High	PreB	98	Negative	ND	8600	ND	7.8
P20	4Y 9M	Debut	F	Standard	PreB	96	Negative	ND	19900	ND	5.2
P21	4Y	Debut	F	Standard	PreB	96	TCF3-PBX1	ND	2780	ND	13.8
P22	10Y 5M	Debut	F	High	PreB	99.5	Negative	ND	46300	ND	10.1

14. APPENDIX 2

Patient	Age	Type	Sex	Risk	Immunophenotype	BM blasts %	Translocations	Response to steroids	Leukocytes (x10^3)	PB blasts %	Hemoglobine (g/dL)
P1	4Y 6M	Debut	F	High	ProB/PreB	96	Negative	Yes	43.03	88	6.45
P2	5Y10M	Debut	F	High	ProB	91.1	t(9;22)(q34;p13)	ND	882.20	100	9.28
P3	8Y 11M	Debut	F	Standard	ProB	96.7	Negative	Yes	1.00	4	11.7
P4	13Y 11M	Debut	M	High	ProB	98.7	t(9;22)(q34;p13)	Yes	169.00	96	8.9
P5	1Y 2M	Debut	F	High	PreB	94.4	t(9;11)(p22;q23)	ND	166.20	85	10.98
P6	7Y 9M	Relapse	M	Relapse	ProB	96.4	Negative	Yes	41.10	76	12.5
P7	6M	Debut	M	High	PreB	96.3	t(9;11)(p22;q23)	Yes	168.50	69	8.86
P8	2Y 8M	Debut	M	Standard	ProB	86	Negative	Yes	9.93	0.05	5.04
P9	9Y 2M	Debut	F	High	ProB/Pre B	92.9	Negative	Yes	2.76	10	9.48
P10	14Y 10M	Debut	F	High	ProB	87	t(9;12)(q34;p13) ETV6 ex5 - ABL1 ex2:	Yes	13.25	9	12.17
P11	7Y 11M	Debut	F	Standard	ProB	89.9	Negative	Yes	5.50	36	2.44
P12	14Y 5M	Debut	M	High	ProB	95	t(16;21)(p11;q22)	Yes	1.70	8	7.5
P13	3Y 11M	Debut	F	Standard	ProB	63.8	t(12;21)(p13;q22)	Yes	2.20	30	14
P14	4Y 2M	Debut	M	High	ProB/Pre B	82.7	t(12;21)(p13;q22)	Yes	157.50	84	7.9
P15	7Y 2M	Relapse	F	Relapse	ProB	83.4	Negative	ND	21.90	69	11.3
P16	13Y 3M	Debut	M	High	ProB/PreB	94.7	Negative	ND	92.00	87	8.8
P17	6Y 3M	Debut	F	High	ProB	31.1	Negative	Yes	4.50	4	15.1
P18	7Y 10M	Debut	M	High	ProB/PreB	86.7	Negative	Yes	6.14	0	2.83
P19	1Y2M	Debut	M	ND	ProB/PreB	96	Negative	ND	2.1	5	4.7
P20	1Y4M	Debut	F	High	ProB/PreB	82	Negative	Yes	81.2	68	11.7
P21	1Y2M	Debut	M	High	PreB	80	t(1;19)(q23;p13) TCF3 ex16 – PBX ex3	No	128	90	8.43
P22	9Y	Debut	F	Standard	PreB	89.54	ND	ND	ND	ND	ND
P23	4Y	Debut	M	Standard	PreB	59.87	ND	ND	ND	ND	ND
P24	3Y	Debut	F	Standard	PreB	88.83	ND	ND	ND	ND	ND
P25	8Y	Debut	F	Standard	PreB	88.19	ND	ND	ND	ND	ND
P26	15Y	Debut	M	High	PreB	94.84	ND	ND	ND	ND	ND
P27	17Y	Debut	F	High	PreB	80.88	ND	ND	ND	ND	ND
P28	3Y	Debut	F	Standard	PreB	90.77	ND	ND	ND	ND	ND
P29	6Y2M	Debut	F	High	ProB	96	Negative	Yes	123.00	90	10.1
P30	12Y3M	Debut	M	Standard	PreB	80	Negative	Yes	17.00	100	8.9
P31	9A2M	Debut	F	Standard	PreB	91	Negative	Yes	5.4	85	12.1
P32	10A1M	Debut	M	High	PreB	90	t(9;22)(q34;p13)	Yes	72.5	99	2.49
P33	7A2M	Debut	M	High	ProB/PreB	77	t(1;19)(q23;p13) TCF3 ex16 – PBX ex3	Yes	35.1	84	11.9
P34	10A3M	Debut	F	Standard	PreB	89	Negative	Yes	39	90	9.1
P35	17A1M	Debut	M	High	ProB/PreB	87	t(9;22)(q34;p13)	Yes	8.8	45	7.5
P36	1A5M	Debut	F	High	ProB/PreB	90	Negative	No	145	99	8
P37	16A2M	Debut	F	High	ProB	88	t(1;19)(q23;p13) TCF3 ex16 – PBX ex3	Yes	5300	56	10.1
P38	10A1M	Relapse	M	Relapse	ProB	80	Negative	Yes	23000	85	9.2
P39	6A2M	Relapse	F	Relapse	ProB	90	Negative	Yes	8500	80	9.4
P40	10A1M	Relapse	F	Relapse	ProB	77	t(12;21)(p13;q22)	No	45000	88	4.6
P41	14Y10M	Debut	M	High	Pro-B	37.7	Negative	Yes	3.8	8	4.8
P42	16Y	Relapse	M	Relapse	ProB	95.6	ND	Yes	145.43	94	10.34
P43	1M	Debut	F	High	Pro-B	95	t(11;19)(q23;p13.3) KMT2A ex9 - MLLT1 ex2	Yes	6.64	0	3.13
P44	6M	Relapse	F	Relapse	Pro-B	79.6	ND	Yes	52.38	90	7.98
P45	12Y11M	Debut	F	High	Pro-B	85	Negative	Yes	99.2	96.4	4.4
P46	14Y2M	Relapse	F	Relapse	Pro-B	99.1	Negative	Yes	36.65	31	12.12
P47	11Y6M	Debut	M	High	Pro-B	95.1	Negative	No	149	100	5.6
P48	11Y8M	Relapse	M	Relapse	Pro-B	73.2	Negative	ND	4.1	*0*	11.9
P49	5Y3M	Relapse	M	Relapse	Pre-B	22	Negative	ND	7.4	0	13.2

Patient	LDH (U/L)	Platelets	Infections	Anemia	Neutropenia	Thrombocytopenia	Hepatomegaly	Splenomegaly	Adenomegaly	Death	HDAC6 fold change	Hospital
P1	445	93	No	Yes	No	Yes	Yes	No	Yes	No	3.25	Hospital para el Niño (Instituto Materno Infantil) del Estado de México (Toluca, Mexico)
P2	1187	55	ND	Yes	Yes	Yes	Yes	No	Yes	Yes	1.82	Hospital para el Niño (Instituto Materno Infantil) del Estado de México (Toluca, Mexico)
P3	210	161	No	Yes	Yes	No	No	No	Yes	No	2.20	Hospital para el Niño (Instituto Materno Infantil) del Estado de México (Toluca, Mexico)
P4	602	30	No	Yes	Yes	Yes	Yes	Yes	Yes	No	1.77	Hospital para el Niño (Instituto Materno Infantil) del Estado de México (Toluca, Mexico)
P5	6918	53	ND	Yes	No	Yes	Yes	Yes	Yes	No	1.64	Hospital para el Niño (Instituto Materno Infantil) del Estado de México (Toluca, Mexico)
P6	1947	214	No	No	No	No	No	No	No	No	2.28	Hospital para el Niño (Instituto Materno Infantil) del Estado de México (Toluca, Mexico)
P7	476	40	Yes	Yes	No	Yes	Yes	Yes	Yes	No	3.00	Hospital para el Niño (Instituto Materno Infantil) del Estado de México (Toluca, Mexico)
P8	264	71	No	Yes	Yes	Yes	Yes	No	Yes	No	2.52	Hospital para el Niño (Instituto Materno Infantil) del Estado de México (Toluca, Mexico)
P9	1022	164	No	Yes	Yes	No	No	No	No	No	2.53	Hospital para el Niño (Instituto Materno Infantil) del Estado de México (Toluca, Mexico)
P10	540	231	No	No	No	No	Yes	No	Yes	No	2.25	Hospital para el Niño (Instituto Materno Infantil) del Estado de México (Toluca, Mexico)
P11	146	43	No	Yes	Yes	Yes	No	No	No	No	2.91	Hospital para el Niño (Instituto Materno Infantil) del Estado de México (Toluca, Mexico)
P12	163	65	No	Yes	Yes	Yes	No	No	No	No	1.72	Hospital para el Niño (Instituto Materno Infantil) del Estado de México (Toluca, Mexico)
P13	287	67	Yes	No	Yes	Yes	Yes	Yes	Yes	No	2.10	Hospital para el Niño (Instituto Materno Infantil) del Estado de México (Toluca, Mexico)
P14	355	18	No	Yes	No	Yes	Yes	Yes	No	No	1.90	Hospital para el Niño (Instituto Materno Infantil) del Estado de México (Toluca, Mexico)
P15	1663	57	Yes	No	Yes	Yes	No	No	No	No	2.98	Hospital para el Niño (Instituto Materno Infantil) del Estado de México (Toluca, Mexico)
P16	1312	14	ND	Yes	No	Yes	Yes	Yes	Yes	ND	1.98	Hospital para el Niño (Instituto Materno Infantil) del Estado de México (Toluca, Mexico)
P17	537	316	Yes	No	No	No	No	No	Yes	No	1.92	Hospital para el Niño (Instituto Materno Infantil) del Estado de México (Toluca, Mexico)
P18	326	165	No	Yes	Yes	No	Yes	Yes	Yes	No	1.45	Hospital para el Niño (Instituto Materno Infantil) del Estado de México (Toluca, Mexico)
P19	235.7	51	ND	Yes	Yes	Yes	Yes	Yes	Yes	ND	1.78	Hospital para el Niño (Instituto Materno Infantil) del Estado de México (Toluca, Mexico)
P20	3095	51	No	Yes	Yes	Yes	Yes	Yes	Yes	ND	2.04	Hospital para el Niño (Instituto Materno Infantil) del Estado de México (Toluca, Mexico)
P21	3799	13.7	No	Yes	No	Yes	Yes	No	No	ND	1.53	Hospital para el Niño (Instituto Materno Infantil) del Estado de México (Toluca, Mexico)
P22	ND	ND	Yes	ND	ND	ND	No	No	No	No	0.88	Hospital para el Niño Poblano (Puebla, Mexico)
P23	ND	ND	ND	ND	ND	ND	ND	ND	ND	No	2.65	Hospital de la Niñez Oaxaqueña (Oaxaca, Mexico)
P24	ND	ND	ND	ND	ND	ND	ND	ND	ND	No	1.84	Hospital de la Niñez Oaxaqueña (Oaxaca, Mexico)
P25	ND	ND	Yes	ND	ND	ND	No	No	Yes	No	2.74	Hospital para el Niño Poblano (Puebla, Mexico)
P26	ND	ND	Yes	ND	ND	ND	No	No	Yes	No	1.16	Unidad Médica de Alta Especialidad (UMAE)-Hospital de Especialidades IMSS San José (Puebla, Mexico)
P27	ND	ND	ND	ND	ND	ND	ND	ND	ND	No	1.90	Hospital de la Niñez Oaxaqueña (Oaxaca, Mexico)
P28	ND	ND	Yes	ND	ND	ND	No	No	No	No	2.44	Hospital Infantil de Tlaxcala (Tlaxcala, Mexico)
P29	512	42000	No	Yes	ND	Yes	Yes	Yes	Yes	No	3.49	Hospital Infantil de Mexico “Federico Gómez” (Mexico City)
P30	480	43000	ND	Yes	ND	Yes	Yes	Yes	Yes	Yes	2.32	Hospital Infantil de Mexico “Federico Gómez” (Mexico City)
P31	390	15000	No	Yes	ND	Yes	No	Yes	No	No	3.27	Hospital Infantil de Mexico “Federico Gómez” (Mexico City)
P32	1150	44000	No	Yes	ND	Yes	Yes	Yes	No	No	2.08	Hospital Infantil de Mexico “Federico Gómez” (Mexico City)
P33	640	80000	No	Yes	ND	Yes	Yes	Yes	Yes	No	4.15	Hospital Infantil de Mexico “Federico Gómez” (Mexico City)
P34	520	1980	No	Yes	ND	Yes	Yes	Yes	No	No	2.58	Hospital Infantil de Mexico “Federico Gómez” (Mexico City)
P35	640	35000	No	Yes	ND	Yes	Yes	Yes	Yes	No	1.49	Hospital Infantil de Mexico “Federico Gómez” (Mexico City)
P36	2200	8000	No	Yes	ND	Yes	Yes	Yes	Yes	No	2.28	Hospital Infantil de Mexico “Federico Gómez” (Mexico City)
P37	560	114000	No	Yes	ND	Yes	No	Yes	Yes	No	1.61	Hospital Infantil de Mexico “Federico Gómez” (Mexico City)
P38	450	56000	No	Yes	ND	Yes	Yes	Yes	Yes	No	7.22	Hospital Infantil de Mexico “Federico Gómez” (Mexico City)
P39	380	87000	No	Yes	ND	Yes	Yes	Yes	Yes	No	7.15	Hospital Infantil de Mexico “Federico Gómez” (Mexico City)
P40	890	23000	No	Yes	ND	Yes	Yes	Yes	Yes	No	11.17	Hospital Infantil de Mexico “Federico Gómez” (Mexico City)
P41	165	88	No	Yes	No	Yes	Yes	No	No	No	3.53	Hospital para el Niño (Instituto Materno Infantil) del Estado de México (Toluca, Mexico)
P42	6089	28	ND	Yes	No	Yes	No	No	No	No	3.80	Hospital para el Niño (Instituto Materno Infantil) del Estado de México (Toluca, Mexico)
P43	619.16	38.4	Yes	Yes	Yes	Yes	Yes	Yes	Yes	No	1.12	Hospital para el Niño (Instituto Materno Infantil) del Estado de México (Toluca, Mexico)
P44	433	70	ND	Yes	No	Yes	No	No	No	No	3.38	Hospital para el Niño (Instituto Materno Infantil) del Estado de México (Toluca, Mexico)
P45	408.8	42	No	Yes	Yes	Yes	No	No	Yes	No	3.99	Hospital para el Niño (Instituto Materno Infantil) del Estado de México (Toluca, Mexico)
P46	461.99	328	No	Yes	No	No	No	No	No	No	5.10	Hospital para el Niño (Instituto Materno Infantil) del Estado de México (Toluca, Mexico)
P47	191.3	185	No	Yes	Yes	No	Yes	Yes	No	No	3.91	Hospital para el Niño (Instituto Materno Infantil) del Estado de México (Toluca, Mexico)
P48	145.5	391	No	Yes	No	No	ND	ND	ND	No	4.48	Hospital para el Niño (Instituto Materno Infantil) del Estado de México (Toluca, Mexico)
P49	144	156	ND	No	No	No	No	No	No	No	4.20	Hospital para el Niño (Instituto Materno Infantil) del Estado de México (Toluca, Mexico)